Proceedings of Anticancer Research

Editors-in-Chief

Bahman Nasiri

School of Biosciences, Faculty of Health and Medical Sciences, Taylor's University, Malaysia

Rajesh K. Singh

Shivalik College of Pharmacy, Nangal, District Rupnagar, Punjab, India

BIO-BYWORD SCIENTIFIC PUBLISHING PTY LTD
(619 649 400)
Level 10
50 Clarence Street
SYDNEY NSW 2000

ISSN (ONLINE): 2208-3553
ISSN (PRINT): 2208-3545

Proceedings of Anticancer Research

Focus and Scope

Proceedings of Anticancer Research is an international peer-reviewed and open access journal, which is devoted to the rapid publication of high quality original articles, reviews, case reports, short communication and letters on all aspects of experimental and clinical oncology.

- Cellular research and bio-markers
- Identification of bio-targets and agents with novel mechanisms of action
- Preventative and integrated treatment for cancer patients
- Radiation and surgery
- Palliative care
- Patient adherence, quality of life, satisfaction
- Anticancer medicine

About Publisher

Bio-Byword Scientific Publishing is a fast-growing, peer-reviewed and open access journal publisher, which is located in Sydney, Australia. As a dependable and credible corporation, it promotes and serves a broad range of subject areas for the benefit of humanity. By informing and educating a global community of scholars, practitioners, researchers and students, it ndeavors to be the world's leading independent academic and professional publisher. To realize it, it keeps creative and innovative to meet the range of the authors' needs and publish the best of their work.

By cooperating with University of Sydney, University of New South Wales and other world-famous universities, Bio-Byword Scientific Publishing has established a huge publishing system based on hundreds of academic programs, and with a variety of journals in the subjects of medicine, construction, education and electronics.

PublisherHeadquarter

BIO-BYWORD SCIENTIFIC PUBLISHING PTYLTD Level 10
50 Clarence Street
Sydney NSW 2000
Website: www.bbwpublisher.com Email: info@bbwpublisher.com

Table of Contents

Call for papers–Proceedings of Anticancer Research

ISSN (Online): 2208-3553
ISSN (Print): 2208-3545

Submission open for September 2023

Dear Researchers,

Proceedings of Anticancer Research is an international peer-reviewed and open access journal, which is devoted to the rapid publication of high quality original articles, reviews, case reports, short communication and letters on all aspects of experimental and clinical oncology.

- Cellular research and bio-markers
- Identification of bio-targets and agents with novel mechanisms of action
- Preventative and integrated treatment for cancer patients
- Radiation and surgery
- Palliative care
- Patient adherence, quality of life, satisfaction
- Anticancer medicine

Proceedings of Anticancer Research is published by Bio-Byword Scientific Publishing Company, it is a fast growing peer-reviewed and open access journal publisher, which is located in Sydney, Australia. As a dependable and credible corporation, it promotes and serves a broad range of subject areas such as medicine, construction, education and electronics for the benefit of humanity. By informing and educating a global community of scholars, practitioners, researchers and students, it endeavour's to be the world's leading independent academic and professional publisher.

All Bio-Byword journals are free from all access barriers, allowing for the widest possible global dissemination of their manuscripts and highest possible citations. Bio-Byword publisher online submission will go through a rapid peer review and production, making the process of publishing simpler and more efficient, which benefit from its user friendly online submission system that reduces the overall time from submission to publication.

Acceptance Notification: Within 21 days from the date of manuscript submission

Send your manuscript to the editor at: **info@bbwpublisher.com**

Kind regards,
Editorial Office
Proceedings of Anticancer Research

Proceedings of Anticancer Research, 2023, Volume 7, Issue 4
http://ojs.bbwpublisher.com/index.php/PAR
ISSN Online: 2208-3553
ISSN Print: 2208-3545

Biosynthesis and Characterization of Silver Nanoparticles Coated with Metabolites Extracted from *Clerodendron phlomoides* with Its Biochemical Studies in Liver Tissue

Subha Veeramani[1], Kirubanandan Shanmugam[2]*

[1]National Centre for Nanoscience and Nanotechnology, University of Madras, Chennai 600025, India

[2]Saveetha School of Engineering, Saveetha Institute of Medical and Technical Sciences (SIMATS), Thandalam, Chennai 602105, India

***Corresponding author:** Kirubanandan Shanmugam, kirubanandan.shanmugam@gmail.com

Abstract: Silver nanoparticles (AgNPs) have been used as a potential nanomaterial-based drug delivery vehicle for liver cancer treatment, as it induces cell death and produces cytotoxicity against cancerous cells at a low concentration. The biosynthesis of green metallic nanoparticles uses secondary metabolites in plant extracts instead of toxic chemicals for a reduction-oxidation (redox) reaction. The biosynthesis of AgNPs with the aqueous extract of *Clerodendron phlomoides* was performed in this study. The phytochemical analysis of *C. phlomoides* extract using gas chromatography-mass spectrometry (GC-MS) confirmed the presence of redox metabolites. The peak at 489 nm in UV-visible spectra confirmed the formation of bioactive AgNPs reduced from silver nitrate solution, whereas the Fourier-transform infrared (FTIR) spectra indicated the bioactive molecules of plant extracts that are responsible for the formation. Scanning electron microscope (SEM) micrograph revealed the formation of spherical and ovoid structures of AgNPs, whereas transmission electron microscope (TEM) micrograph confirmed the size of AgNPs, which varies from 25 nm to 100 nm. X-ray diffraction (XRD) spectra showed the crystalline nature of AgNPs, and the size of crystallite was 4 nm, while dynamic light scattering (DLS) analysis confirmed the average particle size of AgNPs to be around 125 nm. *In vivo* studies showed that bioactive AgNPs have a significant anticancer potential against liver cancer, whereas biochemical studies of rats' liver tissue samples confirmed that bioactive AgNPs produced a potential hepatoprotective effect against diethylnitrosamine-induced liver cancer.

Keywords: Silver nanoparticles; *Clerodendron phlomoides*; Aqueous extract; SEM; TEM; Liver cancer

Online publication: July 05, 2023

1. Introduction

One of the most important organs is the liver and it functions mainly for various metabolism involved in the body. It predominantly works for glucose homeostasis, storage of vitamins and minerals, lipid synthesis and metabolism, maintenance of excess amino acids, ammonia, and bile production [1]. Apart from these functions, the liver plays a major role in the detoxification and metabolism of toxic and xenobiotics and produces enzymes such as cytochrome P450 (CYP 450). This enzyme converts toxic chemicals into hydrophilic substances for easy excretion in the urine via metabolism [2]. Hepatocellular carcinoma (HCC) is a form of liver cancer that is caused by genetic alterations, albeit the progression of HCC remains obscure

in the pathophysiology. The predicted genetic alterations for HCC included mutations, amplifications, and deletions in genomic aspects, as well as epigenetic alterations such as abnormal changes in methylation patterns [3]. HCC has a high metastatic potential and confrontation with contemporary therapeutic approaches that is the most challenging in the field of clinical oncology [4]. Therefore, there is a critical requirement for developing new therapeutic drugs and more efficient site/target-specific drug delivery vehicles [4].

In past decades, metallic nanoparticles have played an important role in medicine for the treatment of various ailments, such as cancer [5]. Precious metal nanoparticles have notable properties, such as excellent biocompatibility, stability, and photostability. In addition to that, metallic nanostructures have favorable physical, chemical, and biological properties as well as functionality in view of their nanoscale size [6,7]. Silver and its oxide nanoparticles (AgNPs) are the predominant metallic nanomaterials used for various functional applications [8]. It has considerable properties such as catalytic, optical, and antimicrobial properties. AgNPs play a predominant role as potential antimicrobial bionanomaterials against various microorganisms and pathogens. Through various mechanisms such as cell membrane breakage and penetration, silver ion in AgNPs eradicates and combats pathogens effectively [9].

AgNPs have not only a bacteriostatic and chemotherapeutic effect but also the capacity for inducing apoptosis in cancerous cells [10,11]. The reported mechanism of AgNPs-induced cell apoptosis is the cleavage of double-strand DNA, follow by oxidative stress production via the formation of free radicals, leading to the instability of chromosomes [12]. The size of AgNPs is one of the biggest advantages in producing anticancer potential against cancerous cells. Smaller nanoparticles penetrate the cancerous cells much more efficiently as compared to larger particles and interact with the nucleus by delivering either the anticancer agents or the biotherapeutic agents and producing more cytotoxic against the cancerous cells. Hence AgNPs can be used as a base biomaterial for the fabrication of drug targeting and delivery into the cells [13]. AgNPs also contribute as diagnostic agents, image contrast agents, and also biosensors to achieve the specific imaging process in biomedical applications. A recent study also showed that AgNPs can be used as chemotherapeutic material for the treatment of diethylnitrosamine (DEN)-induced liver cancer and gives hepatoprotective activity to the liver cells against DEN toxicity [14].

Numerous investigations on silver nanoparticle synthesis were reported. However, the chemical and physical methods for the synthesis of AgNPs have several limitations in the formation of nanoparticles, as there was consumption of toxic and expensive chemicals. To eliminate these limitations, green synthesis of silver nanoparticles via plant extract promotes the reduction and oxidation (redox) of silver nitrate solution into silver nanoparticles. The plant extract consists of various secondary metabolites functioning as agents for redox reactions leading to the formation of nanoparticles. Furthermore, these secondary metabolites make nanoparticles bioactive via coating nanoparticles [15].

Clerodendrum phlomidis Linn is a well-known medicinal plant used in Traditional practice and culture, and its leaves have been used in Ayurvedic and Siddha Medicine. This plant medicine was used for the treatment of inflammation, diabetes, nervous disorder, asthma, rheumatism, digestive disorders, urinary infection and disorders, and bitter tonic. The alcoholic and aqueous extract of the leaves has properties such as analgesic, anti-diarrheal, anti-plasmodial, hypoglycemic, minor tranquilizers, anti-asthmatic, anti-fungal, nematicidal, anti-amnestic, and anti-arthritic. Therefore, it was considered a material used for the green synthesis of nanoparticles considering its wide therapeutic potential [16].

This paper investigated the anticancer potential of silver nanoparticles against liver cancer induced in albino rats and biochemical studies of tissue taken from the liver treated by silver nanoparticles. The silver nanoparticles will be synthesized via a green synthetic approach with the extract from the leaves of *Clerodendrum phlomidis Linn*, hereby known as *C. phlomidis*.

2. Materials and methods

Analytical grade chemicals were supplied by Merck Sigma-Aldrich (USA), HiMedia Laboratories (India), and S.D. Fine Chem Ltd. (India), and were used throughout this scientific work. Silver nitrate (AR Grade) was the major precursor used in the synthesis of silver nanoparticles (AgNPs).

2.1. Plant extract preparation:

Five grams of *C. phlomidis* dried leaves were well grounded and soaked in 100 ml of the double-distilled water for 3 hours and then boiled for 30 min at a temperature of 100 ± 5°C until the solution turned completely brownish and turbid with crude plant extract. The given solution was cooled down to room temperature of nearly 15°C to 20°C, followed by filtered with Whatman 1 filter paper for the collection of the resultant filtrate, which contained the potential secondary metabolites and various bioactive molecules. This filtrate was then stored in a cold room at a temperature of 4°C for further use in the biosynthesis of silver nanoparticles.

2.2. Biosynthesis of silver nanoparticles

One millimolar of silver nitrate (Sigma AR Grade) was dissolved in 100 mL of double-distilled water and then added to 10 mL of an aqueous plant extract. The whole mixture was mixed under continuous stirring at 70 rpm. This experiment was carried out at a temperature of 50°C and a pH of 7 was maintained. Synthesized silver nanoparticles were centrifugated at 12,000 rpm. The freeze-dried silver nanoparticles were performed by a lyophilizer and the dried AgNPs were used for particle size analysis, morphological and topographical analyses, X-ray diffraction (XRD) studies, and zeta potential studies. The dried silver nanoparticles were used for anticancer activity studies against DEN-induced liver toxicity in albino rats.

2.3. Analysis of plant extract using gas chromatography-mass spectrometry

The given plant extracts were subjected to phytochemical analysis via gas chromatography-mass spectrometer (GC-MS), which evaluates the identification of the types of secondary metabolites. Perkin Elmer Auto System XL GC-MS analyzer was used, where 70 eV has been used for electron ionization energy for GC-MS analysis, and helium gas was used as a mobile gas phase and carrier. Helium was used at a flow rate of 1.51 mL/min with a plant extract sample load of 2 µL. Total GC-MS running time was 22 min. TurboMass software was used to analyze the chromatogram of the plant extracts. Identification of the compounds was carried out with the support of a database in the National Institute of Standards and Technology (NIST).

2.4. UV-visible spectroscopy studies of silver nanoparticles

Ten milliliters of plant extract were mixed with 1 mM $AgNO_3$ solution to synthesize bioactive nanoparticles. The formation of AgNPs was confirmed as the solution changed to brown color within 30 minutes. The plant extract contains plant flavonoids that can reduce $AgNO_3$ into silver nanoparticles. The size, shape, concentration, and agglomeration of AgNPs were investigated using UV-visible (UV-vis) spectrophotometer. The comparison between the free nanoparticles and agglomerated nanoparticles was investigated by studying the surface plasmon resonance (SPR) absorption band. For the agglomerated silver nanoparticles, the absorption band shifts to red (longer wavelength) as compared to the absorption band of free silver nanoparticles.

2.5. Scanning electron microscopy of silver nanoparticles

The morphology and shape of the AgNPs were evaluated using scanning electron microscopy (SEM) JEOL JSM IT1800. Dried AgNPs were subjected to SEM evaluation for analysis of the surface topography of the

nanoparticle. The carbon tape was stuck on the metallic stub and then a small quantity of AgNPs was added to the carbon tape and spread well on the area 5 × 5 mm. Nitrogen was then sprayed on the sample on the stub to remove any free nanoparticles. The images are taken in secondary electron mode in an SEM instrument and the SEM micrographs are captured at 5 microns.

2.6. Transmission electron microscopy of silver nanoparticles

The shape and topography of the silver nanoparticles were evaluated using transmission electron microscopy (TEM), which can be interpreted for anticancer activity. A drop of AgNPs suspension was taken on the copper grid and dried before image capture. The TEM micrographs were captured for the analysis of the size and shape of AgNPs.

2.7. Fourier-transform infrared spectroscopy studies of silver nanoparticles and secondary metabolites:

The silver nanoparticles coated by the secondary metabolites were analyzed using Fourier-transform infrared (FTIR) spectroscopy. In this analysis, the functional groups of secondary metabolites in the plant extract and then coated on the silver nanoparticles are investigated with FTIR spectra. The functional groups in the plant extract responsible for the reduction of silver nitrate into silver nanoparticles were also analyzed using FTIR RX1-Perkin Elmer in the wavelength range 4000-400 cm^{-1}.

2.8. X-ray diffraction analysis

The crystalline nature of biosynthesized silver nanoparticles was evaluated using X-ray diffraction (XRD) analysis with XPERT-PRO using monochromatic Cu kα radiation (λ = 1.5406 Å) operated at 40 kV and 30 mA at a 2θ angle pattern, and the scanning was performed in the region from 20° to 80°. The collected data were analyzed with the support of the Joint Committee on Powder Diffraction Standards (JCPDS) library to account for the crystalline structure of silver nanoparticles.

2.9. Dynamic light scattering analysis

The size distribution and stability of biosynthesized nanoparticles were investigated using a dynamic light scattering (DLS) instrument from Malvern Panalytical. The zeta potential of AgNPs was also determined by this measurement.

2.10. *In vivo* studies for evaluation of the anticancer potential of metallic nanoparticles

The biochemical studies of the anticancer potential of AgNPs were investigated via animal studies using Wister albino rats. Group 1 is considered the control group where the rats were fed with standard rat chow and pure drinking water *ad libitum.* For Groups 2–6, the rats were induced with liver carcinogenesis via intra-peritoneal injection of DEN (25 mg/kg body weight) in a single administration. DEN was dissolved in 0.5 mL of sterile water. In Group 3, the DEN-induced rats were treated with AgNPs to evaluate the anticancer potential of nanoparticles. The oral administration of AgNPs with a concentration of 10 mg/kg body weight was fed into the rats daily for 30 days. Group 4 DEN-induced rats were treated with selenium nanoparticles (SeNPs), group 5 DEN-induced rats were treated with palladium nanoparticles (PdNPs), and group 6 DEN-induced rats were treated with plant extracts.

3. Results and discussion

The phytochemical analysis of the plant extract was evaluated via GC-MS and chemical methods to evaluate the type of secondary metabolites in the extract. These secondary metabolites play a major role in the synthesis of silver nanoparticles and also coat the nanoparticles to achieve biological activity and

produce therapeutic effects such as anticancer potential against cancerous cells in the DEN-induced liver. In addition to that, these secondary metabolites act as redox agents in the biosynthesis of silver nanoparticles in an eco-friendly approach without any harmful products. These secondary metabolites increase the synergistic mechanism of AgNPs via coating the nanoparticles. As a result, the therapeutic effect of the biosynthesized nanoparticles was enhanced [17].

3.1. Phytochemical analysis

Aqueous extract of *C. phlomoides* was tested for their phytochemical constituents using various qualitative assays. In this study, alkaloids, flavonoids, phenols, glycosides, carbohydrates, and terpenoids were found in the aqueous extract of *C. phlomoides.* The results obtained were tabulated in **Table 1** stating that glycosides were present in leaves extract of *C. phlomoides*; flavonoids and alkaloids were present in all parts of the plant. The aqueous leaves extract showed positive for several phytoconstituents and the active constituents act as redox agents for the synthesis of silver nanoparticles.

Table 1. GC-MS data of *C. phlomoides* plant aqueous leaves extract

Chemical compounds	RT	Area	Molecular formulae	Molecular Weight	Compounds
2-Hexadecen-1-ol,3,7,11,15-tetramethyl-,[R-[R*,R*-(E)]]-(CAS)Phytol	33.790	1.40	$C_{20}H_{40}O$	296	Acyclic diterpene alcohol
9,12,15-Octadecatrienoic acid, methyl ester,(Z,Z,Z)-(CAS)Methyl linolenate	37.058	12.39	$C_{19}H_{32}O_2$	292	-
Naringenin	24.032	19.50	$C_{15}H_{12}O_5$	272.068	Polyphenolic compounds
6-Methoxy apigenin (Hispidulin)		19.50	$C_{16}H_{12}O_6$		
α-terpinene	C	0.03	$C_{10}H_8O_3$	136	Terpenoid
1,2,3-Propanetriol (CAS) Glycerol	10.332	2.29	$C_3H_8O_3$	92	Polyol
Geranyl Linalool isomer	38.757	4.68	$C_{20}H_{34}O$	290	Terpenoids
4H-Pyran-4-one, 2,3-dihydro-3,5-dihydroxy-6-methyl	33.142	0.59	$C_6H_8O_4$	144	Flavonoid Fraction
Quercetin	17.17	19.50	CHO	270	Flavonoids
1,2,3-Propanetriol (CAS) Glycerol	10.332	2.29	$C_3H_8O_3$	92	Polyol
Ethyl iso-allocholate	35.367	0.06	$C_{26}H_{44}O_5$	436	Steroid

Table 2 summarizes the presence of the various secondary metabolites in an aqueous plant extract and these metabolites coated on the silver nanoparticles. Carbohydrates, alkaloids, flavonoids, and terpenoids are present on the AgNPs via coating while synthesizing the nanoparticle. These secondary metabolites present on the silver nanoparticles produce anticancer activity against liver cancer that not only targets directly the cancerous cell in the liver but also synergistically produces a therapeutic effect against the cancer cell.

Table 2. Phytochemical analysis of *C. phlomoides* plant aqueous leaves extract and AgNPs

Phytochemical	Plant extract	AgNPs
Carbohydrates	+	+

(Continued on next page)

(Continued from previous page)

Phytochemical	Plant extract	AgNPs
Glycosides	+	-
Alkaloids	+++	++
Flavonoids	+	+
Steroids	+	-
Tannins	+	-
Saponins	+	-
Terpenoids	+	-
Polyphenols	+	+

Figures 1 and **2** show the GC-MS of *C. phlomoides* plant aqueous leaves extract. The spectra confirmed the presence of various secondary metabolites with the elucidated structure of the compounds in the extract. These compounds can produce various pharmacological effects with silver nanoparticles. As discussed earlier, these compounds also act as redox agents for the synthesis of silver nanoparticles.

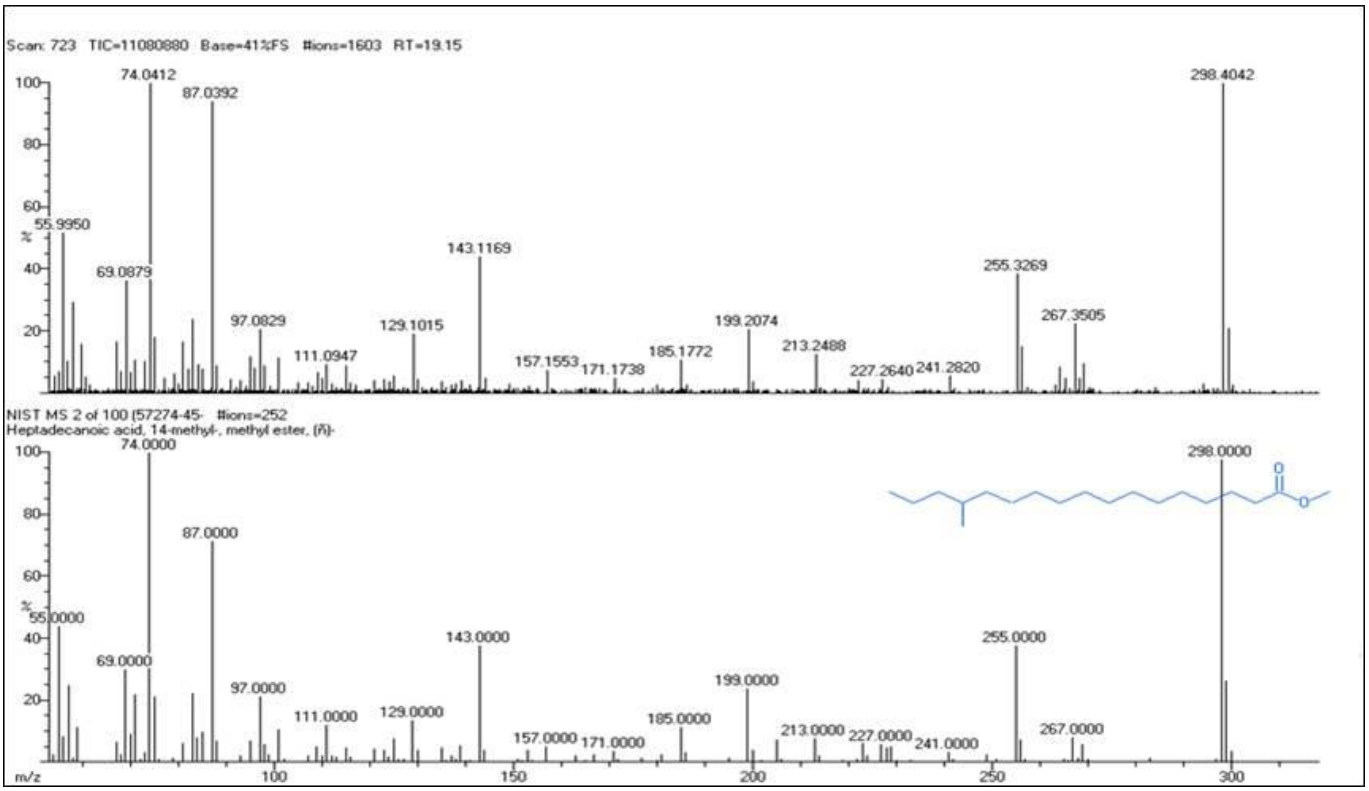

Figure 1. GC-MS data of *C. phlomoides* plant aqueous leaves extract

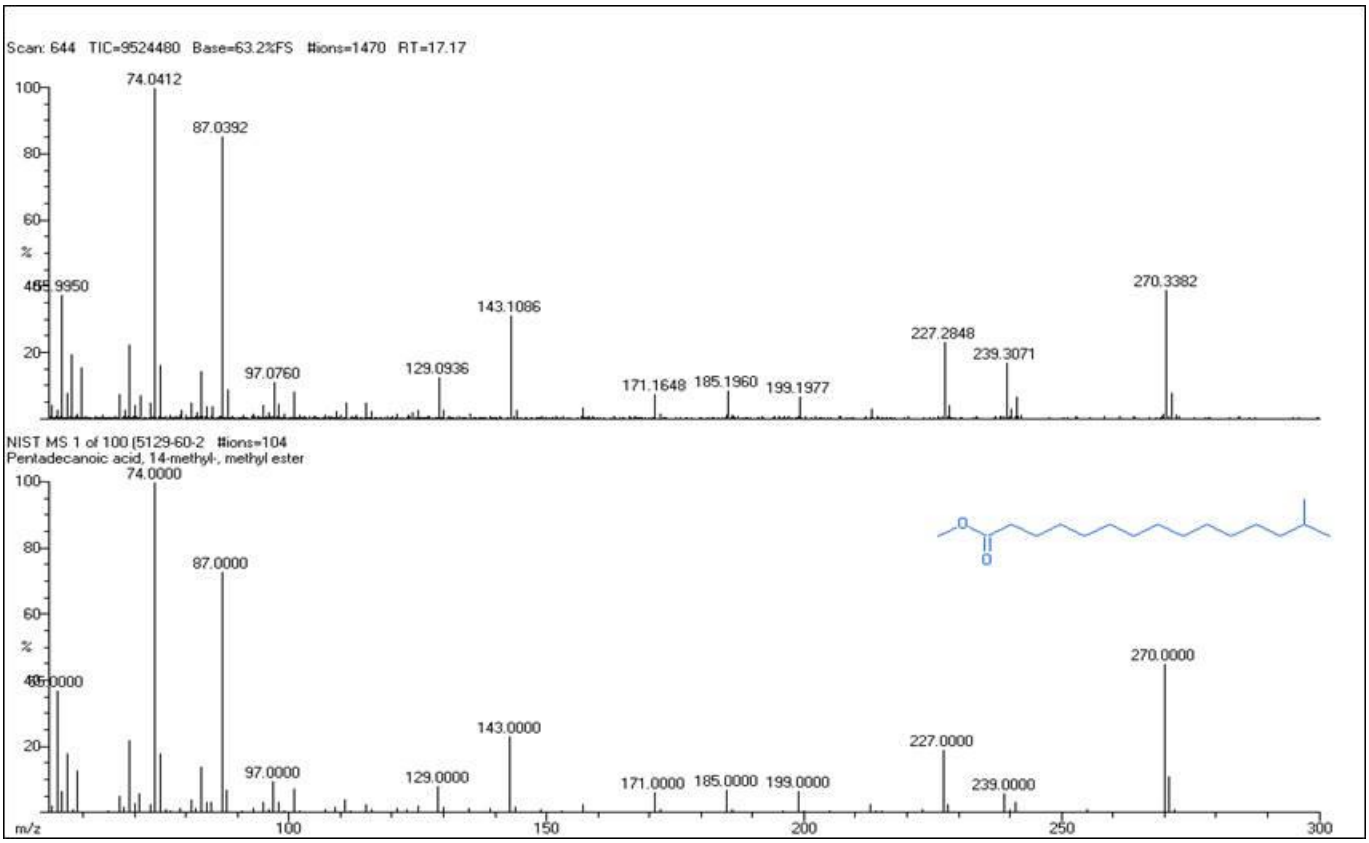

Figure 2. GC-MS data of *C. phlomoides* plant aqueous leaves extract

3.2. UV-visible analysis of AgNPs

Figure 3 reveals the UV-visible spectra of silver nanoparticles confirming that the silver nanoparticles formed at 489 nm. The synthesis of silver nanoparticles using *Peltophorum pterocarphum* plant extract was observed at the same absorption range from 390 to 490 nm. After the addition of plant extract, the colorless silver nitrate solution changed to brown color due to the biological reduction of silver nitrate into silver nanoparticles. The silver nanoparticle has free electrons giving the SPR band. The synthesized nanoparticle absorbs the SPR exactly at 489 nm and the range starts from 360-550 nm.

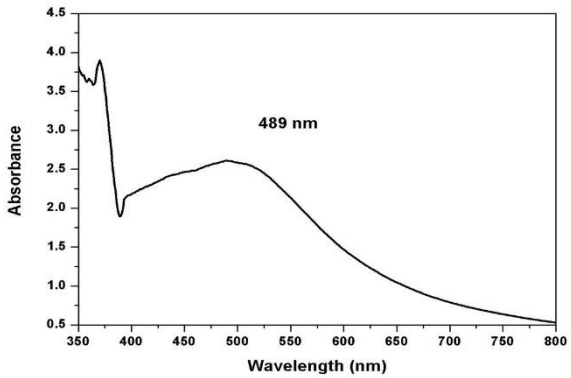

Figure 3. UV-visible spectroscopy analysis of silver nanoparticles

3.3. Fourier-transform infrared analysis of AgNPs

Figure 4 revealed the FTIR spectra of plant extract and silver nanoparticles. FTIR reported the bioactive macromolecules from the plant extract responsible for capping and stabilizing the silver nanoparticle improving their bioactive anticancer potential. **Figure 4A** shows the notable peaks at 3922, 3479, 2097,

and 1639 cm^{-1}. The peaks at 3479 and 1639 cm^{-1} represent the N-H stretching and bending vibration through amines from the proteins and other bioactive compounds of the plant extracts. The peak at 1639 cm^{-1} was observed in plant extract for the presence of NH_2 groups in amino acid. The presence of O-H stretching was noted at the peak of 3922 cm^{-1}. When comparing both FTIR spectra of plant extract and silver nanoparticles, the shift at higher ranges was seen. The polyphenols compounds of the plant are the source of OH groups and are responsible for the reduction of silver ions. This type of shift leads to the bind silver ion with free–NH groups in plant extract resulting in the stabilization of silver nanoparticles [18]. The predominant peaks in FTIR spectra were 1639-1642 cm^{-1} (protein groups), 2097-2103 cm^{-1}, and 3479-3516 cm^{-1} (amide I group). The peak at 2071 cm^{-1} shows the C-H stretching in the aldehyde group.

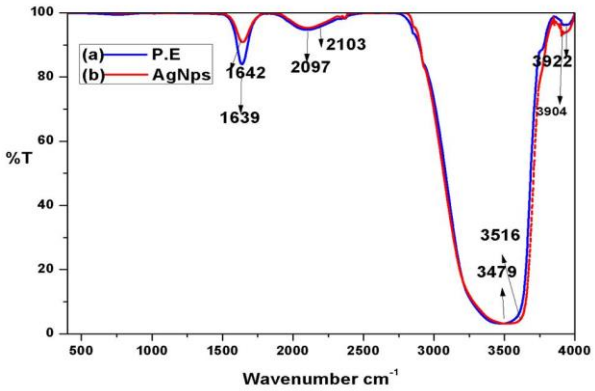

Figure 4. FTIR spectra of (a) Plant leaf extract and (b) Silver Nanoparticles

3.4. Scanning electron microscopy analysis

Figure 5 represents the structure and morphology of the green-synthesized AgNPs in SEM with energy dispersive X-ray (EDX) analysis. The spherical and ovoid structure of AgNPs was observed in the SEM micrograph. The elemental composition of green-synthesized AgNPs was observed from the EDX analysis. The yield of AgNPs was found to be 28.7%. When compared to Ag and O, the presence of other elements such as C and N were found to be present in a negligible amount. The composition of C and N present in the EDX analysis was low as compared to Ag and O, hence it could not be shown. **Table 3** shows the elemental composition of silver nanoparticles. The presence of oxygen in nanoparticles confirmed that a portion of silver was oxidized into silver oxide.

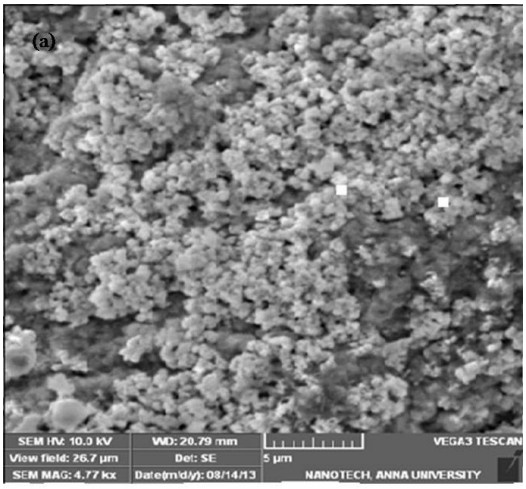

Figure 5. SEM image of green synthesized silver nanoparticles

Table 3. Quantitative analysis of AgNPs

Element	Net count	Weight %	Atom %
O	4462	29.06	73.42
Ag	29051	70.94	26.58
Total		100.00	100.00

3.5. Transmission electron studies:

Figure 6 shows the particle size varying from 25 to 100 nm. The aggregated nanoparticles cause size variation and wide size distribution. TEM reveals nanoparticles are well separated and aggregated. The shape of AgNPs was a sphere and predicted good interaction with cancerous cells due to larger surface volume area as compared to other shapes. As a result, the secondary metabolites on the surface of the AgNPs can penetrate the cancer cells of the liver and produce anticancer activity against the cancerous cell. The smaller particles (< 100 nm) produce more cytotoxic in cancerous cells than larger particles (> 100 nm) and penetrate the cell nucleus more effectively.

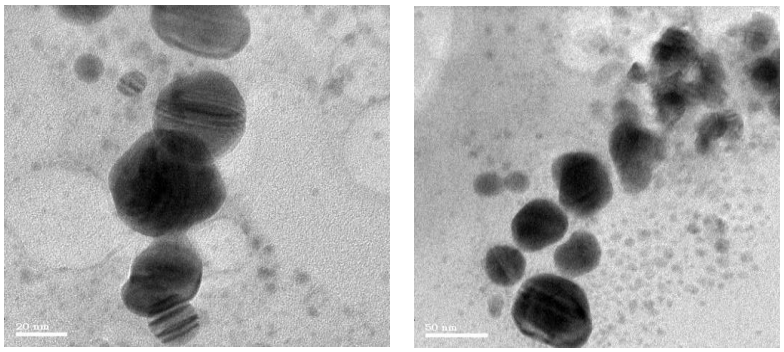

Figure 6. TEM images of silver nanoparticles

3.6. X-ray diffraction analysis

Figure 7 shows the XRD spectra of silver nanoparticles confirming that the nanoparticles were crystalline. The 2θ values were found to be 27.9°, 32.8°, 38.14°, and 46.2°, which corresponds to (220), (311), (111), and (100) planes of pure silver and coincides with ICDD (International Center for Diffraction Data) file No.01-1167. Fewer intensity peaks were observed in the area other than AgNPs, which may be due to the presence of biomacromolecules in an aqueous extract of *C. phlomoides.* Similar XRD results were previously reported for green synthesized silver nanoparticles with face-centered cubic (FCC) structure [18]. From the XRD value, it could be confirmed that the crystalline silver nanoparticles were effectively bio-reduced by *C. phlomoides* plant extract.

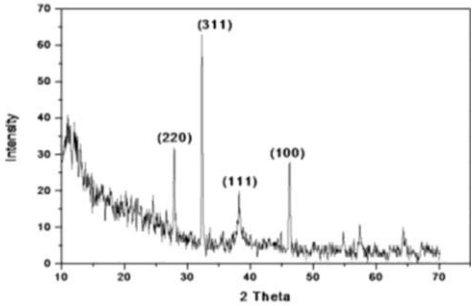

Figure 7. XRD spectra of silver nanoparticles

3.7. Dynamic light scattering and zeta potential analysis

Figure 8 shows the zeta potential for biologically reduced AgNPs. The zeta potential values range between +25 mV and -25 mV confirming highly stable nanoparticles that are highly pH and electrolyte concentration dependent. In the present investigation, AgNPs showed a negative zeta potential value and were found to be -6.02 mV and stable. The maximum particle size distribution falls in the range of 100 nm and next the aggregated particle distribution shows high in the figure of size distribution by density.

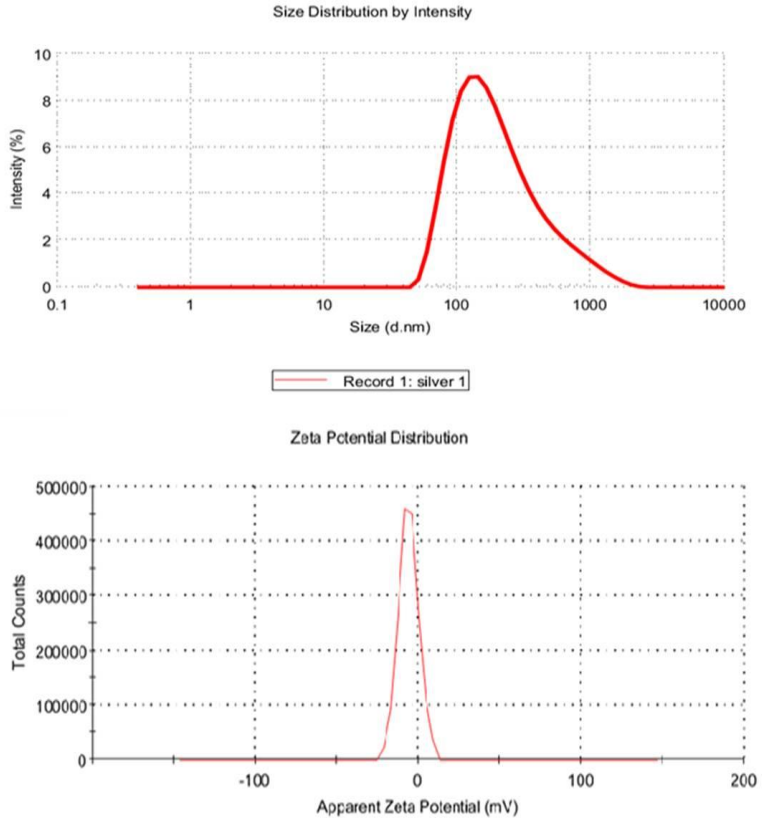

Figure 8. Size distribution of silver nanoparticles

3.8. Biochemical *in vivo* studies

In the biochemical studies, the therapeutic performance of the silver nanoparticle was evaluated and also compared with other metallic nanoparticles such as palladium and selenium nanoparticles. The anticancer potential of these nanoparticles including silver nanoparticles was investigated through the enzymatic analysis via biochemical studies and antioxidant expression in the tissue after the DEN-induced rats were treated with the nanoparticles.

3.8.1. Liver pathological enzyme analysis

As shown in **Figure 9**, the serum pathophysiological enzymes like aspartate aminotransferase (AST), alkaline transferase (ALT), alkaline phosphatase (ALP), and lactate dehydrogenase (LDH) in the control and experimental rats showed no significant difference in their activity. The DEN-induced rats that were administered with AgNPs exhibited about 1.5 times higher AST enzymic activity compared to the control group 1. Similarly, other enzymes like ALT, ALP, LDH, and gamma-glutamyl transferase (γGT) were also found to be increased. It is interesting to note that the treatment of DEN-induced rats with SeNPs decreased the serum pathophysiological enzyme level: AST from 143 to 91.05 U/L, ALT from 134.02 to 90.5 U/L, ALP from 221 to 170.34 U/L, LDH from 241 to 211.5 U/L and γGT 11.05 to 7.2 U/L. In AgNPs treated

group 3 rats, comparatively decreased enzyme activity was seen: AST from 143.21 to 106.34 U/L, ALT from 134.02 to 124.58 U/L, ALP from 221 to 158 U/L, LDH from 241 to 208.43 U/L, and γGT from 11.05 to 9.23 U/L. However, in the case of PdNPs treated group 5 rats, no satisfactory results were obtained. When compared to SeNPs and AgNPs treated groups, the results were shown: AST decreased from 143 to 128 U/L, ALT from 134.02 to 128.01 U/L, ALP from 221 to 142.81 U/L, LDH from 241 to 180.32 U/L, and γGT from 11.05 to 10.42 U/L. Meanwhile, there was not much difference between the DEN-induced group 2 rats and PdNPs-treated group 5 rats. Plant extract-treated group 6 rats, did not show significant changes in their values, which as shown in **Figure 9**.

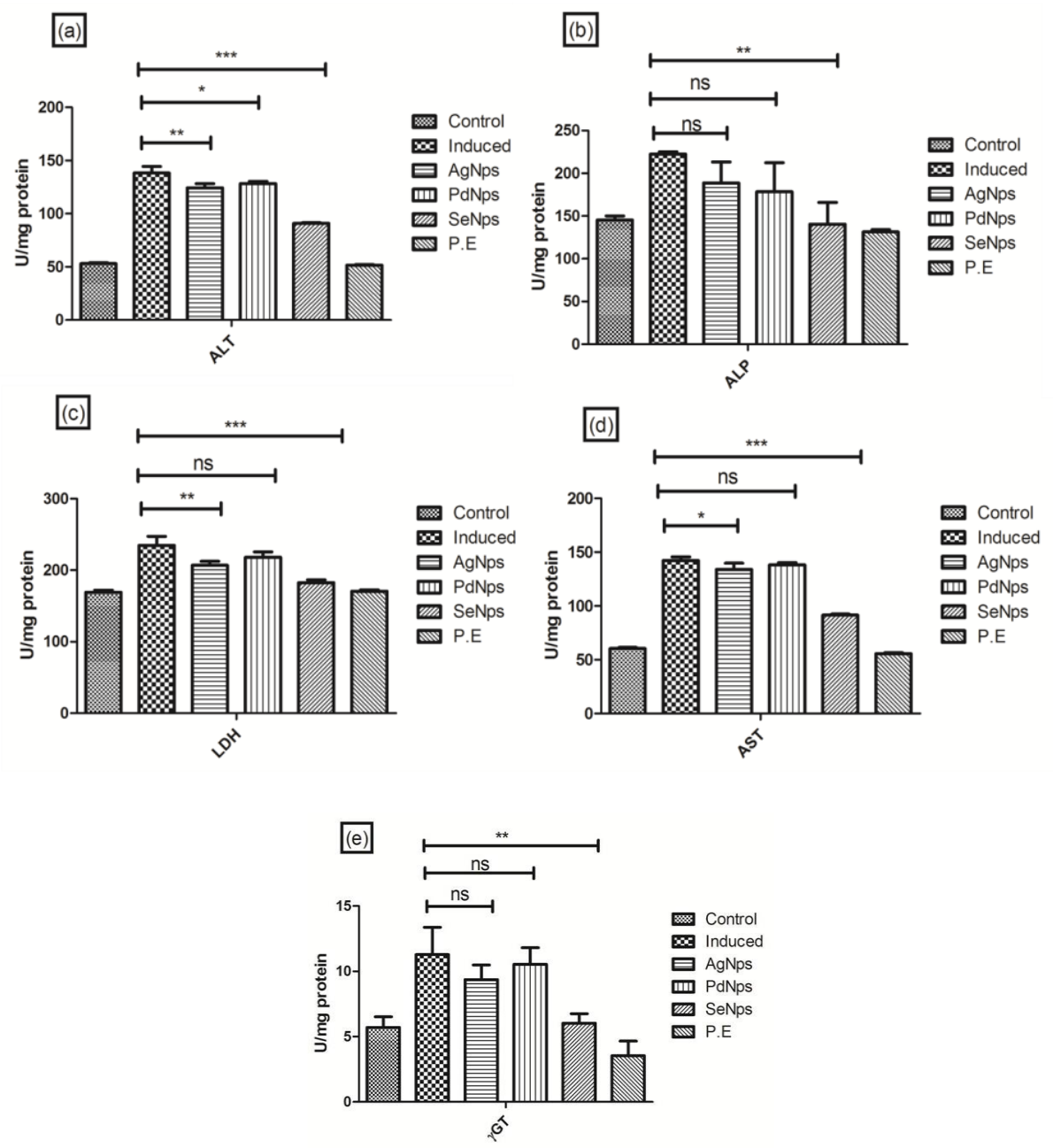

Figure 9. Effect of nanoparticles on serum liver pathological enzymes (a) ALT, (b) ALP, (c) LDH, (d) AST, and (e) γGT. Results were expressed as mean ± standard deviation (SD; n = 6). The significance when compared with the DEN-induced group of rats was shown as ns (not significant), * ($P < 0.05$),** ($P < 0.01$), and *** ($P < 0.005$).

The activities of liver pathophysiological enzymes AST, ALT, ALP, LDH, and γGT in control and experimental rats are presented in **Figure 9**. In the DEN-induced group, there was a significant increase in the activities of all of these enzymes, when compared to the control group. Among all the enzymes, the activity of ALT was found to be drastically increased (221 U/L). Since the liver is the major site for the metabolic enzymatic transformation of DEN molecule, it has been established that the unbearable production of free radicals and toxic reactive oxygen species (ROS) in hepatic cells could be the reason for oxidative stress, which ultimately leads to liver damage [19]. The disease condition pathological changes during the progression of tumors and its inhibition by chemopreventive agents are supposed to be revealed in the biochemical analysis and histopathological studies of the host tumor residing system. Even though there are so many macromolecules, most of the enzymes would leak from the damaged organ tissues, and enzymes are discharged into the body fluids depending on their tissue specificity and catalytic activity. Thus, the study of marker enzymes in serum and tissues is more important in the evaluation of respective tissue damage. Usually, the serum enzymes including transaminases (AST and ALT), LDH, ALP, and GGT denote the phase and function of the liver. Among other enzymes, transaminase elevation is considered to be the most susceptible marker in the examination of hepatocellular damage and loss of membrane functional integrity [20]. Since ALT is considered a promising serum marker, the level of ALT in serum is directly related to the high risk of HCC progression in hosts with chronic hepatitis [21].

LDH is one of the cytosolic enzymes that boost up the reversible oxidation of L-lactate substrate into pyruvate product. Increased LDH activity in serum shows the impairment of hepatic tissues and cellular leakage. The amount of LDH strongly corresponds to the size of the tumor, as the rate of glycolysis takes place in cancerous conditions, which is the only energy source pathway for the tumor cells [22]. ALP is another important liver marker enzyme whose elevated levels in serum indicate diseased conditions and alterations in bile flow. It is established from many studies, that the fast-dividing cells discarded a high amount of ALP as they resided in the bile canalicular plasma membrane [23].

GGT is also considered to be an important marker of liver cancer. It is present on the exterior membrane of the liver cells. An increase in its level leads to cholestasis and bile duct necrosis [24]. Generally, the cellular glutathione homeostasis maintained by GGT and its concentration is often raised in malignancy [25]. If necrosis takes place within the tumor organ or from a nearby invaded non-tumor tissue or leakage from tumor cells, it may lead to such drastic raise of enzymes in the serum [26].

In the present study, the serum pathological enzymes were found to have increased significantly in the SeNPs-treated group which showed the effective anticancer properties of selenium nanoparticles. The proper mechanism behind the anticancer properties of nanoparticles is not well established even though the observed results revealed the anticancer properties of SeNPs against DEN-induced HCC in Swiss Wistar rats.

3.8.2. Enzymic antioxidants

From the results, it was observed that the DEN-induced rats treated with SeNPs showed an increase in the serum enzymic antioxidant level: catalase (CAT) from 18.89 to 50.02 U/L, superoxide dismutase (SOD) from 1.4 to 6.9 U/L, glutathione S-transferase (GST) from 1.77 to 15.6 U/L, glutathione peroxidase (GPx) from 5.79 to 24.79 U/L, and glutathione reductase (GR) from 3.89 to 16.58 U/L. Whereas in AgNPs treated group 3 rats, comparatively increased enzyme activity has shown: CAT from 18.89 to 45.27 U/L, SOD from 1.4 to 6.55 U/L, GST from 1.77 to 13.16 U/L, GPx from 5.79 to 20.05 U/L, and GR from 3.89 to 15.28 U/L.

PdNPs treated group 5 rats doesn't show good results as compared to SeNPs and AgNPs treated groups. While there was an increase in the enzymic antioxidant level: CAT from 18.89 to 23.35 U/L, SOD from 1.4 to 5.45U/L, GST from 1.77 to 10.05 U/L, GPx from 5.79 to 19.1 U/L, and GR from 3.89 to 12.5 U/L,

there was no considerable difference between the DEN-induced group 2 and PdNPs treated group 5 rats.

The antioxidant enzyme activities of the experimental rat groups did not exhibit any significant variation between the control and plant extract-treated rats. DEN-induced group 2 rats showed a reduction in antioxidant activities of all the enzymes as compared to the group 1 control.

Serums from the experimental animal were analyzed for their antioxidant levels in the blood. Serum enzymic antioxidants which exist in biological systems, chiefly include SOD, a type of enzymic antioxidant that breaks down the toxic superoxide anion into oxygen and hydrogen peroxide by catalyzing the reaction [27,28]; CAT, a type of antioxidant enzyme that switches hydrogen peroxide to water and oxygen using either an iron or manganese as a co-factor [29,30]; and GPx, an enzyme containing four selenium-cofactors that facilitates the conversion of hydrogen peroxide and organic hydroperoxides.

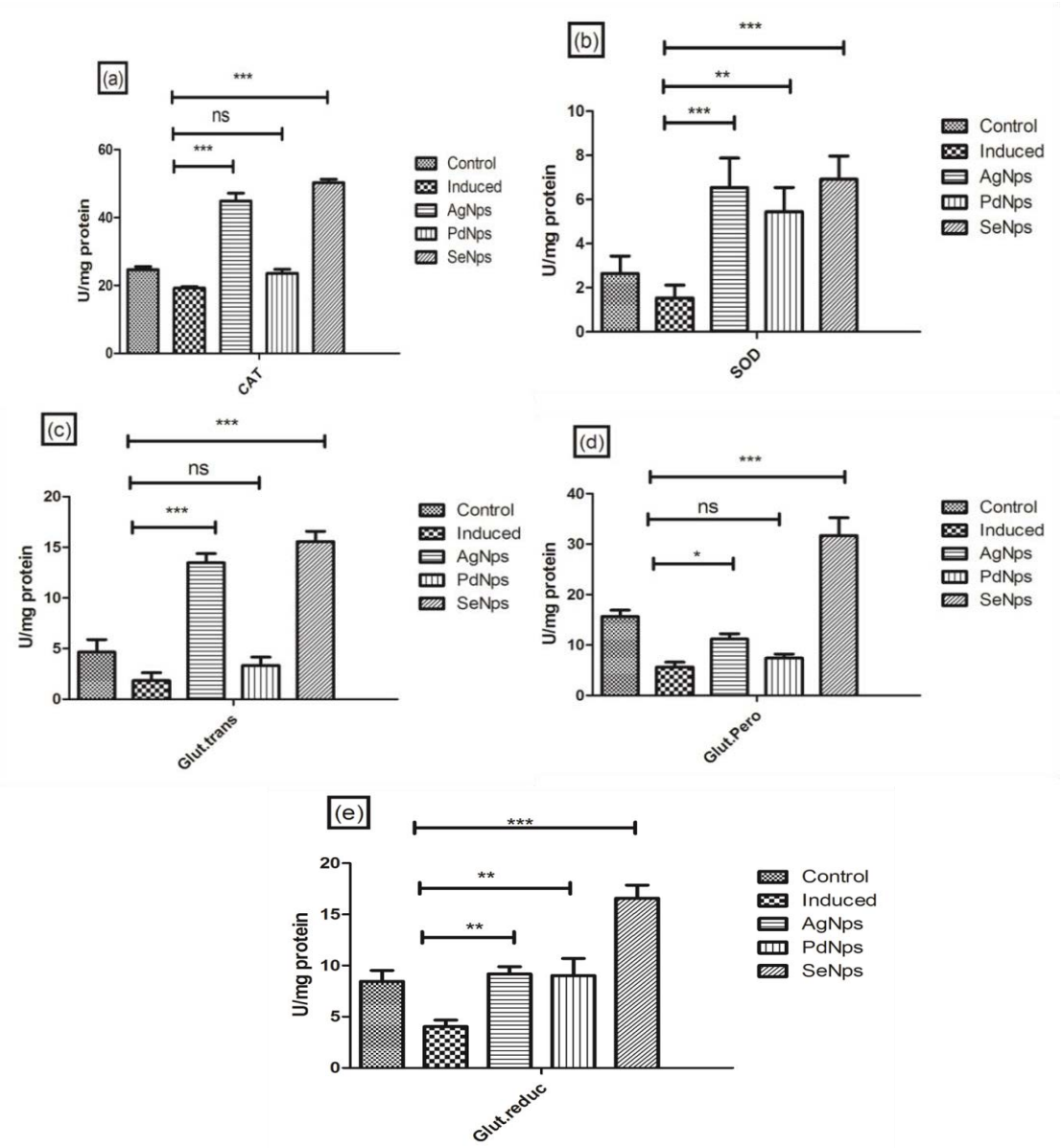

Figure 10. Effect of green synthesized metallic nanoparticles on enzymic antioxidants (a) catalase, (b) superoxide dismutase, (c) glutathione S-transferase, (d) glutathione peroxidase, and (e) glutathione reductase. Results were expressed as mean ± standard deviation (SD, n = 5). The significance when compared with the DEN-induced group of rats was shown as ns (not significant), * ($P < 0.05$),** ($P < 0.01$), and *** ($P < 0.005$).

Figure 10 reveals the effect of green synthesized metallic nanoparticles on enzymic antioxidants such as CAT, SOD, GST, GPx, and GR. Biochemical assay of SOD, CAT, and GPx is a usual step in determining the oxidative stress in a cell and the antioxidative properties of plant extracts [31]. These enzymes are estimated quantitatively to find out the progression of the tumor, the antitumor properties of herbal extracts and their derivatives, cytotoxic effect of toxic chemicals, plant extracts, and nanoparticles [32].

SOD transforms O^{2-} into oxygen and H_2O_2, but with the presence of GPx and CAT, H_2O_2 is transformed into water. In this manner, the enzymic antioxidants help to convert the cytotoxic substance in the body into harmless products [33]. These enzymic antioxidants naturally exist in the healthy body, which, however, turn downs in the case of cancer. The current results showed a significant decline in antioxidant enzyme activity (SOD, CAT, and GPx) in DEN-induced rats as compared to the control rats. However, the SeNPs treated rats showed appreciably increased levels of enzymic antioxidants to near normal. Significant reduction in the development of liver cancer progression in SeNPs oral-administered rats is proved by the reduced tumor markers and antioxidant enzyme levels. Most of the studies showed that patients who underwent chemotherapy and mastectomy for liver cancer had a drastic decrease in antioxidant levels. Hence, it is concluded that the chemotherapeutic agents generate superoxide and hydroxyl radicals during treatment which causes side effects [34-37]. The present study shows that AgNPs could be a good antioxidant supplement, chemopreventive agent, and anticancer agent which could be either due to the triggering of GPx or its highly enhanced permeability and retention (EPR) effect in the liver cancer tissue.

3.8.3. Non-enzymic antioxidant analysis

Figure 11 shows the effect of metallic nanoparticles on non-enzymic antioxidants such as vitamins A, E, and C. Non-enzymic antioxidants assay of vitamins A, E, and C provides protection mechanisms through GSH by GPx, along with vitamin A acting as a co-substrate to detoxify H_2O_2 and to make the free radicals harmless. The non-enzymic antioxidant activity changes of control and experimental rat groups have shown in **Figure 11**. GSH and vitamin A, the potent intracellular antioxidants, defend the cells from ROS damage [38]. Vitamin A is a type of fat-soluble vitamin, which is very important for the growth, maintenance, and duplication of epithelial cells. Vitamin A splits the lipid peroxide (LPO) chain in the cell membrane and prevents its formation. Vitamin A is a great toxic free radical scavenger (O^{-}) and a chain-breaking antioxidant. Among all the other functions, the most important function of Vitamin A is free radical scavenging, which protects the cells from oxidative damage [39]. Raghavan & Kumari studied that *Terminalia arjuna* EtOH extract on alloxan-induced diabetic rats showed a significant increase in SOD, CAT, GPx, GST, GR, GSH, vitamin A, vitamin C, and vitamin E [40]. Gurunagarajan & Pemaiah also established a gradual elevation in vitamin A level, when mice were treated with *Leonotis nepetifolia* EtOH crude extract against EAC cells [41]. When berberine type of an isoquinoline alkaloid is administered against 7,12-dimethylbenz(a)anthracene-induced skin carcinogenesis, it significantly boosted the activities of enzymatic antioxidants as well as nonenzymatic antioxidants including SOD, CAT, GPx, GSH, and vitamin A by which free radicals and lipid peroxidation were reduced [41]. *Ammannia baccifera* significantly reduced the rate of LPO and increased the behavior of enzymic (SOD, CAT, GSH), non-enzymic (vitamins A and D) antioxidants in Dalton's lymphoma ascites (DLA) bearing Swiss albino mice [42]. A significant decrease in vitamins C and E and GSH in DLA-bearing mice could be due to the generation of scavenged free radicals and the products of lipid peroxidation caused by the tumor effect.

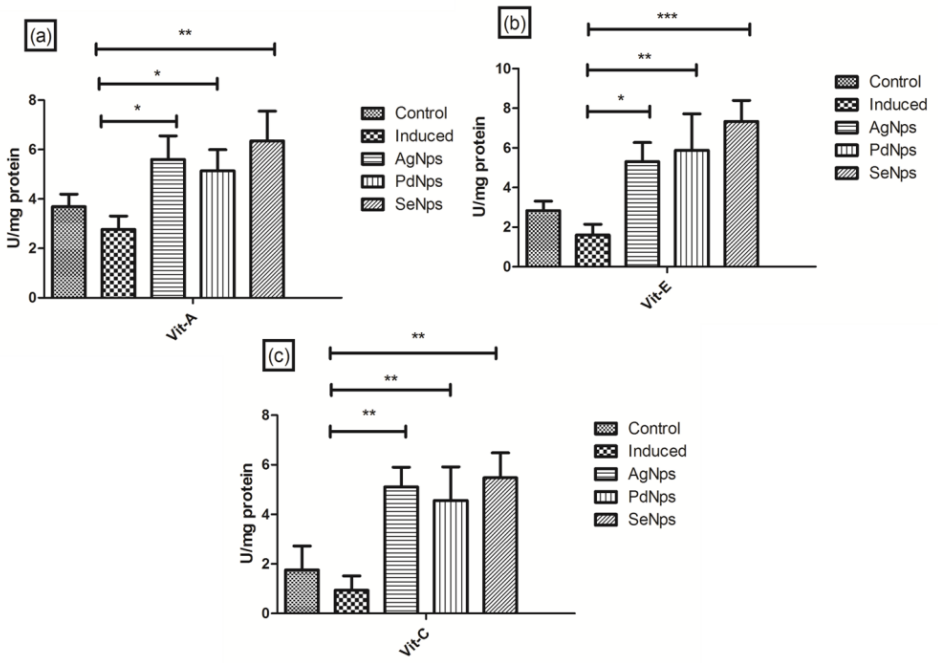

Figure 11. Effect of green synthesized metallic nanoparticles on non-enzymic antioxidants (a) vitamin A, (b) vitamin E, and (c) vitamin C. Results were expressed as mean ± standard deviation SD (n=6). The significance when compared with the DEN-induced group of rats was shown as * ($P < 0.05$),** ($P < 0.01$), and *** ($P < 0.005$).

Vitamin E protects the body from toxic free radicals, which otherwise leads to aging, a process in which oxygen and other free radicals break down the normal body's tissues. It helps to neutralize or scavenge the free radicals, which naturally exist as unstable molecules, hence saving our body from free radical damage by accepting/donating electrons from free radicals to balance themselves. When a saturated amount of vitamin E is present in the living body, unbalanced free toxic radicals accept their electrons from vitamin E molecules and leave the healthy molecules alone, causing comparatively less damage to the tissues [43]. Lower levels of vitamins E and C have been indicated in the DEN-induced rat serum when compared with the control rat, which is due to the high oxidative stress. Tumor growth might also have contributed to the low levels of vitamins E and C.

When oxidative stress is present, it has been found that ascorbic acid is in oxidized form in the body. The change in ascorbic acid level is directly proportional to the level of vitamin E, as a sufficient amount of ascorbic acid is required for the regeneration of vitamin E, an aqueous antioxidant that requires GSH [44]. Since vitamins C and E are synergistic antioxidants, the administration of plant extract and SeNPs significantly improved the vitamin E level in the liver of DEN-induced group 4 rats. The results obtained were found to be similar to a previous study [45], where the levels of non-enzymic antioxidants (vitamins A and E) were significantly enhanced in Swiss albino rats when treated with a protein fraction of *Cynodon dactylon* leaf. The GPx level was found to be decreased from 1 to 6.42 U/mg of protein in DEN-induced rats as compared to the other groups. Nami-A [Imidazoliumtrans-tetrachloro(dimethylsulfoxide)imidazoleruthenium(III)]-loaded NPs demonstrated the greater antitumor effect by inhibiting metastatic tumor growth in T739 mice, both *in-vitro* and *in-vivo* [46].

Vitamin C retains natural antioxidant defense, helping out to inhibit LPO production. Since vitamin C is an electron donor, otherwise called a reducing agent and antioxidant, it prevents other substances from getting oxidized [12]. Vitamin C is an exceptional hydrophilic antioxidant, and it voluntarily scavenges ROS and peroxyl radicals [47]. It also acts as a co-antioxidant, by regenerating vitamins A and E, and GSH from free radicals. It was observed that a decreased level of vitamin C is present in the liver of DEN-bearing rats.

This decreased level could be caused by the increased utilization of vitamin C in deactivating the increased level of ROS or to decrease the GSH level [48]. The administration of AgNPs improved the level of vitamin C in the liver of DEN-induced rats, which is expected to increase the GSH level or trigger the system to recycle the dehydro-ascorbic acid back to ascorbic acid. The level of non-enzymic antioxidant status declined in liver cancer-bearing animals [49], and the present study also correlates with the existing results. It might be due to the overutilization of these antioxidants to scavenge toxic free radicals. The simultaneous administration of SeNPs reversed the changes induced by DEN carcinogen exposure to near normal, and these data support the hypothesis that SeNPs are effective chemopreventive agents.

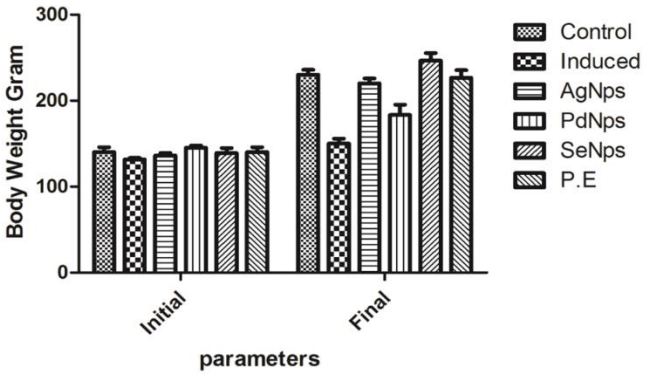

Figure 12. Effect of metallic nanoparticles on body weight of experimental rats. Results of all the groups were expressed as mean ± standard error of the mean (SEM; n = 6), where the $P < 0.005$.

Figure 12 reveals the effect of metallic nanoparticles on the body weight of experimental rats. The anticancer efficacy of green synthesized metal nanoparticles against DEN-induced HCC was studied in male Wistar albino rats. **Figure 12** showed the changes in body weight, before and after treatment, for controlled and experimental rats. The initial rats' body weight of 190 g increased gradually up to 230 g in all the experimental groups. During treatment, the body weight of the experimental groups decreased step by step with visible hair loss on the skin which might be due to the impairment of hepatic cells accordingly with chemical induction of DEN, whereas the control group rats remained the same weight. At the final stage of the experiment, the body weight of control group 1 rats (250 g) did not show any weight loss, but the weight of DEN-induced group 2 rats drastically decreased to 180 g. As compared to the group 2 rats, the AgNPs-treated group 3 rats showed relatively improved body weight (200 g). However, no significant changes in body weight were observed in the palladium nanoparticles treated group 5 rats, which showed almost the same weight as group 2 rats, and decreased when compared to group 3 rats. HCC is a highly malignant cancer that has high morbidity and mortality rate and a poor prognosis. It is highly resistant to chemotherapeutic agents [50], and is associated with distinct symptoms of weight loss and tissue wasting [51]. A quick loss in body weight can be observed in HCC-bearing animals.

4. Conclusion

The present investigation reveals that the biosynthesis of silver nanoparticles was achieved with an aqueous extract of leaves from the *Clerodendron phlomoides* plant. The size and shape of the biosynthesized silver nanoparticle range from 25 to 100 nm, and are spherical for the potential to interact with the cancerous cell in the liver of Wister rats. During the biosynthesis process, the secondary metabolites reduce the silver nitrate solution to silver nanoparticles and coat the nanoparticles with secondary metabolites of the plant extract into a potential drug delivery vehicle to cancer cells. The XRD investigation of the AgNPs confirmed the nanoparticles are crystalline and the DLS studies revealed that the size of the AgNPs varies

from 50 to 100 nm. Due to the aggregation of nanoparticles, the size of the aggregates shows higher and particles are stable in negative potential. The anticancer potential of AgNPs was evaluated in DEN-induced liver cancer in Wister Rats, where the biochemical studies of the anticancer potential via enzymatic analysis and anti-oxidants were carried out. Additionally, AgNPs have a considerable chemoprevention potential when compared with other metallic nanoparticles. In summary, the biosynthetic process of AgNPs is an eco-friendly process for metallic nanoparticle synthesis and a good drug delivery vehicle for the treatment of liver cancer.

Disclosure statement

The authors declare no conflict of interest.

References

[1] Kiernan F, 1833, XXIX. The Anatomy and Physiology of the Liver. Philos Trans R Soc, 123: 711–770.

[2] Nelson DR, 2009, The Cytochrome P450 Homepage. Hum Genomics, 4(1): 59.

[3] Liu CY, Chen KF, Chen PJ, 2015, Treatment of Liver Cancer. Cold Spring Harb Prespect Med, 5(9): a021535.

[4] Rajeshkumar S, 2016, Anticancer Activity of Eco-Friendly Gold Nanoparticles Against Lung and Liver Cancer Cells. J Genet Eng Biotechnol, 14(1): 195–202.

[5] Evans ER, Bugga P, Asthana V, et al, 2018, Metallic Nanoparticles for Cancer Immunotherapy. Mater Today, 21(6): 673–685.

[6] Desai N, Momin M, Khan T, et al, 2021, Metallic Nanoparticles as Drug Delivery System for the Treatment of Cancer. Expert Opin Drug Deliv, 18(9): 1261–1290.

[7] Sharma A, Goyal AK, Rath G, 2018, Recent Advances in Metal Nanoparticles in Cancer Therapy. J Drug Target, 26(8): 617–632.

[8] Ravindran A, Chandran P, Khan SS, 2013, Biofunctionalized Silver Nanoparticles: Advances and Prospects. Colloids Surf B Biointerfaces, 105: 342–352.

[9] Rai M, Yadav A, Gade A, 2009, Silver Nanoparticles as a New Generation of Antimicrobials. Biotechnol Adv, 27(1): 76–83.

[10] Rai M, Kon K, Ingle A, et al, 2014, Broad-Spectrum Bioactivities of Silver Nanoparticles: the Emerging Trends and Future Prospects. Appl Microbiol Biotechnol, 98(5): 1951–1961.

[11] Durán N, Durán M, De Jesus MB, et al, 2016, Silver Nanoparticles: a New View on Mechanistic Aspects on Antimicrobial Activity. Nanomedicine, 12(3): 789–799.

[12] Wei L, Lu J, Xu H, et al, 2015, Silver Nanoparticles: Synthesis, Properties, and Therapeutic Applications. Drug Discov Today, 20(5): 595–601.

[13] Hembram KC, Kumar R, Kandha L, et al, 2018, Therapeutic Prospective of Plant-Induced Silver Nanoparticles: Application as Antimicrobial and Anticancer Agent. Artif Cells Nanomed Biotechnol, 46(sup3): S38–S51.

[14] Saratale RG, Shin HS, Kumar G, et al, 2018, Exploiting Antidiabetic Activity of Silver Nanoparticles Synthesized Using *Punica Granatum* Leaves and Anticancer Potential Against Human Liver Cancer Cells (Hepg2). Artif Cells Nanomed Biotechnol, 46(1): 211–222.

[15] Srikar SK, Giri DD, Pal DB, et al, 2016, Green Synthesis of Silver Nanoparticles: A Review. Green Sustain Chem, 6(1): 34–56.

[16] Sriranjani R, Srinithya B, Vellingiri V, et al, 2016, Silver Nanoparticle Synthesis Using *Clerodendrum Phlomidis* Leaf Extract and Preliminary Investigation of its Antioxidant and Anticancer Activities. J Mol Liq, 220: 926–930.

[17] Lakshmi V, Bai GVS, 2016, In Vitro Anticancer Activity of *Clerodendrum Phlomidis* Leaves and Its Silver Nanoparticles on Human Breast Cancer Cell Line (MCF-7). Asian J Innov Res, 1(2): 1–5.

[18] Khalil MM, Ismail EH, El-Baghdady KZ, et al, 2014, Green Synthesis of Silver Nanoparticles Using Olive Leaf Extract and Its Antibacterial Activity. Arab J Chem, 7(6): 1131–1139.

[19] Gey KF, 1993, Prospects For The Prevention of Free Radical Disease, Regarding Cancer and Cardiovascular Disease. Br Med Bull, 49: 679–699.

[20] Plaa GL, Hewitt WR, 1989, Principle and Methodology of Toxicology, 2nd ed., Raven Press, New York.

[21] Tarao K, Takemiya S, Tamai S, et al, 1997, Relationship Between the Recurrence of Hepatocellular Carcinoma (HCC) and Serum Alanine Aminotransferase Levels in Hepatectomized Patients with Hepatitis C Virus-Associated Cirrhosis and HCC. Cancer, 79(4): 688–694.

[22] Prasad SB, Giri A, 1999, Effect of Cisplatin on The Lactate Dehydrogenase Activity and Its Isozyme Pattern in Dalton's Lymphoma Bearing Mice. Cytologia, 64(3): 259–267.

[23] Frederiks WM, Van Noorden CJ, Aronson DC, et al, 1990, Quantitative Changes in Acid Phosphatase, Alkaline Phosphatase and 5'-Nucleotidase Activity in Rat Liver After Experimentally Induced Cholestasis. Liver, 10(3): 158–166.

[24] Bulle F, Mavier P, Zafrani ES, et al, 1990, Mechanism of Γ-Glutamyl Transpeptidase Release in Serum During Intrahepatic and Extrahepatic Cholestasis in The Rat: a Histochemical, Biochemical and Molecular Approach. Hepatology, 11(4): 545–550.

[25] Daubeuf SP, Leroy A, Paolicchi A, et al, 2002, Enhanced Resistance of HELA Cells to Cisplatin by Overexpression of Gamma-Glutamyl Transferase. Biochem Pharmacol, 64(2): 207–216.

[26] Schwartz MA, West M, Walsch WS, et al, 1962, Serum Enzymes in Disease. VIII. Glycolytic and Oxidative Enzymes and Transaminases in Patients With Gastrointestinal Carcinoma. Cancer, 15(2): 346–353.

[27] Bannister JV, Bannister WH, Rotilio G, 1987, Aspects of the Structure, Function, and Applications Of Superoxide Dismutase. CRC Crit Rev Biochem, 22(2): 111–180.

[28] Zelko IN, Mariani TJ, Folz RJ, 2002, Superoxide Dismutase Multigene Family: a Comparison of the CuZn-SOD (SOD1), Mn-SOD (SOD2), and EC-SOD (SOD3) Gene Structures, Evolution, and Expression. Free Radic Biol Med, 33(3): 337–349.

[29] Chelikani P, Fita I, Loewen PC, 2004, Diversity of Structures and Properties Among Catalases. Cell Mol Life Sci, 61(2): 192–208.

[30] Zámocký M, Koller F, 1999, Understanding the Structure and Function of Catalases: Clues from Molecular Evolution and in Vitromutagenesis. Prog Biophys Mol Biol, 72(1): 19–66.

[31] Siddiqui IA, Raisuddin S, Shukla Y, 2005, Protective Effects of Black Tea Extract on Testosterone Induced Oxidative Damage in Prostate. Cancer Lett, 227(2): 125–132

[32] Cragg GM, Grothaus PG, Newman DJ, 2009, Impact of Natural Products on Developing New Anticancer Agents. Chem Rev, 109(7): 3012–3043.

[33] Ray G, Husain SA, 2002, Oxidants, Antioxidants and Carcinogenesis. Indian J Exp Biol, 40(11): 1213–1232.

[34] Lipinski B, 2011, Hydroxyl Radical and Its Scavengers in Health and Disease. Oxid Med Cell

Longev, 2011:809696.

[35] Zou Z, Chang H, Li H, et al, 2017, Induction of Reactive Oxygen Species: an Emerging Approach for Cancer Therapy. Apoptosis, 22(11): 1321–1335.

[36] Tas F, Hansel H, Belce A, et al, 2005, Oxidative Stress in Breast Cancer. Med Oncol, 22(1): 11–15.

[37] Singh G, Maulik SK, Jaiswal A, et al, 2010, Effect on Antioxidant Levels in Patients of Breast Carcinoma During Neoadjuvant Chemotherapy and Mastectomy. Malays J Med Sci, 17(2): 24–28.

[38] Circu ML, Moyer MP, Harrison L, et al, 2009, Contribution of Glutathione Status to Oxidant Induced Mitochondrial DNA Damage in Colonic Epithelial Cells. Free Radic Biol Med, 47(8): 1190–1198.

[39] Raghavan B, Kumari SK, 2006, Effect of Terminalia Arjuna Stem Bark on Antioxidant Status in Liver and Kidney of Alloxan Diabetic Rats. Indian J Physiol Pharmacol, 50(2): 133–142.

[40] Gurunagarajan S, Pemaiah B, 2010, Anti-Tumor and Antioxidant Potentials of Ethanolic Extract of *Leonotis Nepetefolia R.Br.* Against Ehrlich Ascites Carcinoma Cell Lines. J Pharm Res, 3(12): 2990–2992.

[41] Manoharan S, Vasanthaselvan M, Silvan S, et al, 2010, Carnosic Acid: a Potent Chemopreventive Agent Against Oral Carcinogenesis. Chem Biol Interact, 188(3): 616–622.

[42] Loganayaki N, Manian S, 2012, Antitumor Activity of the Methanolic Extract of *Ammannia Baccifera L.* Against Dalton's Ascites Lymphoma Induced Ascitic and Solid Tumors in Mice. J Ethnopharmacology, 142(1): 305–309.

[43] Traber MG, Atkinson J, 2007, Vitamin E, Antioxidant And Nothing More. Free Radic Biol Med, 43(1): 4–15.

[44] Sies H, Stahl W, 1995, Vitamins E and C, Beta-Carotene, and Other Carotenoids as Antioxidants. Am J Clin Nutr, 62(6 Suppl): 1315S–1321S.

[45] Ashokkumar K, Selvaraj K, Muthukrishnan SD, 2013, *Cynodon Dactylon* (L.) Pers.: an Updated Review of Its Phytochemistry and Pharmacology. J Med Plants Res, 7(48): 3477–3483.

[46] Chiniadis L, Giastas P, Bratsos I, et al, 2021, Insights into the Protein Ruthenation Mechanism by Antimetastatic Metallodrugs: High-Resolution X-Ray Structures of the Adduct Formed between Hen Egg-White Lysozyme and NAMI-A at Various Time Points. Inorg Chem, 60(14): 10729–10737.

[47] Packer L, Tritschler HJ, Wessel K, 1997, Neuroprotection by the Metabolic Antioxidant Alpha-Lipoic Acid. Free Radic Biol Med, 22(1-2): 359–378.

[48] Chatterjee IB, Nandi A, 1991, Ascorbic Acid: a Scavenger of Oxyradicals. Indian J Biochem Biophys, 28(4): 233–236.

[49] Thirunavukkarasu C, Prince Vijeya Singh J, Thangavel M, et al, 2002, Dietary Influence of Selenium on the Incidence of N-Nitrosodiethylamine-Induced Hepatoma with Reference to Drug and Glutathione Metabolizing Enzymes. Cell Biochem Function, 20(4): 347–356.

[50] Alsowmely AM, Hodgson HJF, 2002, Non-Surgical Treatment of Hepatocellular Carcinoma. Aliment Pharmacol Ther, 16(1): 1–15.

[51] Suriawinata AA, Thung SN, 2002, Malignant Liver Tumors. Clin Liver Dis, 6(2): 527–554.

Proceedings of Anticancer Research, 2023, Volume 7, Issue 4
http://ojs.bbwpublisher.com/index.php/PAR
ISSN Online: 2208-3553
ISSN Print: 2208-3545

Successful Treatment of White Lung in Elderly Patients with COVID-19

Chao Fang, Nuan Xiao*, Shengnan Huang, Jiannan Wu, Lili Tan, Hongmei Zhao

Department of Geriatrics/Special Needs Ward, Affiliated Hospital of Hebei University, Baoding 071000, China

***Corresponding author:** Nuan Xiao, 2314528820@qq.com

Abstract: Novel coronavirus (SARS-CoV-2, hereby known as COVID-19) has the characteristics of rapid variation and multiple variants, which has caused a huge impact on human health worldwide. At the end of 2022, the Omicron variant was widely spread in China, and the patients infected with COVID-19 were mainly concentrated in the elderly over 80 years old and people with serious basic diseases. Pathologically, diffuse lung injury can be seen in the advanced stage of severe and critical diseases, with a large number of inflammatory cells and fibrous mucus exudation, alveolar epithelial cells shedding and necrosis, severe pulmonary edema, hyaline membrane formation, and diffuse ground-glass shadow or consolidation on imaging, which is manifested as "white lung" [1], and its mortality rate has significantly increased. This study reported two cases of elderly patients admitted to the Affiliated Hospital of Hebei University for the treatment of COVID-19.

Keywords: Advanced age; COVID-19; White lung; Treatment; Experience

Online publication: July 11, 2023

1. Case reports

1.1. Case 1

Zhang XX, female, 87 years old, had a chief complaint of coughing, wheezing, and discomfort for 7 days. Her past medical history showed that she had chronic bronchitis and a history of right artificial knee resurfacing. Seven days before admission, she coughed and wheezed. She had a chest CT scan at a local hospital, which showed that there were infectious lesions and interstitial lesions in both lungs. She was treated with doxofylline, cefoperazone/sulbactam, ambroxol, and other drugs, but the symptoms were not relieved, so she came to the Department of Infectious Diseases of our hospital for further diagnosis and treatment. The COVID-19 nucleic acid test showed negative on admission. Lung auscultation showed coarse breath sounds in both lungs and scattered moist rales, but no wheeze. Diagnosis of lung infection, chronic bronchitis, right artificial knee resurfacing, abnormal liver function, and hypoproteinemia was recorded.

The following are the extracts from her progress notes:

(1) December 22, 2022: The patient coughed and wheezed; under the condition of oxygen inhalation 2 L/min, blood gas: partial pressure of oxygen (PO_2) 69 mmHg, partial pressure of carbon dioxide (PCO_2) 29 mmHg; blood routine: white blood cell count (WBC) 13.72×10^9/L, neutrophil % (N%) 81.6%, lymphocyte % (L%) 10.9%, C-reactive protein count (CRP) 11.08 mg/L, serum amyloid A (SAA) 110.0 mg/L. Azvudine was given for antiviral function, ambroxol + eucalyptus and limonene for reducing phlegm, prophylline for asthma, ceftazidime for anti-infection, nebulized inhalation of

salbutamol sulfate and budesonide, as well as the intermittent prone position, was encouraged for oxygen concentration increase.

(2) December 23, 2022: Due to her critical condition in addition to coughing and wheezing, the oxygenation index ratio of arterial oxygen partial pressure to fractional inspired oxygen (PaO_2/FiO_2 ratio) 237%, the patient was changed to nasal high-flow oxygen inhalation 40 L/min, fractional inspired oxygen (FiO_2) 60%. An injection of Chinese medicine Xuebijing for antagonizing endotoxin *in vitro* and methylprednisolone for anti-inflammatory were given.

(3) December 24, 2022: Considering that COVID-19 can cause hypercoagulation, and the patient had low O_2 and CO_2, pulmonary embolism was not excluded, and low molecular weight heparin calcium was added for anticoagulation; meanwhile, oral probiotics and whole protein enteral nutrition (EN) powder were given.

(4) December 25, 2022: Under the conditions of high flow oxygen inhalation 40 L/min, FiO_2 60%, blood gas analysis PO_2 84 mmHg, PCO_2 34 mmHg.

(5) December 26, 2022: Blood gas analysis PO_2 131 mmHg, PCO_2 35 mmHg, gradually adjusted the high flow parameters according to the oxygenation situation, adjusted to 30 L/min, under the condition of FiO_2 40%, finger pulse oxygen can reach more than 96%.

(6) December 27, 2022: Continued to reduce the high-flow parameters, and gradually transition to nasal cannula oxygen inhalation at 2 L/min, finger pulse oxygen can reach more than 95%. Chest CT scan showed infectious lesions in both lungs (see **Figure 1a**), and blood gas analysis the next morning showed PO_2 90 mmHg and PCO_2 36 mmHg.

(7) December 29, 2022: Blood routine WBC 9.84×10^9/L, N% 74.5%, L% 13.9%, CRP 1.51 mg/L, SAA 6.8 mg/L, infection index improved significantly, albumin was as low as 26 g/L, hence albumin was given 10 g intravenous infusion, four times a day, for 6 days.

(8) December 31, 2022: Under the condition of nasal cannula oxygen inhalation at 2 L/min, blood gas analysis showed PO_2 113 mmHg and PCO_2 39 mmHg.

(9) January 1, 2023: Re-examination of chest CT scan showed the density of bilateral lung lesions is higher than before (see **Figure 1b**). Considering that imaging studies have entered the consolidation stage, thymosin enteric-coated tablets are added to improve immunity. The patient has an obvious cough, and Suhuang Zhike Capsules are added.

(10) January 5, 2023: Nasal cannula oxygen inhalation 2 L/min, blood gas analysis PO_2 76 mmHg, PCO_2 42 mmHg.

(11) January 7, 2023: Chest CT re-examination showed the lesions in the lower lobes of both lungs are slightly absorbed (see **Figure 1c**).

(12) From January 9 to 11, 2023: Under the condition of nasal cannula oxygen inhalation 2 L/min, finger pulse oxygen fluctuation was 96%–100%.

(13) January 11, 2023: The patient is discharged from the hospital.

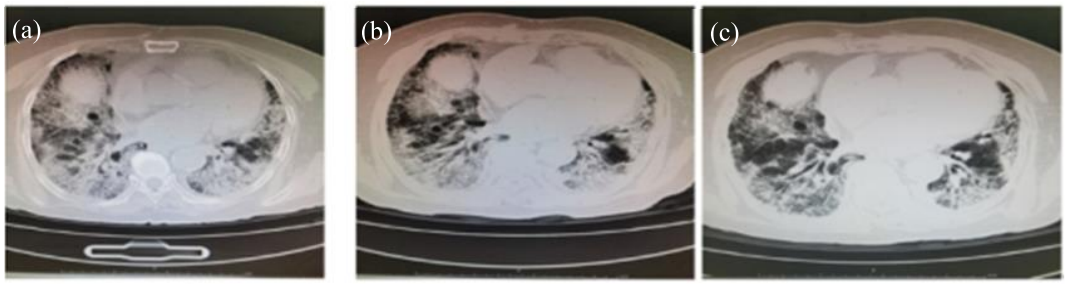

Figure 1. Chest CT scans of the patient in Case 1. (a) Scan on December 27, 2022; (b) Scan on January 1, 2023; (c) Scan on January 7, 2023

1.2. Case 2

Sun XX, male, 89 years old, was admitted to the hospital mainly due to cough, choking, and fever for 8 days. His past medical history consisted of coronary heart disease, coronary stent implantation, and prostatic hyperplasia. The patient developed a cough, suffocation, and fever 8 days before admission, with a body temperature of 38.5°C and coughed white sticky sputum. A chest CT scan was performed in a local hospital 1 day before admission, and showed that there were multiple ground-glass changes in both lungs, and interstitial inflammation was considered. He came to our hospital for further diagnosis and treatment.

The following are the extracts from her progress notes:

(1) December 16, 2022: The patient coughed and suffocated. Under the condition of oxygen inhalation 2 L/min, the blood gas PO_2 57 mmHg, PCO_2 32 mmHg, the comprehensive assessment considers that the patient has severe pneumonia; timely application of nasal high-flow oxygen inhalation 40 L/min, FiO_2 60%; blood routine: WBC 2.2×10^9/L, N% 74.5%, L% 17.3%, CRP 72.6 mg/L, SAA 251.8 mg/L. Bromhexine was given to reduce phlegm, nebulized inhalation of salbutamol sulfate and budesonide, as well as the intermittent prone position, was encouraged to improve oxygenation, oral azvudine for antiviral, low molecular weight heparin calcium as anticoagulant, bicyclol for liver protection as the patient had a poor liver function.

(2) December 18, 2022: High flow as before, blood gas PO_2 43 mmHg, PCO_2 32 mmHg, adjusted high flow to 40 L/min, FiO_2 70%; blood routine: WBC 7.36×10^9/L, N% 88%, L% 6.9%, CRP 97.52 mg/L, SAA 584.1 mg/L. The index of infection was higher than before, and the chest CT scan showed two pneumonia lesions (see **Figure 2a**) leading to obvious wheezing, and the patient was critically ill. Considering that the patient was thin and poor in nutritional status with severe pneumonia, intravenous moxifloxacin was added for anti-infection and oral doxofylline for anti-asthma, in addition to whole protein EN powder nutritional support treatment.

(3) December 20, 2022: High flow as before; blood gas PO_2 88 mmHg, PCO_2 26 mmHg; blood routine: WBC 5.25×10^9/L, N% 83.3%, L% 10.7%, CRP 125 mg/L, SAA 702.2 mg/L. On the next day, the chest CT scan showed an increase in both pneumonia lesions, and a small amount of pleural effusion is found on the right side. Considering that the patient had severe pneumonia and the disease progressed, an intravenous infusion of 40 g methylprednisolone, four times a day for four days was given. The nutritional status was poor, the protein level was low, and lower extremity edema was observed, hence an intravenous infusion of 10 g albumin, four times a day for three days was given, followed by furosemide for diuresis.

(4) December 24, 2022: High flow as before; blood gas PO_2 72 mmHg, PCO_2 37 mmHg; blood routine: WBC 5.76×10^9/L, N% 83.3%, L% 7.5%, lymphocyte ratio progressively decreased, intravenous injection of 5 g human immunoglobulin, four times a day for seven days was given, and oral administration of thymosin enteric-coated tablets was applied.

(5) December 28, 2022: The chest CT scan showed slightly more inflammation in the basal segment of the left lower lobe compared to the scan on December 23, 2022. The patient's condition progressed, and Xuebijing traditional Chinese medicine is added for anti-inflammation, hormones are added again, and the prone position is continued to be encouraged.

(6) January 4, 2023: Re-examination of chest CT compared with December 28, 2022, the range of multiple inflammations in both lungs was slightly smaller than before, bilateral pleural effusion was slightly increased (see **Figure 2b**), blood gas improved to PO_2 80 mmHg and PCO_2 42 mmHg.

(7) January 11, 2023: The patient's condition fluctuated again, and the wheezing worsens. The high-flow oxygen inhalation through the nose is adjusted to 50 L/min, FiO_2 80%; a small amount of sphere-shaped and rod-shaped gram-negative bacteria, sphere-shaped gram-positive bacteria, fungal spores, and bacteria with hypha were found in the sputum smear; the chest CT scan showed a slight increase

in left apical inflammation, left pleural effusion, and a slight decrease in right pleural effusion as compared to the scan on January 4, 2023. Blood routine: WBC 7.31×10^9/L, N% 89.8%, L% 5.6%, CRP 140.56 mg/L, SAA 693.6 mg/L. The patient had viral pneumonia complicated with bacterial and fungal infections, hence piperacillin-tazobactam (total 15 d) and voriconazole (15 d) were given. Doxofylline (13 d), albumin (6 d), and furosemide (16 d) were re-applied.

(8) January 14, 2023: The patient's general condition was poor, with suffocation, sweating, constipation, and phlegm in the throat. After consultation with the Department of Traditional Chinese Medicine, a Chinese herbal decoction was given. Sputum culture included *Acinetobacter baumannii* complex +++. Due to the patient being critically ill and cannot leave the high-flow oxygen inhalation, a chest CT re-examination was not performed, and it was replaced by a bedside chest X-ray: infectious lesions in both lungs, a small amount of pleural effusion. Treatment of piperacillin-tazobactam combined with drug-sensitive antibiotic levofloxacin was given intravenously for 14 days.

(9) January 17, 2023: Sputum culture included *Acinetobacter baumannii* complex +.

(10) January 20, 2023: Under the conditions of nasal high-flow oxygen inhalation 50 L/min, FiO_2 80%, blood gas PO_2 147 mmHg, PCO_2 53 mmHg, oxygenation improved as compared to before, and the high-flow parameters are lowered in time: 40 L/min, FiO_2 70%; blood routine: WBC 8.23×10^9/L, N% 73%, L% 11.9%, CRP 61.05 mg/L, SAA 86.3mg/L; infection indicators improved.

(11) January 21, 2023: The sputum culture was normal, and the fungal spores and hyphae on the sputum smear were positive.

(12) January 25, 2023: The chest X-ray showed a smaller range and less density than the X-rays in both lungs from January 1 to January 17, 2023.

(13) January 26, 2023: Blood routine: WBC 8.28×10^9/L, N% 67.6%, L% 19.7%, CRP 28.24 mg/L; sputum smear showed a small amount of rod-shaped gram-negative bacteria, sphere-shaped gram-positive bacteria, fungal spores and hyphae, as well as normal sputum culture; pulse oxygen fluctuation above 95%, gradually reduced the high flow parameter to 30 L/min, FiO_2 40%, breathing gradually improved.

(14) January 28, 2023: Gradually changed to face mask oxygen inhalation 5 L/min, blood gas PO_2 69 mmHg, PCO_2 44 mmHg.

(15) January 29, 2023: Mask oxygen inhalation 5 L/min, blood gas PO_2 101 mmHg, PCO_2 49 mmHg.

(16) January 30, 2023: He got better and was discharged from the hospital.

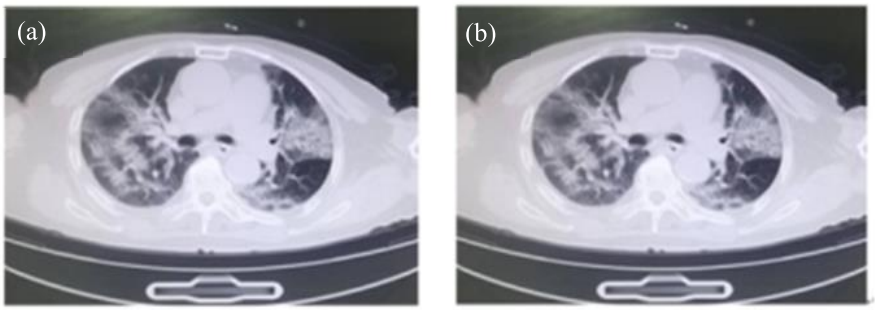

Figure 2. Chest CT scans of the patient in Case 2. (a) Scan on December 18, 2022; (b) Scan on January 4, 2023.

2. Treatment experience

2.1. Early application of antiviral drugs

Antiviral treatment is a key link, and the early and standardized use of antiviral drugs can significantly reduce the viral load in infected patients, reduce the body damage induced by high-load viruses, and especially reduce the hospitalization of groups with high-risk factors such as the elderly rate, severe disease rate and mortality rate [2].

2.1.1. Nematevir/ritonavir combination package (Paxlovid)

This drug acts on the main protease of COVID-19, inhibits the processing of protein precursors mediated by this enzyme, inhibits virus replication, reduces patients' disease progress from severe to mild or moderate, and greatly reduces the mortality rate [3]. It is suitable for infected adult patients with mild to moderate infection within 5 days of onset and with high-risk factors that may progress to severe disease. Due to its multiple interactions with many drugs, it is essential to carefully read the instructions before use.

2.1.2. Azvudine

Azvudine tablet is the first domestically produced oral small-molecule antiviral drug in China. It has the characteristics of a significant curative effect, strong accessibility, and is available for home use. People infected with COVID-19 should use it as soon as possible, with its best time of 5 days before the onset of infection symptoms, and recommended to be taken for ≤ 14 days. It is not recommended to stop the drug without a doctor's authorization if it is tolerable. Patients with mild hepatic and renal insufficiency should monitor liver and kidney function during the consumption of medication, and patients with moderate to severe hepatic and renal insufficiency should use it with caution. Azvudine is a P-glycoprotein (P-gp) substrate and a weak P-gp inducer [4], hence it is required to read the instructions carefully before use.

2.2. Importance of improvement in oxygenation

For COVID-19, patients with underlying diseases and elderly patients are likely to develop severe and critical conditions. If the patient's respiratory rate is ≥ 30 times/min, and the oxygen saturation is ≤ 93% at rest, this indicates that the clinical classification is severe [5]. Patients with PaO_2/FiO_2 < 300 mmHg should be given oxygen therapy immediately. For critically ill patients who receive nasal cannula and mask oxygen inhalation, if respiratory distress and/or hypoxemia do not improve in a short time (1–2 hours), nasal high-flow oxygen therapy (HFNC) or non-invasive ventilation (NIV) should be used.

2.2.1. Use of high flow rate

If it meets the diagnostic criteria for severe new coronary pneumonia [6], HFNC can be considered. For patients with type I respiratory failure, the recommended initial flow rate is 30–40 L/min. The acceptance rate should be adjusted to the highest flow rate that can be tolerated, and the blood oxygen saturation (SpO_2) is maintained at 92%~96%. For patients with type II respiratory failure, the recommended initial flow rate is 20–30 L/min. If the patient has significant PCO_2 retention, it can be increased to 45–55 L/min to the highest flow rate that the patient can tolerate and maintain SpO_2 at 88%~92% [5].

2.2.2. Prone position ventilation

Prone position ventilation is currently one of the most effective adjuvant treatments. Early prone position mechanical ventilation can improve clinical efficacy and significantly reduce mortality in patients with severe acute respiratory distress syndrome (ARDS). It has high application value and is worthy of promotion [7]. Moderate, severe, and critical cases with a high risk of severe disease and rapid disease progression should be treated in the prone position, and it is recommended not less than 12 hours a day [8]. However, it is unacceptable for many frail elderly people. Therefore, individualized body positions are formulated for different patients to ensure both patient tolerance and blood oxygen improvement.

2.3. Precaution to combined bacterial, fungal, and atypical pathogenic bacteria infections

Studies have shown that the abundance of bacteria in throat swabs of patients infected with COVID-19 increased significantly, and these bacteria can stimulate the expression of COVID-19 ACE2 receptor to

promote virus infection, suggesting that the pharyngeal bacteria of patients with new coronary pneumonia play a role in COVID-19 infection. COVID-19 infection is involved in the interaction between the virus and the host [9]. Due to the decline of immunity after the COVID-19 infection, it is necessary to be vigilant against the combination of mycoplasma, chlamydia, influenza A, influenza B, and other pathogen infections, the resurgence of tuberculosis, and fungal infections. As the patients are elderly and critically ill, their clinical manifestations are often atypical. Therefore, it is essential to closely monitor infection indicators, sputum etiology, and chest imaging for viral pneumonia.

2.4. Traditional Chinese medicine treatment

Traditional Chinese medicine (TCM) has played a unique advantage in the treatment of COVID-19. Several studies have shown that heat-clearing and detoxifying TCM treatments have clear clinical effects in anti-COVID-19, especially in clinical aspects such as anti-infection, fever reduction, shortening hospital stay, and improving curative effect [10-14]. On the one hand, it helps the body to quickly clear the virus and improve the state of immunosuppression. On the other, it also regulates the balance of the immune system, prevents the occurrence of cytokine storms and the potential damage of the body's immune system to normal cells, and reduces the mortality rate [15].

2.5. Immunotherapy

Experience in the treatment of severe acute respiratory syndrome (SARS) and Middle East respiratory syndrome (MERS) has shown that high viral titers and subsequent strong inflammatory and chemokine responses are associated with high morbidity and mortality during coronavirus infection. Reducing the viral load through early intervention and controlling the inflammatory response through immunomodulators are effective measures to improve the prognosis of patients [16,17].

Intravenous immune globulin (IVIG) can block Fc receptors, reduce cytokine storm [18], and can be used to enhance the immunity of severe and critically ill patients. A meta-analysis showed that IVIG has a good clinical effect on critically ill patients with the new coronavirus pneumonia [19]. The clinical efficacy of IVIG may be positively correlated with the severity of COVID-19.

Tocilizumab (TCZ) can prevent the binding of IL-6 to its receptor and exert the immunosuppressive effect promoted by IL-6. Michot et al reported a 42-year-old man with respiratory failure due to COVID-19 infection [20]. After 4 days of TCZ treatment, CRP decreased from 225 mg/L to 33 mg/L and he finally recovered completely clinically. Likewise, some case reports have shown that TCZ is an effective and safe approach for the treatment of COVID-19 [21-23].

Thymus preparations can induce the production of macrophages, interferon, interleukin, and other factors, thereby improving the suppressed immune function of the body, and can affect peripheral immune organs to enhance immunity. Fang et al used the thymus method as a neoadjuvant therapy for elderly patients with severe pneumonia, and the results showed that the thymus method can increase the proportion of CD4 and T lymphocyte subsets *in vivo* [24]. Commonly used thymus preparations are thymosin, thymofaxin, and so on.

2.6. Glucocorticoids

The “double-edged sword” effect of glucocorticoids should be fully utilized. For severe and critical cases with progressive deterioration of oxygenation indicators, rapid disease progression shown in imaging, and excessive activation of the body's inflammatory response, glucocorticoids should be used appropriately, and it is recommended not to exceed 10 days. Commonly used glucocorticoids included dexamethasone 5 mg/d or methylprednisolone 40 mg/d, where large doses and long-term use of glucocorticoids are avoided in order to reduce the occurrence of side effects [8].

2.7. Nutritional support

Before patients receive any nutritional support, hypovolemia and water, electrolyte, and acid-base imbalances should be corrected first. According to age, nutritional risk, oral intake, whether accompanied by heart, lung, kidney diseases, etc., the appropriate nutritional support route, energy, and nutritional components are chosen, and an individualized nutritional support plan is then formulated. In the process of nutritional support, the functional status of important organs and the effect of nutritional support should be addressed, and the nutritional plan should be evaluated and adjusted promptly. Enteral nutrition is the first choice for elderly patients with normal gastrointestinal function, and parenteral nutrition should be considered only when the intestines cannot tolerate enteral nutrition, or when enteral nutrition is far from enough for the body's needs [25,26].

2.8. Anticoagulant therapy

Like most patients with severe infection accompanied by disseminated intravascular coagulation, some patients with severe COVID-19 have abnormal coagulation function, manifested by a significant increase in D-dimer and fibrinogen degradation products [28]. Unfractionated or low-molecular-weight heparin can be given to moderate cases with high-risk factors for severe disease and rapid disease progression, as well as severe and critical cases without contraindications.

2.9. Care of functions of other important organs and maintaining the internal environment

People infected with COVID-19 are often accompanied by water and electrolyte disorders, protein and energy imbalances, which all cannot be ignored. Some patients with COVID-19 infection may have elevated liver enzymes, muscle enzymes, lactate dehydrogenase, myoglobin, troponin, ferritin, and other indicators [8]. Therefore, it is necessary to closely monitor the biochemical indicators of patients and intervene in time.

3. Conclusion

For patients with severe or critical pneumonia, especially for high-risk elderly people, strengthening monitoring of vital signs, giving effective oxygen inhalation methods promptly, improving oxygenation, and strengthening airway management are the initial steps, followed by early application of antiviral drugs, as well as close monitoring of blood infection indicators, sputum etiology detection, and chest CT to guard against concurrent bacterial, fungal, and other viral infections. Reasonable anticoagulant therapy, immune support, and comprehensive nutritional support are equally important. Meanwhile, it is also indispensable to take care of the functions of other organs. When the COVID-19 epidemic occurs on a large scale, we must make rational use of medical resources and strive to improve the success rate of treatment.

Funding

The Hebei Provincial Department of Finance's Geriatric Disease Prevention and Control Project (361007) and the Hebei Provincial Postgraduate Innovation Funded Project (HBU2023SS004)

Disclosure statement

The authors declare no conflict of interest.

References

[1] Liu X, Qu J, Yang X, et al, 2020, CT Imaging Features of Novel Coronavirus Pneumonia. Journal of

Heze Medical College, 32(1): 12–16.

[2] Chen Y, Huang W, 2023, Expert Consensus on the Application of Azivudine Tablets in the Treatment of Novel Coronavirus Infection. China Pharmaceutical Industry, 32(3): 1–6.

[3] Zhang J, Hu X, Zhao Z, et al, 2022, The Mechanism of Action and Clinical Research Progress of Naimatevir Tablets/Ritonavir Tablets for the Treatment of COVID-19. Chinese Journal of Pharmaceutical Sciences, 57(10): 845–850.

[4] Yu B, Chang J, 2020, Azvudine (FNC): a Promising Clinical Candidate for COVID-19 Treatment. Signal Transduct Target Therapy, 5(1): 236.

[5] The Respiratory Critical Care Medicine Group of the Respiratory Society of the Chinese Medical Association, the Respiratory Physician Branch of the Chinese Medical Association, the Critical Care Medicine Working Committee, et al, 2019, Expert Consensus on the Clinical Application of High-Flow Nasal Humidified Oxygen Therapy for Adults. Chinese Tuberculosis and Respiratory Journal, 42(2): 83–91.

[6] Ni Z, Qin H, Li J, et al, 2020, Expert Consensus on the Use and Management of Nasal High-Flow Oxygen Therapy for Patients with Novel Coronavirus Pneumonia. Chinese Journal of Respiratory and Critical Care, 19(2): 110–115.

[7] Huang P, 2022, Analysis of the Application Value of Early Mechanical Ventilation in Prone Position in the Clinical Treatment of Severe ARDS. Systematic Medicine, 7(16): 85-88. https://doi.org/10.19368/j.cnki.2096-1782.2022.16.085

[8] National Health Commission of the People's Republic of China, 2023, Diagnosis and Treatment Plan for Novel Coronavirus Infection (Trial 10th Edition). Chinese Journal of Clinical Infectious Diseases, 6(1): 1–9. https://doi.org/10.3760/cma.j.issn.1674-2397.2023.01.001

[9] Xiong D, Muema C, Zhang X, et al, 2021, Enriched Opportunistic Pathogens Revealed by Metagenomic Sequencing Hint Potential Linkages between Pharyngeal Microbiota and COVID-19. Virologica Sinica, 36(5): 924–933.

[10] Lau JTF, Leung PC, Wong ELY, et al, 2005, The Use of an Herbal Formula by Hospital Care Workers During the Severe Acute Respiratory Syndrome Epidemic in Hong Kong to Prevent Severe Acute Respiratory Syndrome Transmission, Relieve Influenza-Related Symptoms, and Improve Quality of Life: a Prospective Cohort Study. J Altern Complement Med, 11: 49–55. https://doi.org/10.1089/acm.2005.11.49

[11] Lau JTF, Leung PC, Wong ELY, et al, 2005, Using Herbal Medicine as a Means of Prevention Experience During the SARS Crisis. Am J Chin Med, 33: 345–356. https://doi.org/10.1142/S0192415X05002965

[12] Zou J, Hua B, Chen C, et al, 2003, Clinical Features of 42 Patients with SARS and Integrated Chinese and Western Medicine. Chin J Integr Tradition West Med Intensive Critical Care, 23: 486–488.

[13] Pan J, Yang H, Yu Q, et al, 2003, Clinical Study on 71 Cases of SARS Patients Intervened with Traditional Chinese Medicine. Chin J Integr Tradition West Med Intensive Crit Care, 10: 204−207.

[14] Tong X, Li A, Zhang Z, et al, 2003, Clinical Observation on 16 Cases of Infectious Atypical Pneumonia Treated by Traditional Chinese Medicine. J Tradition Chin Med, 44: 506–507. https://doi.org/10.13288/j.11-2166/r.2003.07.020

[15] Yang A, Liu Y, Lin L, et al, 2021, Research Progress of Heat-Clearing and Detoxifying Traditional Chinese Medicines Against Novel Coronavirus Pneumonia. Chinese Journal of Traditional Chinese Medicine, 39(1): 181–186. https://doi.org/10.13193/j.issn.1673-7717.2021.01.045

[16] Omrani AS, Saad MM, Baig K, et al, 2014, Ribavirin and Interferon Alfa-2a for Severe Middle East Respiratory Syndrome Coronavirus Infection: a Retrospective Cohort Study. Lancet Infect Dis, 14(11): 1090–1095.

[17] Falzarano D, de Wit E, Rasmussen A, et al, 2013, Treatment with Interferon-α2b and Ribavirin Improves Outcome in MERS-CoV-Infected Rhesus Macaques. Nat Med, 19: 1313–1317. https://doi.org/10.1038/nm.3362

[18] Liu J, Guo H, Li A, 2020, Some Thoughts on the Diagnosis and Treatment of Novel Coronavirus Pneumonia. Journal of Capital Medical University, 41(3): 328–335.

[19] Xiang HR, Cheng X, Li Y, et al, 2021, Efficacy of IVIG (Intravenous Immunoglobulin) for Coronavirus Disease 2019 (COVID-19): a Meta-Analysis. Int Immunopharmacol, 96: 107732. https://doi.org/10.1016/j.intimp.2021.107732.

[20] Michot JM, Albiges L, Chaput N, et al, 2020, Tocilizumab, an Anti-IL6 Receptor Antibody, to Treat Covid-19-Related Respiratory Failure: a Case Report. Ann Oncol, 31: 961–964. https://doi.org/10.1016/j.annonc.2020.03.300.

[21] Zhang X, Song K, Tong F, et al, 2020, First Case of COVID-19 in a Patient with Multiple Myeloma Successfully Treated with Tocilizumab. Blood Adv, 4: 1307–1310. https://doi.org/10.1182/bloodadvances.2020001907

[22] Ferrey AJ, Choi G, Hanna RM, et al, 2020, a Case of Novel Coronavirus Disease 19 in a Chronic Hemodialysis Patient Presenting with Gastroenteritis and Developing Severe Pulmonary Disease. Am J Nephrol, 51: 337–342. https://doi.org/10.1159/000507417

[23] Odièvre MH, de Marcellus C, Ducou Le Pointe H, et al, 2020, Dramatic Improvement After Tocilizumab of a Severe COVID-19 in a Child with Sickle Cell Disease and Acute Chest Syndrome. Am J Hematol, 95(8): E192–E194. https://doi.org/10.1002/ajh.25855.

[24] Fang X, Wu L, Li S, et al, 2014, Effects of Thymofasin for Injection on T Lymphocyte Subsets and Serum Immune Proteins in Elderly Patients with Community-Acquired Severe Pneumonia. Guangdong Medicine, 35(3): 451–452.

[25] Geriatric Nutritional Support Group, Chinese Medical Association Parenteral and Enteral Nutrition Branch, 2013, Chinese Expert Consensus on Parenteral and Enteral Nutrition in Elderly Patients. Chinese Journal of Geriatric Medicine, 32(9): 913–929. https://doi.org/10.3760/cma.j.issn.0254-9026.2013.09.001

[26] Sobotka L, Schneider SM, Berner YN, et al. 2009, ESPEN Guidelines on Parenteral Nutrition: Geriatrics. Clin Nutrit, 28(4): 461–466. https://doi.org/10.1016/j.clnu.2009.04.004

[27] Mei H, Hu Y, 2020, Etiological Analysis and Diagnosis and Treatment Strategies of Coagulation Dysfunction in Patients with Novel Coronavirus Pneumonia (COVID-19). Chinese Journal of Hematology, 41(3): 185–191.

Proceedings of Anticancer Research, 2023, Volume 7, Issue 4
http://ojs.bbwpublisher.com/index.php/PAR
ISSN Online: 2208-3553
ISSN Print: 2208-3545

Clinical Value of Hepatitis B Virus RNA Detection in Patients with Chronic Hepatitis B Infection

Yu Li[1], Yifei Lyu[2], Feng-Yu Xi[3]*

[1]Department of Infectious Diseases, Shaanxi Provincial People's Hospital, Xi'an 710068, Shaanxi Province, China

[2]Department of Gastroenterology, Shaanxi Provincial People's Hospital, Xi'an 710068, Shaanxi Province, China

[3]Department of Clinical Laboratory, Shaanxi Provincial People's Hospital, Xi'an 710068, Shaanxi Province, China

***Corresponding author:** Feng-Yu Xi, Drlee2810@126.com

Abstract: *Objective:* To study the clinical value of hepatitis B virus pregenomic RNA (HBV-pgRNA) detection in the treatment of hepatitis B. *Methods:* 60 patients with hepatitis B were included in the study. Serum HBV-pgRNA and HBV DNA levels in different phases of infection and during treatment were detected, and serum hepatitis B surface antigen (HbsAg) titer was detected by chemiluminescent immunoassay. DNA was extracted from liver biopsy tissue, and covalently closed circular DNA was detected to predict the therapeutic value in patients. *Results:* At the initial stage of treatment, the level of HBV-pgRNA in phase I, II, III, and IV showed a gradual decrease. Comparing the levels of HBV-pgRNA before and after treatment, we found that the level of HBV-pgRNA was significantly lower after treatment ($P < 0.05$). Among the indicators for predicting HBsAg seroconversion, the accuracy of HBV-pgRNA level was 85.0% (51/60). *Conclusion:* The clinical value of HBV-pgRNA detection in the treatment of hepatitis B is high.

Keywords: Hepatitis B virus pregenomic RNA; HBV-pgRNA ; Detection; Hepatitis B; Treatment; Clinical value

Online publication: July 18, 2023

1. Introduction

Hepatitis B is an infectious disease caused by hepatitis B virus (HBV). It is a global health problem, especially in Asia. Hepatitis B is a chronic viral infection that can lead to serious consequences, such as cirrhosis and liver cancer. At present, the treatment for hepatitis B is antiviral therapy, but there are great differences in the treatment effect; some patients may even experience treatment failure or relapse [1-4]. HBV-pgRNA is the pregenomic RNA of HBV, which plays an important role in HBV replication. In recent years, several studies have shown that the detection of HBV-pgRNA can be used to evaluate the effect of antiviral therapy [5,6]. Therefore, we explore the clinical value of HBV-pgRNA detection in the treatment of hepatitis B. The natural history of chronic HBV infection can be divided into four phases: (1) immune tolerance; (2) immune clearance; (3) low replicative or inactive carrier, and (Ⅳ) reactivation [7]. In this study, 60 patients were selected.

2. Materials and methods

2.1. Baseline data

From June 2021 to May 2022, 60 patients with chronic hepatitis B were selected from the Department of Infectious Diseases and Department of Gastroenterology of Shaanxi Provincial People's Hospital. Their

diagnosis was in line with the Guidelines for the Prevention and Treatment of Chronic Hepatitis B (2019) [7]. The ratio of male to female was 30:30, and their age ranged from 23 to 61 (25.2 ± 2.5). There were 3, 29, 9, and 19 cases in phase I, II, III, and IV, respectively. The research protocol was approved by the Ethics Committee of Shaanxi Provincial People's Hospital, and all patients signed the informed consent.

2.2. Methods

Upon admission to the hospital, blood was collected from patients with chronic hepatitis B virus infection on an empty stomach in the morning, and alanine transaminase (ALT) and aspartate transaminase (AST) were determined by rate method.

Using 200 μL of serum, quantitative polymerase chain reaction was performed, and relevant kits were used to extract RNA and obtain complementary DNA (cDNA) through reverse transcription. Serum HBV RNA was determined, and quantitative detection of HBV DNA was performed.

Chemiluminescence immunoassay was used to measure serum hepatitis B surface antigen (HbsAg) titer. The detection limit was 0.05 IU/mL, and the initial value was higher than the detection limit of 250 IU/mL. The sample was diluted at 1:500 for detection.

After cutting the 30 mm formalin-fixed paraffin-embedded liver biopsy tissue into 6 mm, DNA was extracted, double-stranded (ds)DNA and single-stranded (ss)DNA were replicated using relevant reagents, and HBV covalently close circular DNA (cccDNA) was further quantified.

2.3. Statistical analysis

SPSS 25.0 was used for data processing. Measurement data were expressed as mean ± standard deviation, and *t*-test was performed; count data were expressed as percentage (%), and chi-square test was performed. $P < 0.05$ indicates statistically significant results.

3. Results

At the initial stage of treatment, the level of HBV-pgRNA in phase I, II, III, and IV showed a gradual decrease (7.32 ± 1.17 $\log_{10}$ copies/mL, 6.64 ± 0.44 $\log_{10}$ copies/mL, 4.66 ± 1.05 $\log_{10}$ copies/mL, and 5.25 ± 0.37 $\log_{10}$ copies/mL).

Comparing the levels of HBV-pgRNA before and after treatment, the HBV-pgRNA level was singificantly lower after 12 months of treatment (6.22 ± 1.15 $\log_{10}$ copies/mL versus 3.66 ± 0.42 $\log_{10}$ copies/mL; $P < 0.05$, $t = 16.1968$).

In this study, among the indicators for predicting HBsAg seroconversion, the accuracy of HBV-pgRNA was 85.00% (51/60).

4. Discussion

HBV-pgRNA is an important component in the replication of HBV and plays a key role in HBV infection. Recent studies have shown that HBV-pgRNA detection has certain clinical value in evaluating the treatment response and efficacy in hepatitis B patients [8,9]. In the present study, we explore the clinical value of HBV-pgRNA detection in the treatment of hepatitis B and analyze its advantages and limitations in clinical application.

4.1. Clinical application of HBV-pgRNA detection in the treatment of hepatitis B

The application of HBV-pgRNA detection in the treatment of hepatitis B is mainly reflected in three aspects. First, HBV-pgRNA detection can be used to evaluate the efficacy of antiviral therapy. Some studies have shown that a decrease in HBV-pgRNA level reflects the treatment response and efficacy of antiviral therapy in hepatitis B patients [10,11]. For example, the greater the reduction in HBV-pgRNA levels, the better the

treatment response and efficacy. Therefore, HBV-pgRNA detection can be used to guide the treatment plan and thus improve the treatment effect. Second, HBV-pgRNA detection can be used to predict drug resistance. Several studies have shown that changes in HBV-pgRNA levels can predict drug resistance in HBV. For example, HBV-pgRNA levels that do not decline or rebound might suggest that the virus has developed drug resistance. Therefore, HBV-pgRNA detection can be used to guide the selection and adjustment of drugs to prevent the emergence of drug resistance in HBV [12]. Third, HBV-pgRNA detection can be used to assess HBV replication activity. Some studies have shown that the level of HBV-pgRNA can reflect the replication activity of HBV [13-15]. Therefore, HBV-pgRNA detection can be used to assess HBV replication activity before and after treatment to guide treatment options and monitor treatment effects.

4.2. Advantages and limitations of HBV-pgRNA detection

The advantages of HBV-pgRNA detection are as follows: (1) HBV-pgRNA detection can directly reflect HBV replication activity; it is more sensitive and accurate than traditional serological indicators; (2) HBV-pgRNA detection can be used to evaluate the efficacy of antiviral therapy and drug resistance in HBV to guide treatment plans and drug adjustments [16]; (3) HBV-pgRNA detection can be used to monitor HBV replication activity and predict the progress of the disease.

However, HBV-pgRNA detection has several limitations, such as (1) the relatively complicated detection method, which is costly and requires high-tech laboratories and equipment support; (2) a lack of standardized detection methods and standard reference values, which may render differences in results between different laboratories; and (3) the numerous factors that affect the level of HBV-pgRNA, including the patient's immune status, virus serotype and genotype, *etc*., thereby requiring a comprehensive analysis. The study concluded that the level of HBV-pgRNA in phase I, II, III, and IV showed a gradual decrease at the initial stage of treatment. Comparing the levels of HBV-pgRNA before and after treatment, we found that level of HBV-pgRNA was significantly lower after treatment ($P < 0.05$). Among the indicators for predicting HBsAg seroconversion, the accuracy of HBV-pgRNA level was 85.00% (51/60).

Overall, HBV-pgRNA detection has clinical value in hepatitis B treatment and in predicting HBsAg seroconversion. Although there are certain limitations, with the advancement of technology and the establishment of standardization, we anticipate that the clinical application of HBV-pgRNA detection in the treatment of hepatitis B will grow.

Funding

This work was supported by the grant from SPPH Foundation for Development of Science and Technology (2021BJ-26), International Science and Technology Cooperation Projects of Shaanxi Province (2022KW-14).

Disclosure statement

The authors declare no conflict of interest.

References

[1] Huang Y, Gu W, Zhu H, et al., 2022, Effect of Partial or Complete Deletion of Post-Transcriptional Regulatory Elements on Extranuclear Export of Hepatitis B Virus Pregenomic RNA. Chinese Journal of Practical Diagnosis and Therapy, 36(10): 1017–1021.

[2] Ling X, Wang R, Su M, et al., 2022, The Clinical Significance of Dynamic Monitoring of Serum Hepatitis B Virus Pregenomic RNA in the Treatment of Nucleotide Analogues in Patients with Chronic

Hepatitis B. Chinese Journal of Practical Internal Medicine, 42(05): 404–408.

[3] Chen J, Qi W, Hu M, et al., 2022, Correlation Between HBV Pregenome RNA Level and Recurrence Risk After Drug Withdrawal in Patients with Chronic Hepatitis B. Liver, 27(04): 413–417 + 425.

[4] Yan J, Wang C, Liu J, et al., 2022, Predictive Value of Serum Hepatitis B Virus Pregenome RNA Level in Nucleoside (Acid) Analogue-Naïve Chronic Hepatitis B Patients. Practical Hepatology Journal, 25(01): 22–25.

[5] Ma H, Zhao L, Chen W, et al., 2021, Diagnostic Value of Serum Pregenomic RNA Detection in Patients with Hepatitis B Virus Infection with Different Clinical Outcomes. Liver, 26(10): 1150–1153.

[6] Guo Z, Li F, Mo H, 2021, The Relationship Between HBV Pregenomic RNA, Alpha-Fetoprotein Isoform 3 and Hepatitis B X Antibody Levels and HBV-Induced Liver Cancer and the Prognosis of Patients. International Test Journal of Medicine, 42(19): 2390–2393.

[7] Society of Infectious Diseases, Chinese Medical Association, Society of Hepatology, et al., 2019, Guidelines for the Prevention and Treatment of Chronic Hepatitis B (2019 Edition). Chinese Journal of Infectious Diseases, 37(12): 711–736. https://doi.org/10.3760/cma.j.issn.1000-6680.2019.12.003

[8] Ma X, Zheng X, Huang Y, et al., 2022, Effect of Pre-mRNA Splicing Factor 19 Protein on Viral Replication of Hepatitis B Virus Infected Huh7 Cells. Chinese Journal of Practical Diagnosis and Therapy, 36(9): 900–904.

[9] Li X, Li L, Yuan S, et al., 2021, Analysis of the Level of Serum Hepatitis B Virus Pregenome RNA in 70 Cases of Chronic Hepatitis B Patients with Negative Hepatitis B Virus DNA. Chinese Journal of Infectious Diseases, 39(9): 558–561.

[10] Zhang H, Li Y, 2021, Research on the Clinical Significance of Five Items of Hepatitis B and Quantitative Detection of Hepatitis B Virus DNA in Patients with Chronic Hepatitis B. Diet and Health Care, 2021(43): 13–14.

[11] Ren J, 2021, Effect Observation and Detection Rate Analysis of Chemiluminescence Method and Enzyme-Linked Immunoassay in Hepatitis B Virus Serological Test. Diabetes World, 18(3): 141.

[12] Zeng Y, Wang C, He Y, et al., 2022, Clinical Significance of Serum Hepatitis B Virus Pregenomic RNA in Patients with Chronic Hepatitis B Treated with Nucleoside (Acid) Analogues. Journal of Clinical Internal Medicine, 39(11): 751–754.

[13] Lu D, Zheng H, Xi J, et al., 2021, Mechanism of Hepatitis B Virus Pregenomic RNA Selective Translation of Polymerase Protein. Chinese Journal of Hepatology, 29(10): 1035–1040.

[14] Zhang Q, 2022, Application Progress of Serum HBV RNA in Antiviral Therapy. Chongqing Medicine, 51(5): 890–894.

[15] Xu G, Li P, Wu X, 2023, The Value of Hepatitis B Virus Pregenome RNA in Evaluating the Efficacy of Entecavir in the Treatment of Hepatitis B E Antigen Positive Chronic Hepatitis B. Big Doctor, 8(1): 111–113.

[16] Liu Q, Zhang L, Zhang M, et al., 2023, Effect of Pegylated Interferon A-2b on Serum Markers HBsAg, HBV-pgNRA, HBV-RNA in Patients with Chronic Hepatitis B. International Journal of Laboratory Medicine, 44(2): 192–195.

Proceedings of Anticancer Research, 2023, Volume 7, Issue 4
http://ojs.bbwpublisher.com/index.php/PAR
ISSN Online: 2208-3553
ISSN Print: 2208-3545

Effects of IL-6/JAK2/STAT3 on the Biological Behavior of Oral Squamous Cell Carcinoma

Yan Hu[1], Zhizheng Zhuang[1]*, Hongyue Liu[2]

[1]Department of Stomatology, Affiliated Hospital of Hebei University, Baoding 071000, Hebei Province, China

[2]Second Department of Stomatology, The Second People's Hospital of Hengshui, Hengshui 053099, China

***Corresponding author:** Zhizheng Zhuang, 45914633@qq.com

Abstract: *Objective:* To investigate the effect of interleukin 6/Janus kinase 2/signal transducer and activator of transcription 3 (IL-6/JAK2/STAT3) on the biological behavior of oral squamous cell carcinoma (OSCC). *Methods:* OSCC cells were transfected with the designed lentiviral vector plasmid pGMLV-SB3 (experimental group) and the corresponding negative control plasmid pGMLV-SB3-shNC (control group); 48 hours after transfection, a liposome transfection kit (Sigma, USA) was used for lentivirus packaging; after virus packaging, a medium containing pGMLV-SB3 lentiviral vector was added and cultured for 24 h; the cells were harvested, and RNA was extracted; Transwell chamber assay (Sigma, USA) was used to detect cell migration and invasion ability; dot-enzyme-linked immunosorbent assay (ELISA) kit was used to detect the level of interleukin 6 (IL-6) in the culture supernatant, while serum IL-6 level was measured by ELISA. *Results:* The expressions of IL-6, JAK2, and STAT3 in the experimental group were significantly raised, as compared to the control group ($P < 0.05$); the apoptosis rate of OSCC cells in the experimental group, which was detected by flow cytometry 48 h after transfection, was significantly higher than that of cells in the control group ($P < 0.05$); and there was a significant improvement in the experimental group's cell migration and invasion ability, as compared to that of the control group ($P < 0.05$). *Conclusion:* The IL-6/JAK2/STAT3 signaling pathway plays an important role in the migration and invasion of OSCC cells. Inhibiting the expression of IL-6 can inhibit the growth and proliferation of OSCC cells as well as reduce their ability to invade and migrate. These results provide a new target for the treatment of OSCC.

Keywords: IL-6; JAK2; STAT3; Oral squamous cell carcinoma

Online publication: July 20, 2023

1. Introduction

Oral squamous cell carcinoma (OSCC) is one of the most common oral tumors, with high morbidity and mortality, and about 90% of them are squamous cell carcinomas. Although OSCC has a high cure rate, its therapeutic effect is largely limited due to its abnormal biological behavior and ease of recurrence and metastasis. Therefore, it is of great significance to explore its pathogenesis and find effective treatment methods. The pathogenesis of OSCC is related to many factors, including the interleukin 6 (IL-6) signaling pathway. The IL-6 signaling pathway regulates many biological processes, including cell proliferation, migration, and invasion, through molecules such as protein tyrosine kinase 2 (Janus kinase 2, JAK2) and signal transducer and activator of transcription 3 (STAT3) [1-5]. In recent years, studies have found that IL-6 is a cytokine that widely exists as an inflammatory mediator and plays an important role in the occurrence and development of many tumors. The expression of IL-6 has been found to be significantly increased in

OSCC. IL-6 is a natural immune regulatory factor secreted by T lymphocytes, which has immune regulation, anti-inflammation, anti-virus, and anti-tumor roles. Current studies have revealed the role of IL-6 in a variety of malignant tumors; however, its role in OSCC has not been reported [6-8]. The JAK2/STAT3 signaling pathway is one of the important cell-signaling pathways. The abnormal activation of this signaling pathway is also closely related to the occurrence and development of various malignant tumors. In this study, we explore the effect of the IL-6/JAK2/STAT3 signaling pathway on the biological behavior (proliferation, invasion, metastasis, and apoptosis) of OSCC cells and transfect it into OSCC cells through the lentiviral vector to observe its effect on OSCC. The influence on the biological behavior of OSCC cells provides a new strategy for the treatment of OSCC.

2. Materials and methods

2.1. Materials and instruments

The materials and instruments used included cell culture flask (Shanghai SPEF Biotechnology Co., Ltd.), cell incubator (Shanghai Boxun Industrial Co., Ltd.), polymerase chain reaction (PCR) instrument (Thermo Company), electrophoresis instrument (Thermo Company), PCR buffer and enzyme plate (Thermo Company), cell DNA extraction reagent kit (Biochem Company), real-time fluorescence quantitative PCR instrument (Thermo Company), and lentiviral vector pcDNA3.1/ml-gp53 recombinant plasmid (Shanghai Zhicheng Biotechnology Co., Ltd.).

2.2. Lentivirus transfection and identification

OSCC cells were transfected with the designed lentiviral vector plasmid pGMLV-SB3 (experimental group) and the corresponding negative control plasmid pGMLV-SB3-shNC (control group). A liposome transfection kit (Sigma, USA) was used 48 hours after transfection. Lentivirus packaging was performed, and after virus packaging, a medium containing pGMLV-SB3 lentiviral vector was added and cultured for 24 h. Cells were harvested, and RNA was extracted. RT-PCR amplification was performed, and the relative expression of the target gene was determined.

2.3. Detection of cell biological behavior

Transwell chamber assay (Sigma, USA) was used to detect cell migration and invasion ability. Dot-enzyme-linked immunosorbent assay (ELISA) kit was used to detect the level of IL-6 in the culture supernatant, while serum IL-6 level was measured by ELISA.

2.4. Statistical processing

Statistical analysis was performed using SPSS 24.0. Measurement data were expressed as mean ± standard deviation, and count data were expressed as n (%). For comparison between groups, the *t*-test and χ^2 test were used. $P < 0.05$ indicates a statistically significant result.

3. Results

3.1. Lentivirus transfection and virus titer

The expression of the target gene was detected by Western blot 24 h after transfection, and the results are shown in **Table 1**. It can be seen from **Table 1** that the expression of IL-6, JAK2, and STAT3 in the experimental group increased significantly as compared to the control group ($P < 0.05$).

Table 1. Lentivirus transfection and virus titer detection results

Group	JAK2 (μg/mL)	STAT3 (ng/mL)	IL-6 (pg/mL)	IL-12 (pg/mL)
Control group	31.26 ± 14.12	32.14 ± 18.79	401.23 ± 24.36	1.32 ± 0.14
Experimental group	74.12 ± 14.78	113.25 ± 19.45	612.12 ± 36.98	4.12 ± 0.56
t	16.0572	23.0314	33.6768	31.2380
P	0.0000	0.0000	0.0000	0.0000

3.2. Lentivirus transfection and cell apoptosis

Lentiviral particles were diluted with sterile saline to three concentrations (2 μg/mL, 4 μg/mL, and 6 μg/mL) and transfected into the experimental group's OSCC cells. Cell apoptosis was detected by flow cytometry 48 h after transfection. The results are shown in **Table 2**. After 48 h, we found that the apoptosis rate of the cells in the experimental group was significantly higher than that of cells in the control group ($P < 0.05$).

Table 2. Lentivirus transfection and apoptosis detection results

Group	Apoptosis rate (%)
2 μg/mL	2.53 ± 0.12
4 μg/mL	24.01 ± 2.14
6 μg/mL	23.89 ± 2.13
P	< 0.001

3.3. Effect of IL-6 knockdown on OSCC cell migration and invasion

As shown in **Table** 3, there was a significant improvement in the migration and invasion ability of OSCC cells in the experimental group, as compared to the control group ($P < 0.05$).

Table 3. Effect of IL-6 knockdown on OSCC cell invasion and migration

Group	Migration	Invasion
Experimental group	461.62 ± 51.37	367.89 ± 42.52
Control group	104.54 ± 27.05	85.9 ± 12.17

$P < 0.05$ for comparison between groups.

4. Discussion

OSCC is a common oral cancer, and its occurrence and development are related to various factors, including cytokine-mediated signaling pathways. The IL-6/JAK2/STAT3 signaling pathway is one of the important signaling pathways that play an important role in the biological behavior of OSCC cells, such as proliferation, invasion, and metastasis.

IL-6 is a cytokine with complex physiological functions and is produced by a variety of tissue cells, including inflammatory cells, tumor cells, *etc*. [9,10]. IL-6 can induce B cells to differentiate into plasma cells, produce antibodies, and play an immune-response role. At the same time, IL-6 can also promote the proliferation and differentiation of T cells as well as regulate immune response; it can inhibit and reduce inflammatory response by downregulating the production and release of other inflammatory factors; in addition, it can promote the growth and differentiation of certain cells, such as hematopoietic stem cells and neurons; IL-6 is known to be closely related to the occurrence and development of tumors, as it can

also promote the growth and proliferation of tumor cells. IL-6 can activate the JAK2/STAT3 signaling pathway to promote the proliferation, invasion, and metastasis of tumor cells. Studies have shown that the expression of IL-6 in OSCC tissues is significantly higher than that in normal tissues and it is closely related to the clinicopathological features of OSCC, such as pathological grade, lymph node metastasis, and distant metastasis.

JAK2 is a key enzyme in the IL-6 signaling pathway, which can mediate IL-6 signal transduction. Studies have shown that the expression of JAK2 in OSCC tissues is significantly higher than that in normal tissues and its activation is closely related to the invasion and metastasis of OSCC. STAT3, on the other hand, is a downstream molecule of JAK2, which can be phosphorylated by JAK2 and enter the nucleus, thereby regulating the expression of target genes [11-15].

The JAK2/STAT3 signaling pathway is an important cell signaling pathway involved in many biological processes, including cell proliferation, migration, invasion, and apoptosis. JAK2 is a non-receptor tyrosine-protein kinase that can bind to many cell surface receptors, including gp130, EPOR, IGF1R, *etc*. The binding of a ligand to a cellular receptor triggers the activation of JAK2 and the phosphorylation of tyrosine. STAT3 is a signal transducer and transcription activator. When JAK2 is activated, STAT3 will be phosphorylated, form homologous or heterodimers, enter the nucleus, bind to specific gene promoters, and activate gene transcription. The JAK2/STAT3 signaling pathway can regulate the expression of many key genes, such as Cyclin D1, MMP2, VEGFA, *etc*., thereby participating in biological processes, such as cell proliferation, migration, and invasion. In addition, the JAK2/STAT3 signaling pathway can also affect processes such as apoptosis and autophagy as well as play complex biological roles. Studies have shown that the expression of STAT3 in OSCC tissues is significantly higher than that in normal tissues, and its activation is closely related to the proliferation, invasion, and metastasis of OSCC.

Cytokines play an important role in the occurrence and development of many tumors, among which IL-6 is a cytokine widely present as an inflammatory mediator that can induce tumor cell apoptosis and promote tumor growth. Current studies have found that IL-6 is abnormally expressed at varying degrees in malignant tumors, including colon cancer, breast cancer, lung cancer, and ovarian cancer. At the same time, IL-6 has also been found to be abnormally expressed in OSCC, as evidenced by the significantly higher serum IL-6 levels in patients with OSCC, as compared to those in normal patients. Therefore, IL-6 plays a certain role in the occurrence and development of OSCC. Several studies have found that the JAK2/STAT3 signaling pathway is activated in OSCC, while the expressions of STAT1 and STAT3 are significantly reduced. Therefore, the JAK2/STAT3 signaling pathway is considered to be one of the important mechanisms for the development of OSCC.

The results of the present study showed significantly increased expressions of IL-6, JAK2, and STAT3 in OSCC tissues. The IL-6/JAK2/STAT3 signaling pathway can inhibit tumor growth by regulating the biological behavior of OSCC cells, such as proliferation, invasion, metastasis, and apoptosis.

With regard to the occurrence and development of OSCC, IL-6 participates in tumor cell proliferation, invasion, and metastasis by regulating the JAK2/STAT3 pathway. At the same time, IL-6 can also change the tumor microenvironment by regulating the secretion of extracellular matrix. In the treatment of OSCC, a variety of treatment methods have been used clinically, including surgery, chemotherapy, radiotherapy, and immunotherapy, among which immunotherapy is one of the most widely used methods. However, the curative effect of immunotherapy on OSCC is still unsatisfactory. A combined IL-6 targeted therapy with immunotherapy may be an effective option for patients with OSCC. At the same time, IL-6 has a favorable application prospect, as it can be used as one of the biomarkers to predict the prognosis of patients with OSCC.

In conclusion, the IL-6/JAK2/STAT3 signaling pathway plays an important role in the occurrence and

development of OSCC. Therefore, therapeutic strategies targeting this signaling pathway may become a new avenue for OSCC treatment. For example, specific inhibitors can be developed to inhibit the activity of JAK2 or STAT3, thereby blocking IL-6 signal transduction and inhibiting OSCC proliferation, invasion, and metastasis. In addition, OSCC can also be treated by modulating the expression or activity of IL-6. However, these therapeutic strategies still require further research and validation.

Disclosure statement

The authors declare no conflict of interest.

References

[1] Wang N, Jin W, Peng X, 2023, Research Progress of Human Xenograft Model of Oral Squamous Cell Carcinoma. Modern Stomatology, 37(3): 195–199.

[2] Yang Y, Song X, Wu Y, 2023, Notch1 (P1641S) Mutation Promotes the Proliferation of Oral Squamous Cell Carcinoma Through PI3K/Akt Pathway. Stomatological Medicine, 43(5): 393–399.

[3] Zhang H, Jiang Y, Sun L, et al., 2023, The Expression of SMARCA5 in Oral Squamous Cell Carcinoma and Its Effect on the Proliferation, Migration and Invasion of HSC4 Cells. Chongqing Medicine, 52(9): 1292–1297.

[4] Wu R, Liu H, Zheng S, et al., 2023, MCU Maintains Mitochondrial Calcium Homeostasis Through LETM1 to Regulate Oral Squamous Cell Carcinoma Metastasis. Journal of Chongqing Medical University, 48(4): 411–416.

[5] Zheng S, Meng L, Ren F, et al., 2023, Cell-Free DNA from Oral Squamous Cell Carcinoma Regulates Stemness and Migration of Oral Cancer Cell Lines by Inducing Macrophage Polarization. Journal of Sichuan University (Medical Edition), 54(3): 510–516.

[6] Zhang C, Li C, 2023, Relationship Between TP53 Gene Mutation and Prognosis of Oral Squamous Cell Carcinoma. Modern Oncology, 31(11): 2169–2172.

[7] Yang K, Sun Y, Hu Y, et al., 2023, The Predictive Effect of Cyclin D1 Expression Pattern Deep Learning Recognition and Prediction Model on the Prognosis of Patients with HPV-Negative Oral Squamous Cell Carcinoma and Oropharyngeal Squamous Cell Carcinoma. Stomatology Research, 39(4): 308–315.

[8] Xu L, Huang Z, Lu D, et al., 2022, The MiR-663b/ALDH6A1 Axis Regulates the Proliferation of Oral Squamous Cell Carcinoma Cells Through ROS. Journal of Local Surgery, 31(9): 747–753.

[9] Li W, Cao J, Guo X, et al., 2022, Tumor-Associated Macrophage-Derived IL-6 Promotes the Invasion and Migration of Oral Squamous Cell Carcinoma CAL27 Cells by Up-Regulating the Expression of LIF in Tumor Cells. Journal of Jilin University (Medical Edition), 48(4): 946–953.

[10] Tong X, Zhou X, Zhong H, et al., 2022, Effects of IL-6/JAK2/STAT3 on Biological Behavior of Oral Squamous Cell Carcinoma. Chinese Journal of Otorhinolaryngology and Skull Base Surgery, 28(1): 89–97.

[11] Qu Y, He Y, Yang Y, et al., 2019, Proceedings of the 2019 First National Oral and Maxillofacial - Head and Neck Tumor Academic Conference, December 20–22, 2019: ALDH3A1 as a Prognostic Marker for Oral Squamous Cell Carcinoma Inhibits the Epithelial-Mesenchymal Transition of Tumor Cells Through the IL-6/STAT3 Signaling Pathway. Convergence Leading, 94–95.

[12] Zhang S, 2019, Bit-1 Regulates the Migration, Invasion and Apoptosis of Oral Squamous Cell Carcinoma Through the IL-6/IL-6R-STAT3 Pathway, thesis, Zhengzhou University.

[13] Yang J, 2018, The Role of SOCS3 Gene Silencing in Regulating the Differentiation and Maturation of Dendritic Cells in Candida albicans Infection and Its Immunological Mechanism, thesis, Peking Union Medical College, Chinese Academy of Medical Sciences, Tsinghua University School of Medicine.

[14] Xu X, Zhang R, 2014, Research Progress on the Correlation Between Interleukin-6 and Oral Diseases. Stomatological Medicine, 34(6): 470–472.

[15] Du J, Yan Y, 2010, Detection of CEA, IL-6 and IL-8 in Saliva of Patients with Oral Squamous Cell Carcinoma. Journal of Anhui Medical University, 45(4): 579–581.

Proceedings of Anticancer Research, 2023, Volume 7, Issue 4
http://ojs.bbwpublisher.com/index.php/PAR
ISSN Online: 2208-3553
ISSN Print: 2208-3545

Efficacy of Low-Dose Rituximab in Primary Immune Thrombocytopenia

Ben Niu, Lan Li*

Department of Hematology, Shaanxi Provincial People's Hospital, Xi'an 710068, Shaanxi Province, China

***Corresponding author:** Lan Li, lilanlanxin@163.com

Abstract: *Objective:* To explore the effect of low-dose rituximab in primary immune thrombocytopenia. *Methods:* From January 2022 to January 2023, 60 patients with primary immune thrombocytopenia were randomly divided into two groups. The control group was treated with standard doses of rituximab, and the observation group was treated with low doses of rituximab. Rituximab was used for treatment, and the clinical curative effect of the two groups was observed. *Results:* Before treatment, there was no statistically significant difference in platelet count (PLT), anti-GPIIb/IIIa antibody, and anti-GPIb/IX antibody between the two groups ($P > 0.05$). After treatment, the PLT of the two groups increased significantly. Antibodies were all decreased, and there was no significant difference between the two groups ($P > 0.05$). The incidence of adverse reactions in the observation group was 13.33%, and that in the control group was 40.00%. The adverse reactions in the observation group were significantly lower than the control group ($P < 0.05$). *Conclusion:* In the clinical treatment of primary immune thrombocytopenia, low-dose rituximab can control the progression of the disease, improve blood routine indicators, and have fewer adverse reactions.

Keywords: Rituximab; Primary; Immune thrombocytopenia

Online publication: July 20, 2023

1. Introduction

Primary immune thrombocytopenia (formerly idiopathic thrombocytopenia purpura, ITP) is an autoimmune disease, and the main clinical symptoms of this disease are thrombocytopenia and bleeding. When treating ITP, the traditional treatment plan can achieve certain effects, but there are still a small number of patients who found the treatment being ineffective [1]. After continuous clinical practice and research, rituximab is gradually used in the clinical treatment of immune thrombocytopenia. This drug belongs to a human-mouse chimeric CD20 monoclonal antibody, which can eliminate B cells. Currently, rituximab is used as second-line therapy. In order to explore the therapeutic effect of low-dose rituximab on ITP, 60 patients were selected in this study and divided into two groups. The results are as follows.

2. Materials and methods

2.1. General information

During the period from January 2022 to January 2023, 60 patients with ITP were selected from the Shaanxi Provincial People's Hospital, and randomly divided into two groups, with 30 cases in both groups; the observation group had 16 males and 14 females, aged 20–75 years, with an average age of 42.2 ± 5.3 years old; the control group had 15 males and 15 females, aged 20–75 years, with an average age of 42.3 ± 5.6 years old. This study was approved by the ethics committee of the Shaanxi Provincial People's Hospital,

all patients or family members signed the informed consent form, and there was no difference in the basic information of the two groups of patients ($P > 0.05$).

2.2. Methods

Before treatment, the patients in the two groups received an intramuscular injection of 12.5 mg diphenhydramine, and an intravenous infusion of 10 mg dexamethasone to prevent allergic reactions. Patients in the control group were treated with a standard dose of rituximab, 375 mg/m^2, by intravenous infusion at a rate of 50 mg/h, once a week. The observation group received a small dose of rituximab, 100 mg/m^2, by intravenous infusion at a rate of 50 mg/h, once a week. The treatment period for both groups was 4 weeks.

2.3. Observation effect

Before and after treatment, relevant blood routine indicators such as platelet count (PLT), anti-GPIIb/IIIa antibody, and anti-GPIb/IX antibody were detected in the two groups. The adverse reactions of the two groups of patients, mainly pulmonary infection, bleeding reaction, allergic reaction, and infusion reaction, as well as the statistical incidence, were observed.

2.4. Statistical methods

The statistical processing of the data adopts SPSS 21.0 version software, the measurement data is expressed in the form of mean ± standard deviation (SD) and the test value is t. The count data is expressed in the form of %, and the test value is χ^2. When the P value is less than 0.05, there is a statistical difference.

3. Results

3.1. Comparison of blood routine indicators related to patients

Before treatment, the PLT, anti-GPIIb/IIIa antibody, and anti-GPIb/IX antibody of the two groups were not statistically significant ($P > 0.05$). After treatment, the PLT of the two groups was significantly increased ($P < 0.0001$), the specific antibodies were all significantly reduced ($P < 0.0001$), and there was no statistically significant difference between the two groups ($P > 0.05$). See **Table 1**.

Table 1. Comparison of blood routine indicators related to patients

Group	Sample sizes	PLT (×10^9/L)		Anti-GPIIb/IIIa antibody		Anti-GPIb/IX antibody	
		Before treatment	After treatment	Before treatment	After treatment	Before treatment	After treatment
Observation group	30	26.36 ± 8.12	86.05 ± 13.11*	0.48 ± 0.03	0.36 ± 0.05*	0.43 ± 0.05	0.37 ± 0.06*
Control group	30	26.17 ± 9.31	86.12 ± 13.25*	0.47 ± 0.05	0.35 ± 0.04*	0.42 ± 0.05	0.36 ± 0.04*
t-value		0.084	0.021	0.939	0.856	0.775	0.760
P value		0.933	0.984	0.352	0.396	0.442	0.451

Note: * $P < 0.0001$ when compared to before treatment.

3.2. Comparison of adverse reactions between the two groups of patients

The incidence of adverse reactions in the observation group was 13.33%, and that in the control group was 40.00%. The adverse reactions in the observation group were significantly fewer than the control group ($P < 0.05$), see **Table 2** for details.

Table 2. Comparison of adverse reactions between the two groups [n (%)]

Group	Number of cases	Lung infection	Bleeding reaction	Allergic reaction	Infusion reaction	Incidence rate
Observation group	30	1	1	1	1	4 (13.33)
Control group	30	2	2	4	4	12 (40.00)
χ^2 value						5.4545
P value						0.020

4. Discussion

Immune thrombocytopenia is a disease of the immune system leading to severe conditions. Its pathogenesis is relatively complicated, and the cause of the disease is ambiguous. When patients develop the disease, the obvious feature included a significant decrease in platelets and an abnormal increase in bone marrow megakaryocytes. If the patients are not accurately diagnosed and given effective treatment, the disease will be progressive [2]. As the condition worsens, the patients will experience gastrointestinal bleeding, which directly endangers their life. The common treatment of immune thrombocytopenia is the usage of glucocorticoids, and some patients require splenectomy. However, the effect of conventional treatment is not ideal [3-6].

Rituximab is a new type of therapeutic drug called a monoclonal antibody, which specifically binds to CD20 protein on the surface of B cells. Under the influence of complement-dependent and antibody-dependent cytotoxicity, it can induce apoptosis of B cells, and B cells that produce antibodies will also be effectively eliminated [7,8]. In the treatment of immune thrombocytopenia, rituximab can increase the number of platelets and improve clinical symptoms. In the clinical treatment of ITP, standard doses of rituximab (375 mg/m^2) can be used. Smaller doses can also be considered because the number of B cells in ITP patients is significantly lesser than that of lymphoma patients, and the use of standard doses of drugs may easily damage normal B cells, further leading to a decline in immune function and an increase in the possibility of infection. Moreover, conventional treatment methods cost more money. Small doses of rituximab can save the costs of treatment and are relatively safe [9,10].

In this study, the PLT, anti-GPIIb/IIIa antibody, and anti-GPIb/IX antibody of the two groups before treatment were not statistically significant ($P > 0.05$). However, after treatment, the PLT of the two groups was significantly increased, the specific antibodies were all lower, and there was no statistically significant difference between the two groups ($P > 0.05$). The incidence rates of adverse reactions in the observation and control groups were 13.33% and 40.00%, respectively. The adverse reactions in the observation group were significantly lesser as compared to the control group ($P < 0.05$).

In summary, when treating ITP, the use of low-dose rituximab can effectively increase the number of platelets, improve various clinical symptoms, and have relatively fewer adverse reactions. Its safety is high, and this treatment method is worthy of clinical promotion.

Disclosure statement

The authors declare no conflict of interest.

References

[1] Liu C, Luan L, 2019, The Effect of Glucocorticoid Combined with Low-Dose Rituximab Injection in the Treatment of Refractory Primary Immune Thrombocytopenia. China Contemporary Medicine, 26(30): 68–70 + 74.

[2] Yan L, Zhang J, Ding X, 2021, Effect Analysis of Low-Dose Rituximab Combined with Prednisone Acetate Tablets in the Treatment of Primary Immune Thrombocytopenia. Clinical Medicine Engineering, 28(11): 1505–1506.

[3] Zhang Y, Du J, 2021, Clinical Curative Effect Analysis of Low-Dose and Standard-Dose Rituximab on Elderly Patients with Chronic Refractory Primary Immune Thrombocytopenia. Shanxi Medical Journal, 50(1): 56–58.

[4] Hu X, Luo Y. Comparison of the Effect of Standard-Dose and Low-Dose Rituximab in the Treatment of Primary Immune Thrombocytopenia. Chinese and Foreign Medical Research, 19(2): 30–32.

[5] Hu X, Bao G, Wang H, et al, 2020, Efficacy of Low-Dose Rituximab and Cyclosporine in the Treatment of Refractory Primary Immune Thrombocytopenia and Safety Analysis. Chinese Medicine and Clinic, 20(20): 3476–3478.

[6] Li J, Chen L, Jiang G, et al, 2021, Efficacy and Safety Analysis of Low-Dose Rituximab in the Treatment of Refractory Thrombocytopenia Secondary to Systemic Lupus Erythematosus. Jilin Medicine, 42(4): 966–969.

[7] Zhu X, Ma J, Gu H, et al, 2021, Analysis of Clinical Characteristics of Primary Chronic Refractory Immune Thrombocytopenia in Children in a Single Center. Journal of Clinical Hematology, 34(11): 781–784.

[8] Zhang Y, Du J, 2021, Clinical Curative Effect Analysis of Low-Dose and Standard-Dose Rituximab on Elderly Patients with Chronic Refractory Primary Immune Thrombocytopenia. Shanxi Medical Journal, 50(1): 56–58.

[9] Yan L, Zhang J, Ding X, 2021, Effect Analysis of Low-Dose Rituximab Combined with Prednisone Acetate Tablets in the Treatment of Primary Immune Thrombocytopenia. Clinical Medicine Engineering, 28(11): 1505–1506.

[10] Zhu X, Ma J, Chen Z, et al, 2022, Comparison of the Efficacy and Safety of Two Small Doses of Rituximab in the Second-Line Treatment of Children with Primary Immune Thrombocytopenia. Chinese Journal of Pediatrics, 60(11): 1185–1190.

Proceedings of Anticancer Research, 2023, Volume 7, Issue 4
http://ojs.bbwpublisher.com/index.php/PAR
ISSN Online: 2208-3553
ISSN Print: 2208-3545

Clinical Value of cfDNA Content in Peripheral Blood of Patients with Triple-Negative Breast Cancer

Jirui Sun, Qiushuang Ma, Hong Chen, Xing Zhou, Bingjuan Zhou, Jinku Zhang*

Department of Pathology, Baoding First Central Hospital, Baoding 071000, Hebei Province, China

***Corresponding author:** Jinku Zhang, zjkblk@sina.com

Abstract: *Objective:* To explore the value of circulating free (cfDNA) content in the clinical diagnosis and treatment of triple-negative breast cancer (TNBC). *Methods:* A total of 39 TNBC patients, 45 non-TNBC patients, and 50 healthy individuals admitted to the Baoding First Central Hospital during 2019–2022 were recruited. The clinical data, peripheral blood cfDNA concentration, and clinicopathological indicators of the patients were observed and analyzed. *Results:* The difference in clinical indicators such as age, age range, tumor size, clinical stage, and lymph node metastasis between patients with TNBC and non-TNBC was insignificant ($P > 0.05$). The cfDNA concentrations (ng/mL) of the TNBC group, non-TNBC group, and healthy group were 24.12 ± 4.98, 15.36 ± 4.12, and 3.12 ± 1.02, respectively, and they are statistically different ($P < 0.05$). The difference in cfDNA concentration was insignificant between TNBC patients with tumors ≤ 2 cm and > 2 cm ($P > 0.05$) but was significant between TNBC patients with clinical stages I+II and III+IV ($P < 0.05$). The cfDNA concentration in TNBC patients with lymph node metastasis was significantly higher than those without lymph node metastasis ($P < 0.05$). *Conclusion:* cfDNA has an important application value in the diagnosis and treatment of breast cancer. By detecting the cfDNA level and its gene variation, valuable information about the progress and treatment effects of breast cancer can be obtained. This non-invasive detection method has a wide range of applications and can be used for early screening, auxiliary diagnosis, efficacy evaluation, and recurrence monitoring of breast cancer.

Keywords: Triple-negative breast cancer; cfDNA; Tumor cells

Online publication: July 25, 2023

1. Introduction

Triple-negative breast cancer (TNBC) refers to three different types of breast cancer: human epidermal growth factor 2 (HER2) protein, estrogen receptor (ER), and progesterone receptor (PR) negative breast cancer [1-6]. TNBC is second only to ductal carcinoma in incidence in women, accounting for about 15% of all cancers in women. The clinical symptoms of TNBC lack specificity, and its diagnosis is mainly based on the tumor histological type, and most patients have no obvious clinical symptoms in the early stage. The treatment of TNBC patients is mainly surgery, but due to its high recurrence rate, high metastasis rate, and poor prognosis, the curative effect is dissatisfactory. In recent years, attention has turned to finding noninvasive biomarkers, with circulating free DNA (cfDNA) attracting widespread interest in its potential role in breast cancer. cfDNA is a kind of DNA in blood circulation, and its sources include tumor cells and normal cells [7-10]. In breast cancer, the level of cfDNA and its gene variation information may reflect tumor progression and treatment effect [11]. cfDNA plays an important role in the diagnosis, treatment, and

monitoring of TNBC and is a potential biomarker. An in-depth study of the relationship between cfDNA and TNBC allows a better understanding of the occurrence and development of TNBC and provides patients with more accurate and effective treatment strategies. This study aimed to investigate the correlation between peripheral blood cfDNA content and clinicopathological features in TNBC patients.

2. Materials and methods

2.1. General information

The clinicopathological data of 39 TNBC patients admitted to the Baoding First Central Hospital from 2019 to 2022 and 45 non-TNBC patients were retrospectively analyzed, and compared with 50 cases of normal physical examination population hospitalized during the same period.

Inclusion criteria: tumor located in lymph node metastasis, tumor diameter ≤ 3 cm, tumor infiltration depth ≤ 3 cm; patients without liver, lung, or bone metastasis; patients and their families gave informed consent and signed an informed consent form.

Exclusion criteria: history of other malignant tumors, radiotherapy, chemotherapy, or endocrine therapy within 1 year before surgery; preoperative chemotherapy time ≥ 1 cycle, or postoperative pathological examination showed local recurrence or distant metastasis. All patients underwent a modified radical mastectomy, and breast-enhanced CT or MRI before operation.

2.2. Methods

Three mL of venous blood were taken, centrifuged at 4°C for 10 min, and the upper plasma was utilized for detection. The cfDNA content in the peripheral blood of TNBC patients was detected using quantitative reverse transcription PCR (qRT-PCR). Reagents were provided by Shanghai Bioengineering Co., Ltd.

2.3. Observation indicators

Clinical data, cfDNA concentration, and clinicopathological indicators of patients were observed and analyzed.

2.4. Statistical methods

Statistical software SPSS 24.0 was used to analyze the data. Measurement data were expressed as mean ± standard deviation (SD), using a *t*-test; count data were expressed as %, using a χ^2 test, and $P < 0.05$ was considered statistically significant.

3. Results

3.1. Clinical analysis

There was no statistical difference in age, extent, tumor size, clinical stage, lymph node metastasis, and other clinical indicators between patients with TNBC and non-TNBC ($P > 0.05$), as shown in **Table 1**.

Table 1. Clinical data

Item		TNBC	Non-TNBC	t / χ^2	*P*
Number (case)		39	45	-	-
Age		51.21 ± 10.32	50.97 ± 11.23	0.1014	0.9195
Age range (years)		31–80	29–79	-	-
Tumor size	≤ 2 cm	21 (53.85)	21 (46.67)	0.4308	0.5116
	> 2 cm	18 (46.15)	24 (53.33)		

(Continued on next page)

(Continued from previous page)

Item		TNBC	Non-TNBC	t / χ^2	*P*
Clinical stage	Phase I+II	26 (66.67)	30 (66.67)	0.0000	1.0000
	Phase III+IV	13 (33.33)	15 (33.33)		
Lymph node metastasis	Have	17 (43.59)	20 (44.44)	0.0062	0.9372
	None	22 (56.41)	25 (55.56)		

3.2. Measurement results of peripheral blood cfDNA concentration of patients in each group

The peripheral blood cfDNA concentrations (ng/mL) of the TNBC group, non-TNBC group, and healthy group were 24.12 ± 4.98, 15.36 ± 4.12, and 3.12 ± 1.02, respectively. There are statistical differences ($P < 0.05$), as shown in **Table 2**.

Table 2. Measurement results of peripheral blood cfDNA concentration of patients in each group (mean ± SD)

Group	Number of cases	cfDNA concentration (ng/mL)
TNBC group	39	24.12 ± 4.98
Non-TNBC group	45	15.36 ± 4.12
Healthy group	50	3.12 ± 1.02

Note: $P < 0.05$ between the comparisons.

3.3. The relationship between the concentration of peripheral blood cfDNA and the clinicopathological indicators of TNBC

There was no statistical difference in the cfDNA concentration between TNBC patients with tumors ≤ 2 cm and > 2 cm ($P > 0.05$), and the cfDNA concentration of TNBC patients with clinical stages I+II and III+IV were statistically different ($P < 0.05$). The peripheral blood cfDNA concentration of TNBC patients with lymph node metastasis is significantly higher than that of TNBC patients without lymph node metastasis ($P < 0.05$), see **Table 3** shown.

Table 3. The relationship between the concentration of cfDNA in peripheral blood and the clinicopathological indicators of TNBC (mean ± SD)

TNBC		cfDNA concentration (ng/mL)	*t*	*P*
Tumor size	≤ 2 cm ($n = 21$)	24.12 ± 4.98	0.1285	0.8984
	> 2 cm ($n = 18$)	24.32 ± 4.68		
Clinical stage	Stage I+II ($n = 26$)	28.12 ± 5.98	3.1894	0.0029
	Stage III+IV ($n = 13$)	22.12 ± 4.48		
Lymph node metastasis	Have ($n = 17$)	27.12 ± 3.88	3.3492	0.0019
	None ($n = 22$)	23.42 ± 3.08		

4. Discussion

TNBC is a highly invasive disease with a poor prognosis. The current treatment of TNBC is mainly surgery, but the curative effect is dissatisfactory. The change of cfDNA content in tumor tissue is a complex process, which is related to many factors such as tumor growth, differentiation, metastasis, and treatment, and the cfDNA content in tumor tissue is closely related to its occurrence and development. Elevated cfDNA content in the peripheral blood of TNBC patients can be used as an independent prognostic factor,

suggesting that it may be an important clinical indicator of poor prognosis in TNBC patients [12-15].

cfDNA is DNA released into the blood circulation by a variety of cells, mainly including the following sources: normal cells will initiate apoptosis at the end of their life cycle, and after cell death, the DNA in them will be released into the blood circulation; Abnormal cells, such as tumor cells, may release a large amount of DNA into the blood circulation; under certain conditions, such as inflammation, trauma, etc., normal cells may actively release DNA into the blood circulation.

The characteristics of cfDNA are as follows: the concentration of cfDNA in the blood circulation is usually very low, generally between several to tens of nanograms per milliliter; the length of cfDNA is usually shorter than that of normal cell DNA because it will be degraded by enzymes during release; In some disease states, such as cancer, cfDNA may carry disease-related gene variations, such as mutations, methylation, etc.; the half-life of cfDNA in blood circulation is usually very short, generally between minutes and hours; due to the diversity of cfDNA sources, its concentration may be affected by various factors, such as diet, drugs, etc. Therefore, it is necessary to ensure the consistency of experimental conditions when performing cfDNA detection to obtain reproducible results. cfDNA is a non-invasive biomarker with a wide range of sources and diverse characteristics, which can reflect the health status and disease progression of the body to a certain extent. Detecting cfDNA can provide more information about the diagnosis, treatment, and monitoring of diseases such as breast cancer.

There is a certain association and influence between cfDNA and breast cancer. Breast cancer is a common malignant tumor, and its occurrence and development are related to changes in cfDNA. The cfDNA released by breast cancer cells into the blood circulation can reflect the status and progress of breast cancer to a certain extent. These genetic variations can be detected and analyzed by high-throughput sequencing and other technologies, providing important information for the diagnosis, treatment, and monitoring of breast cancer. The concentration and level of cfDNA can be used as an indicator of breast cancer prognosis. For example, a high concentration of cfDNA may indicate an increase in the proliferation and release of breast cancer cells, suggesting that the prognosis of patients may be poor. By detecting gene variations in cfDNA, breast cancer patients can be provided with personalized treatment recommendations and monitoring options. For example, if a mutation in a specific gene is detected in a patient's cfDNA, targeted drug therapy for the mutation can be selected. In addition to being used as a biomarker, cfDNA can also be used as an emerging tool for breast cancer research. By analyzing cfDNA, it is possible to explore the pathogenesis, drug resistance, and metastasis of breast cancer, and provide more ideas and basis for the prevention, diagnosis, and treatment.

The cfDNA released by TNBC cells may have some unique characteristics, such as high concentration and high mutation rate. If a mutation in a specific gene is detected in a patient's cfDNA, targeted drug therapy targeting that mutation can be selected. The results of this study show that the cfDNA content in the peripheral blood of TNBC patients has no obvious correlation with tumor stage and clinicopathological features, but there is a correlation with relatively good clinical prognosis. This study suggests that cfDNA content is an important indicator of poor prognosis in TNBC patients, and cfDNA content can be considered as one of the reference indicators when formulating clinical treatment plans for TNBC patients. This study shows that the cfDNA content in the peripheral blood of TNBC patients is correlated with clinicopathological features (tumor size, lymph node metastasis, TNBC pathological type) and hormone receptor expression. Moreover, the content of cfDNA in the TNBC group was higher than that in the non-TNBC group ($P < 0.05$). The results of this study show that cfDNA content can be used as a diagnostic marker of TNBC, which can be used to guide the early diagnosis and treatment of TNBC and provide more treatment opportunities for TNBC patients.

However, the number of cases included in this study is small, and there may be problems such as a small sample size and short follow-up time, which lead to the fact that the research results cannot fully

represent the actual situation of TNBC patients. Therefore, it is necessary to expand the sample size and conduct multi-center follow-ups of patients to further verify the correlation between cfDNA content and clinicopathological features.

In summary, cfDNA offers significant clinical benefits in the detection and management of breast cancer. It is possible to obtain valuable information on the progression and treatment effects of breast cancer by investigating the cfDNA level and its gene variation. This non-invasive detection method has a wide range of applications including early screening, auxiliary diagnosis, curative effect evaluation, and monitoring of recurrence in breast cancer.

Disclosure statement

The authors declare no conflict of interest.

References

[1] Wang Z, Yang L, Huang Y, et al, 2023, Analysis of MutT Homologous Protein 1 Gene Status and Immunotherapy Efficacy and Prognosis in Patients With Triple-Negative Breast Cancer. Chinese Journal of Eugenics and Genetics, 31(6): 1162–1170.

[2] Si G, Shan C, 2023, Research Progress of Exosomal Non-Coding RNA in Triple-Negative Breast Cancer. Journal of Shandong First Medical University (Shandong Academy of Medical Sciences), 44(6): 461–465.

[3] Tao Y, Zhang L, Chen D, 2023, Expression of AR in ER-Positive and Negative Breast Cancer And Its Clinical Significance. Journal of Practical Cancer, 38(6): 879–881 + 887.

[4] Shan S, Wang H, Wang F, et al, 2023, The Predictive Value of NLR Combined With Serum CA15-3, NGF, and BSP for Postoperative Bone Metastasis in Patients with Triple-Negative Breast Cancer. Laboratory Medicine and Clinic, 20(10): 1369–1373.

[5] Yang K, 2023, Factors Influencing the Prognosis of Triple-Negative Breast Cancer. Chinese Contemporary Medicine, 30(2): 109–113.

[6] Xiao H, Zhang L, Gu L, 2022, Research Progress of CDK4/6 Inhibitors in Neoadjuvant Therapy of HR-Positive/HER2-Negative Breast Cancer. Tumor, 42(12): 835–844.

[7] Yang F, Wang L, Liu Y, et al, 2017, Study on the Clinical Value of Peripheral Blood cfDNA and Long Fragment DNA Concentration in Patients With Breast Cancer. Clinical Medicine Literature, 4(94): 18497–18498.

[8] Yi Z, Ma F, Yuan L, et al, 2017, Clinical Analysis of Circulating Tumor DNA in Predicting Resistance to Endocrine Therapy in Patients with Hormone Receptor-Positive Advanced Breast Cancer. Chinese Journal of Breast Diseases (Electronic Edition), 11(3): 132–137.

[9] Cheng Z, Xu W, Chen Y, 2020, Comparison of the Application Value of Combined Detection of Blood CTCs and cfDNA and Traditional Tumor Marker Detection in Auxiliary Diagnosis of Breast Cancer. Journal of Clinical and Experimental Medicine, 19(9): 994–997.

[10] Wang C, Wang Z, Jiang Q, 2022, Observation on the Curative Effect of TX, GX, NX Regimens in the Treatment of Advanced Triple-Negative Breast Cancer and Its Impact on the Long-Term Prognosis of Patients. Journal of Hunan Normal University (Medical Edition), 19(3): 149–151.

[11] Fan X, Fu J, Liu J, 2021, Application of Detection of Circulating Tumor Cells and Circulating Free DNA in Peripheral Blood in Patients with Breast Cancer. Journal of Diagnostic Pathology, 1(28): 47–54.

[12] Chang L, Yang D, Liu D, 2020, Application of Blood CTCs and cfDNA Detection in Breast Cancer. Journal of Molecular Diagnosis and Therapy, 12(10): 1298–1302.

[13] Liu Z, 2020, Effect Analysis of Immunohistochemical Detection in Pathological Diagnosis of Breast Cancer. China Practical Medicine, 15(23): 4–7.

[14] Ghoncheh M, Pournamdar Z, Salehiniya H, 2016, Incidence and Mortality and Epidemiology of Breast Cancer in the World. Asian Pacific Journal of Cancer Prevention, 17: 43–46. https://doi.org/10.7314/apjcp.2016.17.s3.43

[15] Ferlay J, Soerjomataram I, Dikshit R, et al, 2015, Cancer Incidence and Mortality Worldwide: Sources, Methods and Major Patterns in GLOBOCAN 2012. International Journal of Cancer, 136: E359–E386. https://doi.org/10.1002/ijc.29210

Proceedings of Anticancer Research, 2023, Volume 7, Issue 4
http://ojs.bbwpublisher.com/index.php/PAR
ISSN Online: 2208-3553
ISSN Print: 2208-3545

A Study on Yeast Using the Photoreactivation Process to Repair the Pyrimidine Dimer Mutations

Yichen Liu*

Shandong University, Jinan 250100, China

***Corresponding author:** Yichen Liu, mushoufangah@126.com

Abstract: Sunlight has an indispensable importance for living things in nature [1-3]. However, the direct absorption of UV will lead to the formation of pyrimidine dimers between adjacent pyrimidines in DNA strands usually in the form of cyclobutene pyrimidine dimers (CPDs) and pyrimidine (6-4) pyrimidone photoproducts (6-4PPs) which causes great damage [4-6]. A DNA repair system, known as photoreactivation, can effectively repair the dimers using photolyase [7-9], which has currently been found in plants, prokaryotic and eukaryotic cells [10-12]. This study was carried out to determine whether photolyase DNA repair can be observed in yeast. Several yeast Petri dishes were treated with ultraviolet radiation, different treatments were then added to them, and the colonies were counted after culturing, hence verifying that yeasts can use the photoreactivation process.

Keywords: Photoreactivation; DNA repair; Photolyase

Online publication: July 25, 2023

1. Introduction

The yeast *Saccharomyces cerevisiae* (*S. cerevisiae*) is a unicellular eukaryote that has haploid and diploid forms. *S. cerevisiae* is widely distributed in nature, and its growth rate is significantly affected by environmental changes, of which temperature and pH value are the two main aspects [13,14]. It is acidophilic and the optimal growth temperature is 28–30°C. Commonly used as a model organism for studying eukaryotes, *S. cerevisiae* has many identical structures with animal and plant cells and is easy to culture. It is also the most commonly used biological species in fermentation, as people often use it as the main strain for alcohol production and juice fermentation [15,16].

2. Materials and Methods

2.1. Selection of dilution of the yeast culture and the UV-C exposure time

Sixty-three Petri dishes of *S. cerevisiae* were plated with a dilution of 1/10 and 1/100, respectively. They were located under the same UV-C light intensity and other environmental factors. The most suitable UV-C exposure time was determined to achieve LD_{50} (the dose that kills 50% of the test population), ensuring the damaged cells were not too few and not representative due to short duration, or too many due to long duration. Hence, 9 of each dilution were removed every 30 s including time point 0 followed by colonies counting after visible colonies formation. The data was plotted to fit a linear model that indicated the optimal dilution and UV-C LD_{50}, which were 1/100 and 1.5 min, respectively.

2.2. The UV-C radiation and light exposure experimental procedure

A total of 30 yeast dishes with a dilution of 1/100 were distributed under 3 experimental conditions evenly: (1) non-UV radiated yeasts (nonirradiated group); (2) UV-radiated and kept in the dark after radiation 1.5 min (irradiated dark group); and (3) UV-radiated and exposed to the sun after radiation 1.5 min (irradiated light group). These Petri dishes were all placed in the same environment of 25℃, 70% relative humidity, and with the same light irradiation intensity and other confounding factors. Each group had 10 replications. All the Petri dishes were inserted into an incubator to allow living cells for colony formation and counting.

2.3. Statistical analysis

The initial data was plotted to fit a linear model in order to select the optimal dilution and calculate the UV-C LD_{50}. One-way ANOVA and Tukey HSD in the RStudio were used to observe whether there is statistically significant photoreactivation.

In the ANOVA, the null hypothesis was assumed to be no difference between living cell count across the treatment. The outliers in the data were removed and checked with diagnostic plots.

In the Tukey HSD test, the data were made in pairs and divided into 3 categories: (1) the irradiated light and irradiated dark; (2) the nonirradiated and irradiated dark; (3) the nonirradiated and irradiated light. Three null hypotheses were made:

(1) There is no difference between the mean cell count in the irradiated light and irradiated dark groups.
(2) There is no difference between the mean cell count in the nonirradiated and irradiated dark groups.
(3) There is no difference between the mean cell count in the nonirradiated and irradiated light groups.

3. Results

Figure 1 showed the number of cells at 1/10 and 1/100 dilutions at different exposure times. There were hundreds of colonies per plate with 1/10 dilution which were all bigger than that with 1/100 dilution. There were less than 200 cells in all of the 1/100 dilution cultures.

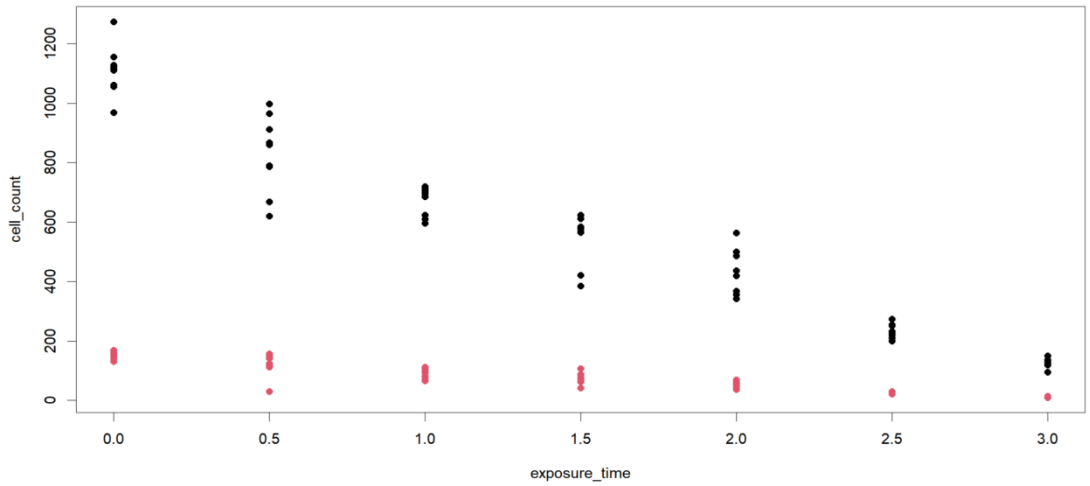

Figure 1. The scatter plot of the 1/10 and 1/100 dilution cultures data at different exposure times.

Figure 2 showed the regression line of the changes in cell count with exposure time where half of the cell population died at 1.5 min. In other words, the LD_{50} is 1.5 min.

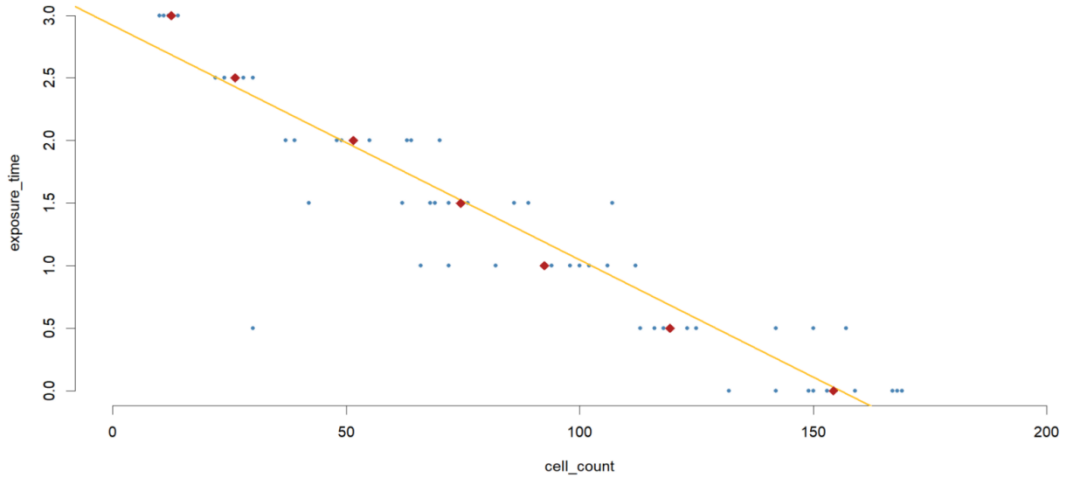

Figure 2. The plot of the regression line showed the changes in cell count with exposure time.

The data of cell numbers in the nonirradiated, irradiated dark, and irradiated light groups were plotted with a boxplot in RStudio. Almost all data were concentrated below 200. However, two plates in each treatment with an unusually high number of colonies were observed.

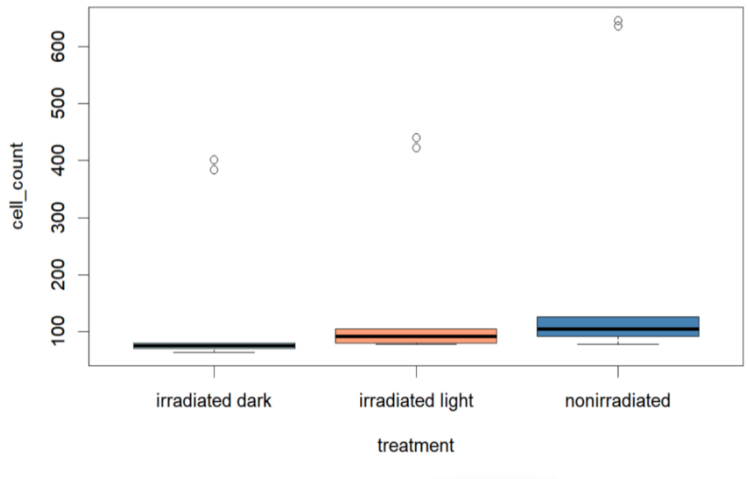

Figure 3. Distribution of yeast colony number in box plot under three environmental conditions.

The data with outliers removed were plotted with a boxplot. As shown in **Figure 4**, the number of living yeast in the nonirradiated group was the highest, whereas the irradiated light group had more living yeast colonies than the irradiated dark group, but both groups had lesser living yeast colonies than the nonirradiated group.

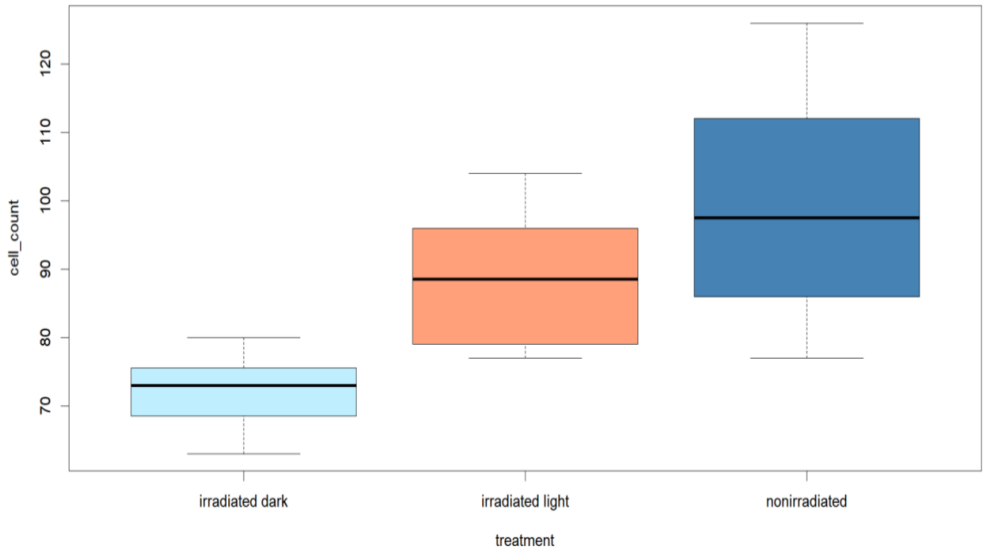

Figure 4. Distribution of yeast colony number in boxplot under three environmental conditions after removing the outliers.

The average number of living yeast in each treatment category was calculated. According to **Table 1**, the nonirradiated group had the highest cell count while the cell count in the dark environment was the least.

Table 1. The mean number of cells calculated in each treatment category

Treatment	Cell count
Irradiated dark	72.125
Irradiated light	88.500
Nonirradiated	99.250

To calculate the mean squares, the *F*-statistic, and the *P*-value, the ANOVA was used (results shown in **Figure 5**). The *P*-value found was 0.000654.

```
            Df Sum Sq Mean Sq F value   Pr(>F)
treatment    2   2985  1492.6   10.61 0.000654 ***
Residuals   21   2954   140.7
---
Signif. codes:  0 ‘***’ 0.001 ‘**’ 0.01 ‘*’ 0.05 ‘.’ 0.1 ‘ ’ 1
```

Figure 5. The ANOVA of data analysis in RStudio.

Figure 6 shows the Tukey HSD test analysis of the data. The Tukey HSD test showed the *P*-values of the 3 categories were 0.03, 0.00047, and 0.19, respectively.

```
  Tukey multiple comparisons of means
    95% family-wise confidence level

Fit: aov(formula = cell_count ~ treatment, data = y.fix)

$treatment
                                    diff       lwr      upr     p adj
irradiated light-irradiated dark  16.375  1.426694 31.32331 0.0301853
nonirradiated-irradiated dark     27.125 12.176694 42.07331 0.0004652
nonirradiated-irradiated light    10.750 -4.198306 25.69831 0.1898423
```

Figure 6. Tukey HSD test of data analysis in Rstudio.

In **Figure 7**, the 95% confidence intervals of the test statistics were plotted, and the intervals of nonirradiated-irradiated light included 0.

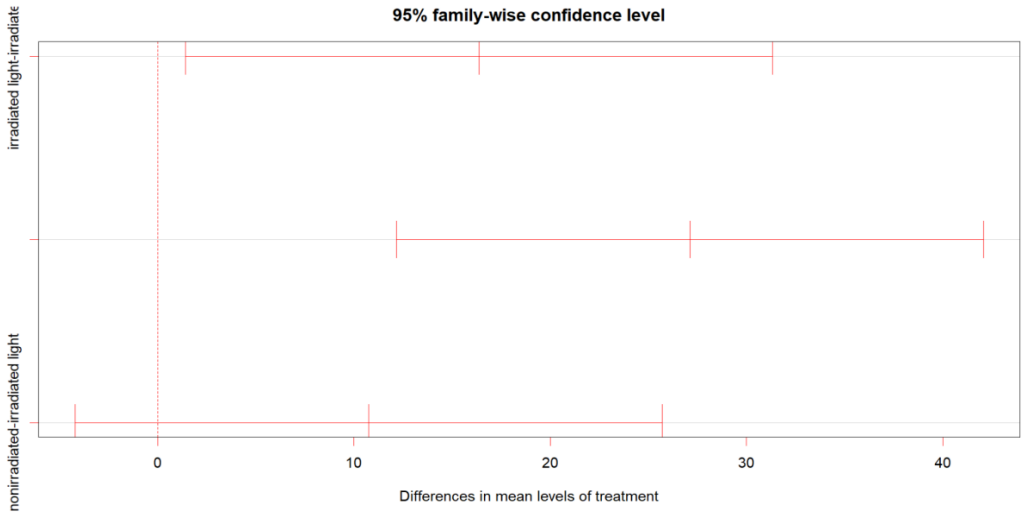

Figure 7. The plot of the 95% confidence intervals of the test statistics.

In **Figure 8**, the 'Residuals vs Fitted' plot showed a red line close to being horizontal at 0, and some of the points were randomly and evenly distributed. In the 'Normal Q-Q' plot, a line of best fit was drawn from the points. The 'Scale-Location' plot showed a steeper red line as compared to the 'Residuals vs Fitted' plot. The 'Constant Leverage: Residuals vs Factor Levels' plot showed a near horizontal red line as there are some points further than 2 units from the 0.

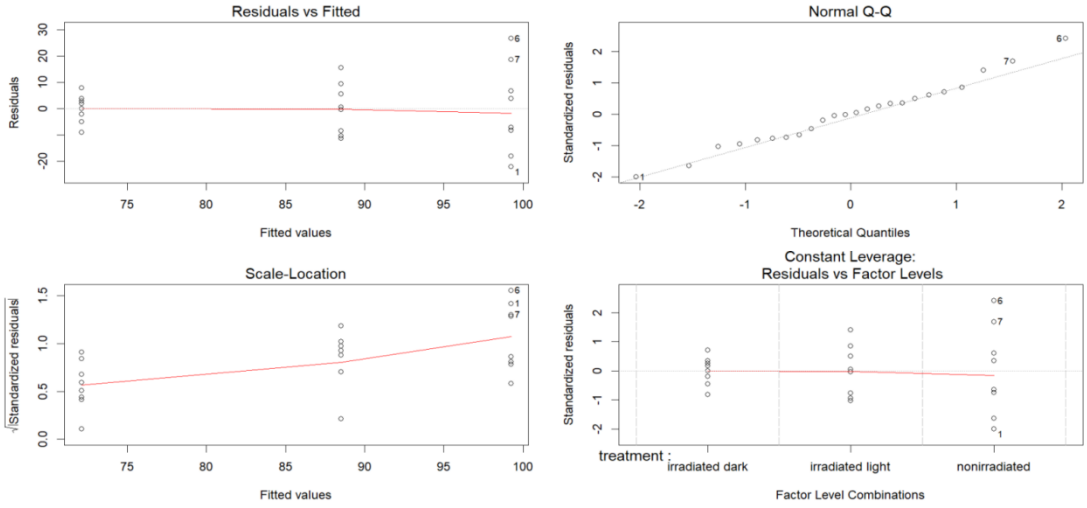

Figure 8. The diagnostic plots to check the assumption of ANOVA.

4. Discussion

4.1. Analysis of the distribution of yeast colony number in the boxplot

According to **Figure 2** and **Table 1**, the number of living cells in both groups after irradiation was lower than that in the nonirradiated group, which indicated that UV irradiation affected the cells. Meanwhile, the boxplot intuitively showed that light, such as sunlight, helps promote the DNA repair of *S. cerevisiae*. However, the efficiency of DNA repair in the dark environment is comparatively low. Hence, it is deduced

that the DNA repair degree of *S. cerevisiae* in light is higher than that in dark environments.

4.2 Analysis of ANOVA

According to ANOVA, the *P*-value is 0.000654 which is much smaller than the significance level $\alpha = 0.05$. Also, the assumption of ANOVA was checked by diagnostic plots shown in **Figure 6**. Therefore, the null hypothesis is rejected, and it is concluded that there is some relation between the living cell count and the treatment. Hence, it is preliminarily found that *S. cerevisiae* had a certain photoactivated DNA repair mechanism.

4.3. Analysis of Tukey HSD test and the 95% confidence intervals

According to the Tukey HSD test, the *P*-value of the nonirradiated-irradiated light groups is 0.19 which is bigger than the significance level $\alpha = 0.05$, and the intervals of nonirradiated-irradiated light groups included 0, making it statistically insignificant, so the null hypothesis is not rejected. On the other hand, the *P*-value in the irradiated light and the irradiated dark groups is 0.03 which is smaller than $\alpha = 0.05$, so the null hypothesis is rejected and there is some difference between the irradiated light and the irradiated dark groups. From this perspective, it is concluded that there is little difference in the viable count between the nonirradiated and irradiated light groups despite the irradiated light group having UV-damaged DNA followed by a period of sunlight exposure. However, the DNA repair rate in the irradiated light group is significantly higher than that in the irradiated dark group, which is consistent with the fact that yeast preferentially uses photolyase to repair non-transcribe strands of active RNA polymerase II and III transcribed genes instead of nucleotide excision repair (NER), leading to higher efficiency in DNA repairing [17-19].

4.4. Limitations of the study

Although the confounding variables of the different groups were controlled to be identical, there may still be variations that existed, for example, the inconsistency in the state of the ultraviolet lamp used in each group, the intensity of light, and the initial cell activity of different yeast groups, which are likely reflected in the outliers in **Figure 3**. Furthermore, some deviations in the statistical analysis are shown as the outliers in 'Residuals vs Factor levels' in **Figure 8**, which makes the ANOVA slightly imprecise. The sample size in subsequent experiments should be increased to reduce the chance of variations in experimental results [20].

5. Conclusion

In this study, there is no difference between the nonirradiated and irradiated light groups, but there is a significant difference in DNA repair rate between the irradiated light and irradiated dark groups, which indicated the efficient DNA repair mechanism of photolyase after a period of sunlight exposure despite DNA being damaged by UV. The photolyase DNA repair mechanism is observed in yeast, and it is concluded that yeast can use the photoreactivation process which uses photolyase and the light energy to repair the pyrimidine dimer mutations.

Disclosure statement

The author declares no conflict of interest.

References

[1] Banaś AK, Zgłobicki P, Kowalska E, et al, 2020, All You Need is Light. Photorepair of UV-Induced

Pyrimidine Dimers. Genes, 11(11): 1–17. https://doi.org/10.3390/genes11111304

[2] Wright KP Jr, McHill AW, Birks BR, et al, 2013, Entrainment of the Human Circadian Clock to the Natural Light-Dark Cycle. Curr Biol, 23(16): 1554–1558. https://doi.org/10.1016/j.cub.2013.06.039

[3] Holick MF, Chen TC, Lu Z, et al, 2007, Vitamin D and Skin Physiology: A D-Lightful Story. J Bone Miner Res, 22 Suppl 2: V28–V33. https://doi.org/10.1359/jbmr.07s211

[4] Schuch AP, Moreno NC, Schuch NJ, et al, 2017, Sunlight Damage to Cellular DNA: Focus on Oxidatively Generated Lesions. Free Radic Biol Med, 107: 110–124. https://doi.org/10.1016/j.freeradbiomed.2017.01.029.

[5] Eischeid AC, Linden KG, 2007, Efficiency of Pyrimidine Dimer Formation in *Escherichia coli* Across UV Wavelengths. J Appl Microbiol, 103(5): 1650–1656. https://doi.org/10.1111/j.1365-2672.2007.03424.x

[6] Douki T, von Koschembahr A, Cadet J, 2017, Insight in DNA Repair of UV-Induced Pyrimidine Dimers by Chromatographic Methods. Photochem Photobiol, 93(1): 207–215. https://doi.org/10.1111/php.12685

[7] Fingerhut BP, Heil K, Kaya E, et al, 2012, Mechanism of UV-Induced Dewar Lesion Repair Catalysed by DNA (6-4) Photolyase. Chemical Science, 3(6): 1794–1797. https://doi.org/10.1039/c2sc20122d

[8] Ramírez-Gamboa D, Díaz-Zamorano AL, Meléndez-Sánchez ER, et al, 2022, Photolyase Production and Current Applications: A Review. Molecules, 27(18): 5998. https://doi.org/10.3390/molecules27185998

[9] Fukui A, Hieda K, Matsudaira Y, 1978, Light-Flash Analysis of the Photoenzymic Repair Process in Yeast Cells. I. Determination of the Number of Photoreactivating Enzyme Molecules. Mutat Res, 51(3): 435–439. https://doi.org/10.1016/0027-5107(78)90133-1

[10] Painter RB, 1974, DNA Damage and Repair in Eukaryotic Cells. Genetics, 78(1): 139–148. https://doi.org/10.1093/genetics/78.1.139

[11] Heelis PF, Kim ST, Okamura T, et al, 1993, The Photo Repair of Pyrimidine Dimers by DNA Photolyase and Model Systems. J Photochem Photobiol B, 17(3): 219–228. https://doi.org/10.1016/1011-1344(93)80019-6

[12] Tuteja N, Ahmad P, Panda BB, et al, 2009, Genotoxic Stress in Plants: Shedding Light on DNA Damage, Repair and DNA Repair Helicases. Mutat Res, 681(2–3): 134–149. https://doi.org/10.1016/j.mrrev.2008.06.004

[13] Belda I, Ruiz J, Santos A, et al, 2019, *Saccharomyces cerevisiae*. Trends Genet, 35(12): 956–957. https://doi.org/10.1016/j.tig.2019.08.009

[14] Duina AA, Miller ME, Keeney JB, 2014, Budding Yeast for Budding Geneticists: A Primer on the *Saccharomyces cerevisiae* Model System. Genetics, 197(1): 33–48. https://doi.org/10.1534/genetics.114.163188

[15] Nielsen J, 2019, Yeast Systems Biology: Model Organism and Cell Factory. Biotechnol J, 14(9): e1800421. https://doi.org/10.1002/biot.201800421

[16] Kouamé C, Loiseau G, Grabulos J, et al, 2021, Development of a Model for the Alcoholic Fermentation of Cocoa Beans by a *Saccharomyces cerevisiae* Strain. Int J Food Microbiol, 337: 108917. https://doi.org/10.1016/j.ijfoodmicro.2020.108917

[17] Suter B, Livingstone-Zatchej M, Thoma F, 1997, Chromatin Structure Modulates DNA Repair by Photolyase *in vivo*. EMBO J, 16(8): 2150–2160. https://doi.org/10.1093/emboj/16.8.2150

[18] Morse NR, Meniel V, Waters R, 2002, Photoreactivation of UV-Induced Cyclobutane Pyrimidine

Dimers in the MFA2 Gene of *Saccharomyces cerevisiae*. Nucleic Acids Res, 30(8): 1799–1807. https://doi.org/10.1093/nar/30.8.1799

[19] Sinha RP, Häder DP, 2002, UV-Induced DNA Damage and Repair: A Review. Photochem Photobiol Sci, 1(4): 225–236. https://doi.org/10.1039/b201230h

[20] Engel SR, Dietrich FS, Fisk DG, et al, 2014, The Reference Genome Sequence of *Saccharomyces cerevisiae*: Then and Now. G3 (Bethesda), 4(3): 389–398. https://doi.org/10.1534/g3.113.008995

Proceedings of Anticancer Research, 2023, Volume 7, Issue 4
http://ojs.bbwpublisher.com/index.php/PAR
ISSN Online: 2208-3553
ISSN Print: 2208-3545

The Effect of TSH Suppression Therapy on the Efficacy and Immune Function of Postoperative Patients with Thyroid Cancer

Quan Shi*

The Affiliated Traditional Chinese Medicine Hospital of Southwest Medical University, Luzhou 646000, China

***Corresponding author:** Quan Shi, shiquan1808@163.com

Abstract: *Objective:* To investigate the efficacy and immune function of thyroid stimulating hormone (TSH) suppression therapy in postoperative thyroid cancer patients. *Methods:* Sixty thyroid cancer patients admitted from July 2020–July 2022 were recruited and randomly divided into two groups. The control group (30 patients) received hormone replacement therapy, while the study group (30 patients) received TSH suppression therapy. The thyroid function, clinical efficacy, immune function, and tumor markers of the two groups were compared. *Results:* After treatment, the levels of free triiodothyronine (FT3) and thyroxine (FT4) in both groups increased significantly, while TSH levels decreased significantly. Moreover, the magnitude of change in the study group was greater than that in the control group ($P < 0.05$). The total effective rate in the study group was significantly higher as compared to the control group ($P < 0.05$). After treatment, the levels of CD3+ and CD4+ cells in both groups of patients increased significantly, with the study group showing significantly higher levels than the control group, whereas the level of CD8+ cells decreased significantly, with the study group having lower levels than the control group ($P < 0.05$). After treatment, the levels of Tg and CEA in both groups were significantly lowered as compared to before treatment, and the levels of Tg and CEA in the study group were significantly lower than the control group ($P < 0.05$). *Conclusion:* TSH suppression therapy in postoperative thyroid cancer patients can improve thyroid function, suppress the levels of tumor markers, and enhance immune function, thereby achieving good clinical outcomes.

Keywords: TSH suppression therapy; Thyroid cancer; Postoperative; Efficacy; Immune function

Online publication: July 27, 2023

1. Introduction

Thyroid cancer is a relatively common malignant tumor in clinical practice [1,2]. It typically grows slowly, but certain types of thyroid cancer can be invasive and have the potential to spread to tissues and organs beyond the thyroid [3,4]. If left untreated, tumor progression can pose a risk to the patient's trachea and recurrent laryngeal nerves, and in severe cases, metastasis may occur, leading to a worsened prognosis [5]. Treatment options for postoperative thyroid cancer include hormone replacement therapy (HRT) and suppression therapy of thyroid-stimulating hormone (TSH). The main difference between these two treatment methods lies in the range of controlling serum TSH levels. There has been an ongoing debate regarding the advantages and disadvantages of these treatment methods in clinical practice [6,7]. Therefore, this study aims to investigate the efficacy and immune function of TSH suppression therapy in postoperative patients with thyroid cancer, aiming to provide insights into the clinical treatment of postoperative thyroid cancer. The findings are reported as follows.

2. Materials and methods

2.1. General information

Sixty patients with thyroid cancer admitted to the Affiliated Traditional Chinese Medicine Hospital of Southwest Medical University from July 2020 to July 2022 were selected as the study subjects. They were randomly assigned using a random number table into a study group and a control group, with 30 patients in each group. In the study group, there were 10 male patients and 20 female patients, with an age range of 25 to 76 years old and an average age of 50.25 ± 9.13 years old. The pathological types included 18 cases of papillary thyroid carcinoma, 5 cases of follicular thyroid carcinoma, 3 cases of medullary thyroid carcinoma, and 4 cases of mixed-type thyroid carcinoma. The tumor stages were as follows: 8 cases in stage I, 14 cases in stage II, and 8 cases in stage III. In the control group, there were 13 male patients and 17 female patients, with an age range of 24 to 78 years old and an average age of 51.25 ± 8.53 years old. The pathological types included 15 cases of papillary thyroid carcinoma, 6 cases of follicular thyroid carcinoma, 4 cases of medullary thyroid carcinoma, and 5 cases of mixed-type thyroid carcinoma. The tumor stages were as follows: 9 cases in stage I, 15 cases in stage II, and 6 cases in stage III. There were no statistically significant differences in general information between the two groups ($P > 0.05$). Both patients and their families were informed about the study protocol and signed informed consent forms approved by the hospital's ethics committee.

2.2. Inclusion and exclusion criteria

Inclusion criteria included patients who meet the requirements for surgical treatment, patients who meet the diagnostic criteria for thyroid cancer and have been confirmed by pathological examination, patients with an estimated survival of more than 12 months, and patients without significant cardiovascular, cerebrovascular, renal, pulmonary, hematological, or mental system diseases, and able to actively participate in the study.

Exclusion criteria included female patients during lactation or pregnancy, patients with significant impairment of vital organs such as the heart, liver, or kidneys, such as congenital heart disease, diabetes, and renal failure, and patients with concomitant other cancers, such as lung cancer.

2.3. Methods

The control group received thyroid HRT. Patients were treated with oral levothyroxine sodium tablets, starting with an initial dose of 50 μg/day, taken in the morning. After two weeks, the dose was increased to 100 μg/day. The study group received TSH suppression therapy, using the same medication and dosage as the control group. During the treatment period, TSH levels were measured monthly for both groups, and the dosage of levothyroxine was adjusted based on the results. In the control group, TSH levels were maintained within the normal range [0.3–5.0 milli-international units per liter (mIU/L)], while in the suppression group, TSH levels were kept within the normal range or slightly elevated but still lower than the range seen in hyperthyroidism (0.05–0.1 mIU/L).

2.4. Observational indicators

Observational indicators in this study included:

(1) Assessment of thyroid function in both groups of patients: Before and after treatment, 5 mL of fasting venous blood was collected in the morning, and serum was obtained through anticoagulation and centrifugation. TSH, free triiodothyronine (FT3), and free thyroxine (FT4) levels were measured using a fully automated biochemical analyzer, following the instructions provided in the reagent kit. The measurements were performed by two laboratory physicians.

(2) Comparison of clinical efficacy between the two groups of patients: This includes clinical symptoms

and thyroid function indicators. If clinical symptoms and thyroid function indicators return to normal or improve by more than 30% compared to before treatment, it is considered significantly effective. If both clinical symptoms and thyroid function indicators show improvement by 10% to 30% compared to before treatment, it is considered effective. If there are no significant changes in clinical symptoms and thyroid function indicators, or if the improvement is less than 10% compared to before treatment, it is considered ineffective. The overall effective rate is calculated as (significantly effective/n + effective/n) × 100%.

(3) Comparison of immune function levels between the two groups of patients: Before and after treatment, 5 mL of fasting venous blood was collected in the morning, and serum was obtained through anticoagulation and centrifugation. Flow cytometry was used to measure the levels of CD3+, CD4+, and CD8+ cells in each group.

(4) Comparison of tumor marker levels between the two groups of patients: This includes the measurement of thyroglobulin (Tg) and carcinoembryonic antigen (CEA) levels. Before and after treatment, 5 ml of fasting venous blood was collected in the morning, and serum was obtained through anticoagulation and centrifugation. Tg levels were measured using a fully automated electrochemiluminescence immunoassay analyzer, and CEA levels were measured using the same analyzer. All measurements were performed according to the instructions provided in the reagent kit, and two laboratory physicians conducted unified testing to ensure the accuracy of the results.

2.5. Statistical methods

The data were analyzed using SPSS 22.0 software. Continuous variables are presented as mean ± standard deviation (SD). The *t*-test was used to compare continuous variables between the two groups. Categorical variables are presented as [n (%)] and compared using the chi-square test between the two groups. A *P* value of < 0.05 was considered statistically significant for determining differences.

3. Results

3.1. Assessment of thyroid function in the two groups of patients.

Before treatment, there were no significant differences in TSH, FT3, and FT4 levels between the two groups ($P > 0.05$). After treatment, the levels of FT3 and FT4 in both groups of patients increased significantly, while TSH levels decreased significantly. Furthermore, the magnitude of change in the study group was greater than that in the control group ($P < 0.05$). Please refer to **Table 1** for detailed information.

Table 1. Comparison of thyroid function between the two groups of patients (mean ± SD)

Time	Group	Number of cases	TSH (mU/L)	FT3 (pmol/L)	FT4 (pmol/L)
Pre-treatment	Study group	30	4.76 ± 0.82	2.17 ± 0.96	10.85 ± 3.78
	Control group	30	4.52 ± 0.68	2.09 ± 0.71	10.42 ± 3.36
	t value		1.234	0.367	0.466
	P value		0.222	0.715	0.643
Post-treatment	Study group	30	0.97 ± 0.60*	6.25 ± 1.32*	25.04 ± 2.57*
	Control group	30	3.01 ± 0.82$^{\#}$	4.24 ± 1.02$^{\#}$	17.38 ± 2.13$^{\#}$
	t value		10.997	6.600	12.569
	P value		0.000	0.000	0.000

Note: $P < 0.05$ when compared to the pre-treatment values within the same group. * for the study group. $^{\#}$ for the control group.

3.2. Comparison of clinical efficacy between the two groups of patients

The overall effective rate of the study group was significantly higher than that of the control group ($P < 0.05$). Please refer to **Table 2** for detailed information.

Table 2. Comparison of clinical efficacy between the two groups of patients [n (%)]

Group	Number of cases	Ineffective	Effective	Significantly effective	Overall response rate
Study group	30	3 (10.00)	13 (43.33)	14 (46.67)	27 (90.00)
Control group	30	10 (33.33)	11 (36.67)	9 (30.00)	20 (66.67)
χ^2 value					4.812
P value					0.028

3.3. Comparison of immune function levels between the two groups of patients

Before treatment, there were no significant differences in the levels of CD3+, CD4+, and CD8+ cells between the two groups of patients ($P > 0.05$). After treatment, the levels of CD3+ and CD4+ cells in both groups of patients increased significantly, with the study group showing significantly higher levels than the control group ($P < 0.05$). Additionally, the level of CD8+ cells decreased significantly, with the study group having lower levels than the control group ($P < 0.05$). Please refer to **Table 3** for detailed information.

Table 3. Comparison of immune function levels between the two groups of patients (mean ± SD)

Time	Group	Number of cases	$CD3^+$	$CD4^+$	$CD8^+$
Pre-treatment	Study group	30	53.26 ± 6.31	28.23 ± 3.12	37.32 ± 5.16
	Control group	30	53.52 ± 5.62	28.04 ± 3.05	37.65 ± 4.87
	t value		0.169	0.239	0.255
	P value		0.867	0.812	0.800
Post-treatment	Study group	30	67.56 ± 7.21*	41.32 ± 4.20*	24.57 ± 3.22*
	Control group	30	60.03 ± 6.57$^{\#}$	34.72 ± 4.36$^{\#}$	30.06 ± 3.72$^{\#}$
	t value		4.228	5.971	6.112
	P value		0.000	0.000	0.000

Note: $P < 0.05$ when compared to the pre-treatment values within the same group. * for the study group. $^{\#}$ for the control group.

3.4. Comparison of tumor marker levels between the two groups of patients

There were no significant differences in the levels of Tg and CEA between the two groups of patients before treatment ($P > 0.05$). However, after treatment, the levels of Tg and CEA in both groups were significantly lowered as compared to before treatment, and the levels of Tg and CEA in the study group were significantly lower than the control group ($P < 0.05$). Please refer to **Table 4** for detailed information.

Table 4. Comparison of tumor marker levels between the two groups of patients (mean ± SD)

Time	Group	Number of cases	Tg (ng/mL)	CEA (U/mL)
Pre-treatment	Study group	30	42.57 ± 8.56	6.75 ± 1.52
	Control group	30	43.82 ± 9.82	6.42 ± 1.38
	t value		0.526	0.880
	P value		0.601	0.382

(Continued on next page)

(Continued from previous page)

Time	Group	Number of cases	Tg (ng/mL)	CEA (U/mL)
Post-treatment	Study group	30	14.12 ± 3.67*	2.92 ± 0.34*
	Control group	30	19.87 ± 5.06#	3.96 ± 0.57#
	t value		5.038	8.583
	P value		0.000	0.000

Note: $P < 0.05$ when compared to the pre-treatment values within the same group. * for the study group. # for the control group.

4. Discussion

Thyroid cancer is a relatively common malignant tumor of the endocrine system, although it accounts for a small proportion of all cancers. However, the incidence rate has been gradually increasing over the years, posing a serious threat to the lives and health of the population [8,9]. Thyroid cancer arises from the uncontrolled proliferation and spread of malignant cells within the thyroid tissue, forming tumors such as papillary carcinoma, follicular carcinoma, medullary carcinoma, and undifferentiated carcinoma [10,11]. Early-stage thyroid cancer usually lacks obvious symptoms, but as the tumor grows and metastasizes, patients may experience symptoms such as neck masses, discomfort in the throat, and hoarseness of voice [12,13]. Compared to some other malignancies, thyroid cancer has a lower degree of malignancy and a slower progression rate. Most thyroid cancer patients achieve good treatment outcomes after surgical removal. However, partial or complete thyroidectomy disrupts the secretion and regulatory stability of thyroid-related hormones in the body, leading to postoperative hypothyroidism. This can significantly impact the body's energy system adjustment, protein metabolism, and stability of endocrine function [14]. Therefore, after thyroid cancer surgery, patients often require endocrine treatment to maintain thyroid hormone levels within a safe range and ensure normal thyroid function [15].

Currently, the endocrine treatment options for post-thyroid cancer surgery patients mainly include HRT and TSH suppression therapy. Most researchers believe that both supplementation and suppression are essential steps because residual thyroid tissue after surgery may grow and recur under the stimulation of TSH [16,17]. Therefore, supplementing levothyroxine can provide normal thyroid hormone levels, while TSH suppression can reduce the stimulation of residual thyroid tissue and decrease the risk of recurrence [18]. However, a small number of researchers believe that the advantages of levothyroxine supplementation outweigh TSH suppression. This is because excessive TSH suppression may lead to side effects, and some studies have shown that TSH suppression does not significantly reduce the recurrence or mortality rate of thyroid cancer [19]. As for the clinical efficacy of the two approaches, there are limited reports available currently, and the results are inconsistent. This may be attributed to the selection of different efficacy endpoints and the influence of other factors [20].

The results of this study showed that after thyroid function treatment, the levels of FT3 and FT4 in both groups of patients significantly increased, while the TSH level significantly decreased, with a greater magnitude of change in the study group compared to the control group ($P < 0.05$). This indicates that TSH suppression therapy can lower TSH levels, increase FT3 and FT4 levels, and reduce thyroid hormone levels. The total effective rate of clinical efficacy in the study group was significantly higher than that in the control group ($P < 0.05$), suggesting that TSH suppression therapy has better clinical efficacy. This is because TSH suppression therapy can increase thyroid hormone levels, and promote protein metabolism and hormone balance.

The results of this study also showed that after TSH suppression therapy, the levels of CD3+ and CD4+ cells in both groups of patients significantly increased, with the study group showing significantly higher levels than the control group, while the level of CD8+ cells significantly decreased, with the study group having lower levels than the control group ($P < 0.05$). This suggests that TSH suppression therapy can

regulate post-thyroid cancer surgery cellular immune function. The development of thyroid cancer is closely related to tumor differentiation and immune function in the body. Thyroid cancer patients have characteristics of immune dysfunction. TSH suppression therapy in post-thyroid cancer surgery can affect tumor differentiation and its relationship with the body's immune function, thereby influencing the characteristics of immune dysfunction in thyroid cancer patients. TSH suppression therapy after thyroid cancer surgery can promote postoperative recovery, reduce the occurrence of tumor recurrence and metastasis, and improve cellular immune function in thyroid cancer patients. Furthermore, the results of this study showed that the levels of tumor markers Tg and CEA after treatment were significantly lower than those in the control group before treatment, and the levels of Tg and CEA in the control group were significantly lower than those before treatment ($P < 0.05$). This indicates that TSH suppression therapy can control the serum levels of Tg and CEA in post-thyroid cancer surgery patients, effectively regulate thyroid hormone levels, stabilize thyroid function, and reduce Tg and CEA levels.

In summary, implementing TSH suppression therapy in post-thyroid cancer surgery patients improves thyroid function, suppresses tumor marker levels of Tg and CEA, and enhances immune function, demonstrating favorable clinical outcomes. These findings are valuable for clinical application and should be promoted.

Disclosure statement

The author declares no conflict of interest.

References

[1] Zhang J, Chen C, Yang Y, et al, 2022, Diagnosis and Treatment of Postoperative Persistent/Recurrent Cervical Lymph Nodes Metastases in Differentiated Thyroid Cancer. International Journal of Radiation Medicine and Nuclear Medicine, 46(11): 692–696.

[2] Ma Y, Yang S, Wang YQ, et al, 2023, Research Progress in Changes of Hormone Levels of Patients with Differentiated Thyroid Carcinoma During Pregnancy and Their Effects on Occurrence and Development of Disease. Journal of Jilin University (Medicine Edition), 49(3): 811–815.

[3] Xu FZ, Jiang CY, Yi DD, et al, 2023, Influence of Gender-Related Factors on the Occurrence and Development of Thyroid Cancer. Journal of Southeast University (Medical Science Edition), 42(1): 154–159.

[4] Yuan NH, Wei P, Liu SL, et al, 2021, Diagnostic Value of Sound Velocity Matching Technique in Thyroid Carcinoma. Imaging Science and Photochemistry, 39(2): 219–223.

[5] Huang JY, Dai QJ, Su J, et al, 2021, Choice of 131 I Ablation in Patients with Differentiated Thyroid Cancer after Partial Thyriodectomy. Journal of Cancer Control and Treatment,34(2): 143–149.

[6] Zhao FL, Kang YL, Ma YJ, et al, 2021, Effect of TSH Suppression Therapy in Elderly Patients with Thyroid Cancer After Total Thyroidectomy and on Serum Tg, TSH, CEA Levels. The Practical Journal of Cancer, 36(12): 1970–1973.

[7] Wang X, Zhao F, Yan S, 2022, Effect of TSH Inhibition Therapy on Bone Metabolism, CD44v6, and sIL-2R Levels in Patients with Differentiated Thyroid Carcinoma, China Journal of Modern Medicine, 32(23): 34–38.

[8] Yue X, Luo Z, Zhu XY, 2023, Diagnostic Value of Serum Tg and TSH in Preoperative N Staging of Thyroid Carcinoma. Chinese Journal of Laboratory Diagnosis, 27(5): 529–532.

[9] Zhang LD, Xi YC, You LQ, et al, 2018, Effects of TSH Inhibition After Total Thyroidectomy on Tg,

VEGF, TSGF, CD44V6, slL-2R and T Lymphocyte Subsets in Patients with Differentiated Thyroid Carcinoma. Journal of Hainan Medical University, 24(2): 242–245.

[10] Wu WJ, Jing JM, Gao JQ, et al, 2022, Effects of TSH Suppression Therapy on TRAb, TPOAb, and TgAb in Patients After Surgery for Differentiated Thyroid Carcinoma. Chinese Journal of Gerontology, 42(6): 1340–1342.

[11] Gao JQ, Wang J, Miao YX, et al, 2020, The Effect of Thyroid Stimulating Hormone Inhibitory Therapy on Prognosis and Serum CD44 V6 Level in Elderly Patients with Thyroid Carcinoma. Journal of North Sichuan Medical College, 35(5): 863–865 + 871.

[12] Wang Y, Pan ZY, Lin ZG, 2018, Effects of TSH Suppression Therapy on Immune Function and Serum CD44V6, FT3, and FT4 Levels in Elderly Patients with Thyroid Cancer. Chinese Journal of Gerontology, 38(5): 1110–1113.

[13] Qian WW, 2019, The Role of TSH Suppression Therapy in the Treatment of Thyroid Cancer and Its Influence on Adverse Reactions in Patients. World Latest Medicine Information (Electronic Version), 19(34): 58 + 60.

[14] Wang X, Zhao YZ, 2021, Analysis of the Effect of TSH Inhibition on Prognosis and T Cell Immune Factors in Elderly Patients with Thyroid Cancer. Chinese Journal of Practical Internal Medicine, 41(11): 978–980.

[15] Wen F, Lu P, Qin CL, et al, 2019, Effects of Atorvastatin Calcium Tablets Combined with TSH Inhibition Therapy on the Efficacy, Blood Lipid Level and Coagulation Function of Patients with Senile Thyroid Cancer After Operation and Hyperlipidemia. Journal of Hunan Normal University (Medical Science), 16(6): 120–123.

[16] Zhang J, Ren HZ, Guo YY, 2022, Relationship between BRAF V600E Mutation and L-T4 Dosage Required for TSH Inhibition Treatment Reaching the Standard After Operation in Patients with Thyroid Papillary Carcinoma. Shandong Medical Journal, 62(32): 37–40.

[17] Mei Y, Wang Q, Zhao LW, et al, 2023, Effects of TSH Inhibition Therapy on Immune Function and Bone Metabolism after Operation in Patients with Differentiation Thyroid Cancer. Chongqing Medicine, 21(6): 686–689.

[18] Zhang XJ, Li FG, Ma YQ, et al, 2023, Effects of Hormone Replacement Therapy on Alanine Aminotransferase, Free Thyroxine, Thyroid Stimulating Hormone Levels and Immune Function in Postoperative Patients with Thyroid Cancer. Oncology Progress, 21(6): 686–689.

[19] Guo YX, Sun XD, Qiang W, et al, 2022, Effect of Helicobacter pylori Infection on Standard Dose of Postoperative Thyrotropin Suppression Therapy for Differentiated Thyroid Cancer. Chinese Journal of Endocrine Surgery, 16(3): 299–302.

[20] Qiu HJ, Fang SY, Luo JG, et al, 2018, Effect of TSH Suppressive Therapy on Bone Mineral Density in Patients with Differentiated Thyroid Carcinoma. Zhejiang Medical Journal, 40(12): 1320–1323 + 1327.

Proceedings of Anticancer Research, 2023, Volume 7, Issue 4
http://ojs.bbwpublisher.com/index.php/PAR
ISSN Online: 2208-3553
ISSN Print: 2208-3545

The Diagnostic Value of Fecal *Fusobacterium nucleatum* Combined with FIT and CA199 in the Diagnosis of Colorectal Cancer

Tianhong Jia[1], Yang Yu[1], Yan Wang[1], Ming Li[2], Shuzhuo Liu[1], Wei Li[1]*

[1]Department of Laboratory Medicine, Affiliated Hospital of Hebei University, Baoding 071000, China

[2]School of Basic Medical Sciences, Hebei University, Baoding 071000, China

***Corresponding author:** Wei Li, 120073839@qq.com

Abstract: *Objective:* To analyze the diagnostic value of fecal *Fusobacterium nucleatum* detection, fecal immunochemical test (FIT), and carbohydrate antigen 19-9 (CA19-9) detection for colorectal cancer (CRC). *Method:* A total of 78 CRC patients and 60 healthy individuals were enrolled in this study. Stool and blood samples were collected for the 3 diagnoses, and ROC curves were analyzed for diagnostic value. *Result:* The 3 diagnoses' positive detection rates in CRC samples were significantly higher than those of healthy samples ($P < 0.05$). The combined CRC diagnoses showed significantly higher sensitivity as compared to individual fecal *F. nucleatum* detection ($\chi^2 = 6.495$, $P = 0.011$), FIT ($\chi^2 = 4.871$, $P = 0.027$), and serum CA19-9 detection ($\chi^2 = 7.371$, $P = 0.007$). The area under the ROC curve for fecal *F. nucleatum* detection was 0.63 [95% confidence interval (CI) = 1.124–6.238], with a sensitivity of 73.08% and specificity of 85.00%, whereas FIT was 0.65 (95% CI = 1.365–9.241), with a sensitivity of 51.28% and specificity of 96.67%, meanwhile, serum CA19-9 detection was 0.62 (95% CI = 1.517–12.342), with a sensitivity of 69.23% and specificity of 98.33%. The combined CRC diagnoses showed an area under the ROC curve of 0.76 (95% CI = 1.213–6.254), with a sensitivity of 87.18% and specificity of 70.00%. *Conclusion:* The combined diagnoses of fecal *F. nucleatum* detection, FIT, and serum CA19-9 detection can significantly improve the sensitivity and accuracy of CRC diagnosis, which has high clinical application value to provide guidance for clinical CRC screening and early intervention treatment.

Keywords: Fecal *Fusobacterium nucleatum*; Fecal immunochemical test; Carbohydrate antigen 19-9; Colorectal cancer

Online publication: July 27, 2023

1. Introduction

Colorectal cancer (CRC) is a common malignant tumor of the gastrointestinal tract. With the increase in its mortality rate, early diagnosis is of great significance in the prevention and treatment of CRC. At present, the clinical diagnosis of CRC is mainly based on stool tests, colonoscopy, and tumor marker determination. However, due to certain limitations of these methods, the diagnostic accuracy is not high. In order to reduce the mortality rate and early diagnosis of CRC, biomarkers and effective diagnostic methods have been investigated to improve the diagnosis of CRC [1,2]. The fecal immunochemical test (FIT) is a non-invasive, convenient, fast, but low-sensitivity examination [3]. Carbohydrate antigen 19-9 (CA19-9) is a tumor marker widely used in clinical practice and has important diagnostic value in tumor diseases [4]. Fecal *Fusobacterium nucleatum* (hereby *F. nucleatum*) can be enriched in the colon and rectum, which can promote the proliferation, metastasis, and invasion of intestinal cancer cells, and participate in the immune

regulation of tumor cells [5]. In this study, the joint diagnoses of fecal *F. nucleatum* detection, FIT, and serum CA19-9 were used to explore their significance in the diagnosis of CRC, aiming to provide an efficient and accurate early diagnosis method for clinical diagnosis, improve the early diagnosis rate of CRC, and further reduce the fatality rate.

2. Materials and methods

2.1. Background

A total of 78 CRC patients admitted to the Affiliated Hospital of Hebei University from January 2020 to December 2020 were continuously selected for retrospective analysis, including 49 males and 29 females, aged 28 to 79 years old, with an average age of 53.36 ± 3.42 years old. A total of 60 healthy individuals were also recruited for data comparison.

The inclusion criteria included patients who meet the diagnostic criteria for CRC in the "Standards for Diagnosis and Treatment of CRC", diagnosed with CRC by postoperative histopathological examination, and aged > 18 years, yet to receive relevant anti-tumor treatment before admission, consist of complete clinical data, and able to fulfill the obligation of disclosure, know the content of the research, and voluntarily sign a consent form.

The exclusion criteria included CRC patients diagnosed with severe heart, liver, kidney, and other vital organ diseases, respiratory system diseases, immune and inflammatory diseases, or consisted of other malignant tumors, or consisted of chronic hepatitis, ulcerative colon cancer, and other digestive system diseases, or had mental disorders or communication difficulties. The research was approved by the Hospital Ethics Committee.

2.2. Methods

2.2.1. Fecal *Fusobacterium nucleatum*

Stool samples were taken from the patients in the morning, and the DNA of fecal *F. nucleatum* was extracted using Beijing Tiangen Biochemical Technology Co., Ltd. DP328 Fecal DNA Extraction Kit. The concentration and quality of the extracted DNA were analyzed using the Nanodrop One UV-Vis spectrophotometer (Thermo Scientific, USA). The ratio of $A_{260\ nm}$ and $A_{280\ nm}$ was 1.7~1.9. The relative expression of *F. nucleatum* DNA was detected using the 7900HT real-time PCR system (Applied Biosystems, USA), and the TB Green qPCR Master Mix reagent from Dalian Bao Biological Co., Ltd. (product number 639676) was used to prepare the reaction buffer and DNA template. The PCR reaction conditions were 45 cycles of pre-denaturation at 95°C for 30 s, denaturation at 95°C for 10 s, and annealing/extension at 60°C for 35 s. The sequence of the primers for *F. nucleatum* is as follows: the upstream primer is 5'-TTCAATAAAAGTGGCAGGTCAAG-3', and the downstream primer is 5'-TAACAACACATGCAGGTCAATGG-3'. The 16S rDNA primer sequence of the total bacterial internal reference gene is as follows: the upstream primer is 5'-CCATGAAGTCGGAATCGCTAG-3', and the downstream primer is 5'-GCTTGACGGGCGGTGT-3'. The relative expression level of target bacterial DNA is represented by 2-ΔCt, ΔCt=Ct target bacterial sequence-Ct16S rDNA.

2.2.2. Fecal immunochemical test (FIT)

Two stool samples were taken from the patient in the morning, and the fecal occult blood colloidal gold detection test paper was used for detection, and the relevant operations are strictly carried out according to the test paper instructions. The criteria for a positive fecal occult blood test are (1) there are differences in the positive or negative results of two fecal occult blood tests in one specimen, and (2) there are differences between positive and negative results in one test specimen.

2.2.3. Carbohydrate antigen 19-9 (CA19-9)

About 3 mL of fasting venous blood was taken from the patient, then placed in a test tube containing separating gel, centrifuged at 3000 r/min for 10 min, and the expression of CA19-9 was detected using a fully automatic electrochemiluminescence instrument and matching kits from Roche, Germany.

2.3. Observation indicators

The observation indicators of this study are as follows:

(1) Comparison of the positive detection rates of fecal *F. nucleatum*, FIT, and serum CA19-9: the positive rates of the three diagnostic methods were compared in CRC patients and healthy individuals.

(2) The diagnostic efficacy of fecal *F. nucleatum* detection combined with FIT and serum CA19-9 detection for CRC: the pathological results were used as the gold standard to evaluate the sensitivity and specificity of individual diagnostic methods and the combined CRC diagnoses for the CRC diagnosis degree and accuracy.

(3) ROC curve of fecal F. nucleatum detection combined with FIT and serum CA19-9 detection for CRC: the ROC curve was drawn according to each diagnostic method and the combined diagnosis of CRC. The larger the area under the ROC curve, the higher the diagnostic accuracy.

2.4. Statistical method

The research statistical data was analyzed using SPSS 21.0 software, the count data was described by number (percentage) [*n* (%)], the χ^2 test was used, and the difference was considered statistically significant when $P < 0.05$.

3. Results

3.1. Comparison of positive detection rates of fecal *F. nucleatum*, FIT, and serum CA19-9

The positive detection rates of fecal *F. nucleatum*, FIT, and serum CA19-9 in CRC patients were significantly higher than those of healthy individuals ($P = 0.000$), see **Table 1**.

Table 1. Comparison of positive detection rates of fecal *F. nucleatum*, FIT, and serum CA19-9 [*n* (%)]

	Number of cases	Fecal *F. nucleatum*	FIT	Serum CA19-9
CRC patients	78	57 (73.1%)	40 (51.3%)	54 (69.2%)
Healthy individuals	60	9 (15.0%)	2 (3.3%)	1 (1.7%)
χ^2 value		45.841	23.698	51.386
P value		0.000	0.000	0.000

3.2. The diagnostic efficacy of fecal *F. nucleatum* combined with FIT and serum CA19-9 detection for CRC

Table 2 showed that the sensitivity of the combined diagnoses of the three was significantly higher than that of the individual detection of F. nucleatum ($\chi^2 = 6.495$, $P = 0.011$), FIT ($\chi^2 = 4.871$, $P = 0.027$), and serum CA19-9 ($\chi^2 = 7.371$, $P = 0.007$).

Table 2. The diagnostic efficacy of fecal *F. nucleatum* combined with FIT and serum CA19-9 detection for CRC [*n* (%)]

Detection method	Number of cases	Sensitivity	Specificity	Accuracy
F. nucleatum	138	73.08% (57/78)	85.00% (51/60)	78.26% (108/138)
FIT	138	51.28% (40/78)	96.67% (58/60)	71.01% (98/138)
CA19-9	138	69.23% (54/78)	98.33% (59/60)	71.74% (99/138)
Joint diagnoses	138	87.18% (68/78)	70.00% (42/60)	79.71% (110/138)

3.3. ROC curve of fecal *F. nucleatum* combined with FIT and serum CA19-9 detection for CRC

The area under the ROC curve for the diagnosis of CRC by fecal *F. nucleatum* detection was 0.63 [95% confidence interval (CI) = 1.124–6.238), and the sensitivity and specificity were 73.08% and 85.00%, respectively. The area under the ROC curve for the diagnosis of CRC by FIT was 0.65 (95% CI = 1.365–9.241), with a sensitivity of 51.28% and specificity of 96.67%. The area under the ROC curve for the diagnosis of CRC by serum CA19-9 detection was 0.62 (95% CI = 1.517–12.342), and the sensitivity and specificity were 69.23% and 98.33%, respectively. The area under the ROC curve for the combined three diagnoses of CRC was 0.76 (95% CI = 1.213–6.254), with a sensitivity of 87.18% and specificity of 70.00%, as shown in **Figure 1**.

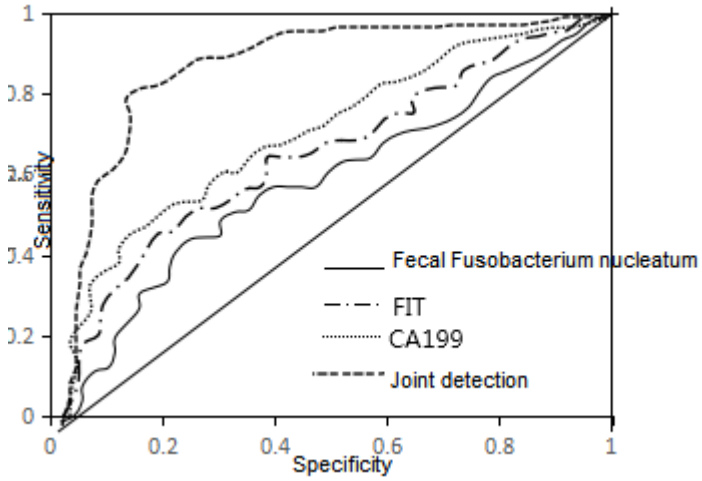

Figure 1: ROC curve of CRC diagnoses using fecal *F. nucleatum* detection, FIT, serum CA19-9, and a combination of all three diagnoses.

4. Discussion

In recent years, with the rapid economic development and changes in people's living habits, the incidence and mortality of CRC in China are gradually increasing [6], and roughly 20% of CRC patients are found to be associated with liver metastases at the early stage of diagnosis and progress to advanced stages. The 5-year survival rate of bowel cancer patients is about 60%. Moreover, due to the CRC patients are being not vigilant enough and performing limited examinations, the misdiagnosis rate of CRC is approximately 30% [7,8]. Therefore, improvement of the early diagnosis and screening of CRC is an essential clinical problem that needs to be solved urgently. In this study, the combined diagnoses of fecal *F. nucleatum* detection, FIT, and serum CA19-9 detection were found to have good sensitivity and accuracy, and it has high clinical application value for the early diagnosis of CRC.

Recently, the research on the relationship between intestinal microecology and CRC has progressed, and the relationship between intestinal microecology and CRC has gradually been recognized. Gut bacteria

have certain carcinogenicity and can drive the occurrence of CRC and change with the development of CRC [9,10]. *F. nucleatum* can form a Fap2/Gal-Gal NAc complex through its bacterial protein Fap2 and become a passive bacterium in the process of CRC lesions, indicating that *F. nucleatum* is closely related to CRC lesions [11,12]. Therefore, fecal *F. nucleatum* has a certain clinical value in the diagnosis of CRC. Although the detection of fecal microbial markers is convenient and economical, the DNA of fecal microorganisms is stable, and the extraction method is mature and simple, but due to the diversity of gastrointestinal flora and its micro-ecological environment, it is easy to obtain errors in the diagnostic results, thereby leading to misdiagnosis, which is inconsistent with several reports in related studies of using fecal *F. nucleatum* as a biomarker for early screening of bowel cancer, which may be due to the differences in the gastrointestinal flora of patients [11,13]. The fecal occult blood test is a simple immunological detection method. However, when the blood concentration in the stool sample is too high, the result will appear as a false negative, resulting in misdiagnosis [3,14]. Tumor marker CA19-9 has good specificity and accuracy for the diagnosis of CRC [15], and CA242 also has a certain value in the diagnosis of CRC [16]. However, there are many tumor markers available and it is impossible to detect them one by one. Therefore, the detection of a single tumor marker has certain exclusivity. It can be seen that a single detection method cannot meet the needs of clinical early diagnosis. In recent years, the application of joint detection has become the preferred method for the diagnosis of CRC [17,18], but there is still a lack of unified standards for joint detection indicators. Several detection methods that have been popular in recent years have been integrated to find a more stable and reliable early diagnosis method for early intervention and treatment, thereby reducing the mortality rate of CRC.

The combined detection results of the three showed that the sensitivity and sensitivity of fecal *F. nucleatum* combined with FIT and CA19-9 detection were significantly higher than that of individual diagnoses ($P < 0.05$), indicating that the combination diagnoses can improve the sensitivity of early diagnosis of CRC, and the ROC curve proves that the accuracy of combined diagnosis of CRC is higher. In the current clinical diagnostic experiments of CRC, combined detection is often used to improve the sensitivity or specificity of diagnosis, thereby improving the efficiency of clinical diagnosis. However, many experiments show that the premise of improving the sensitivity of diagnosis is to reduce the specificity, and the improvement of specificity is at the expense of reducing the sensitivity. In this study, the combined detection of fecal *F. nucleatum*, FIT, and serum CA19-9 significantly improved the sensitivity of diagnosing CRC. The combined detection can make up for the limitation of single index diagnosis to a certain extent, and the ROC curve proves that its diagnostic accuracy is high, indicating that combined detection can improve the sensitivity and accuracy of CRC diagnosis, and can be used as a fast and effective detection method for screening and diagnosing CRC.

In conclusion, fecal *F. nucleatum* combined with FIT and serum CA19-9 detection can efficiently and accurately diagnose CRC with high sensitivity and high diagnostic value, which can provide a reference for early diagnosis of CRC, and is conducive to timely intervention and treatment to improve the quality of life of CRC patients.

Funding

The In-Hospital Fund of the Affiliated Hospital of Hebei University (2017Q004) and the Medical Research Project of Hebei Provincial Health Commission (20190924)

Disclosure statement

The authors declare no conflict of interest.

References

[1] González-González M, Garcia JG, Monstero JAA, et al, 2013, Genomics and Proteomics Approaches for Biomarker Discovery in Sporadic CRC with Metastasis. Cancer Genomics Proteomics, 10(1): 19–25.

[2] Kumar M, Cash BD, 2017, Screening and Surveillance of CRC Using CT Colonography. Curr Treat Options Gastroenterol, 15(1): 168–183. http://doi.org/10.1007/s11938-017-0121-7

[3] Lee JK, Liles EG, Bent S, et al, 2014, Accuracy of Fecal Immunochemical Tests for CRC: Systematic Review and Meta-Analysis. Ann Intern Med, 160(3): 171. http://doi.org/10.7326/M13-1484

[4] Zhu Y, Zhao W, Mao G, 2022, Perioperative Lymphocyte-to-Monocyte Ratio Changes Plus CA199 in Predicting the Prognosis of Patients with Gastric Cancer. J Gastrointest Oncol, 13(3):1007–1021. http://doi.org/10.21037/jgo-22-411

[5] Castellarin M, Warren RL, Freeman JD, et al, 2012, Fusobacterium nucleatum Infection is Prevalent in Human Colorectal Carcinoma. Genome Res, 22(2): 299–306. http://doi.org/10.1101/gr.126516.111

[6] Sung JJY, Lau JYW, Goh KL, et al, 2005, Increasing Incidence of CRC in Asia: Implications for Screening. Lancet Oncol, 6(11): 871–876. http://doi.org/10.1016/S1470-2045(05)70422-8

[7] Aghagolzadeh P, Radpour R. 2016, New Trends in Molecular and Cellular Biomarker Discovery for CRC. World J Gastroenterol, 22(25): 5678–5693. http://doi.org/10.3748/wjg.v22.i25.5678

[8] Sung JJY, Ng SC, Chan FKL, et al, 2015, an Updated Asia Pacific Consensus Recommendations on CRC Screening. Gut, 64(1): 121–132. http://doi.org/10.1136/gutjnl-2013-306503

[9] Yu J, Feng Q, Wong SH, et al, 2017, Metagenomic Analysis of Faecal Microbiome as a Tool Towards Targeted Non-Invasive Biomarkers for CRC. Gut, 66(1): 70–78. http://doi.org/10.1136/gutjnl-2015-309800

[10] Liang Q, Chiu J, Chen Y, et al, 2017, Fecal Bacteria Act as Novel Biomarkers for Noninvasive Diagnosis of CRC. Clin Cancer Res, 23(8): 2061–2070. http://doi.org/10.1158/1078-0432.CCR-16-1599

[11] Ahn J, Sinha R, Pei Z, et al, 2013, Human Gut Microbiome and Risk for CRC. J Natl Cancer Inst, 105(24): 1907–1911. http://doi.org/10.1093/jnci/djt300

[12] McCoy AN, Araújo-Pérez F, Azcárate-Peril A, et al, 2013, Fusobacterium is Associated with Colorectal Adenomas. PLoS One, 8(1): e53653. http://doi.org/10.1371/journal.pone.0053653

[13] Lopez-Siles M, Martinez-Medina M, Surís-Valls R, et al, 2016, Changes in the Abundance of Faecalibacterium prausnitzii Phylogroups I and II in the Intestinal Mucosa of Inflammatory Bowel Disease and Patients with CRC. Inflamm Bowel Dis, 22(1): 28–41. http://doi.org/10.1097/MIB.0000000000000590

[14] Haug U, Hundt S, Brenner H, 2010, Quantitative Immunochemical Fecal Occult Blood Testing for Colorectal Adenoma Detection: Evaluation in the Target Population of Screening and Comparison with Qualitative Tests. Am J Gastroenterol, 105(3): 682–690. http://doi.org/10.1038/ajg.2009.668

[15] Gao Y, Wang J, Zhou Y, et al, 2018, Evaluation of Serum CEA, CA19-9, CA72-4, CA125 and Ferritin as Diagnostic Markers and Factors of Clinical Parameters for CRC. Sci Rep, 8(1): 2732. http://doi.org/10.1038/s41598-018-21048-y

[16] Rao H, Wu H, Huang Q, et al, 2021, Clinical Value of Serum CEA, CA24-2 and CA19-9 in Patients with CRC. Clin Lab, 67(4). http://doi.org/10.7754/Clin.Lab.2020.200828

[17] Wong SH, Kwong TNY, Chow T-C, et al, 2017, Quantitation of Faecal Fusobacterium Improves Faecal Immunochemical Test in Detecting Advanced Colorectal Neoplasia. Gut, 66(8): 1441–1448.

http://doi.org/10.1136/gutjnl-2016-312766

[18] Steer T, Collins MD, Gibson GR, et al, 2001, Clostridium hathewayi sp. nov., from Human Faeces. Syst Appl Microbiol, 24(3): 353–357. http://doi.org/10.1078/0723-2020-00044

Author Guidelines

Before your submission, please check that your manuscript has been prepared in accordance to the step-by-step instructions for submitting a manuscript to our online submission system. We recommend that you keep this page open for your reference as you move through the submission process.

If there are any differences in author guidelines between the print and online version, it is recommended that authors refer to the online version for use.

Manuscript Format

Proceedings of Anticancer Research accepts manuscript that is in MS Word or LaTeX format. All manuscripts must be written in clear, comprehensible English. Both American and British English are acceptable. Usage of non-English words should be kept to a minimum and all must be italicized (except for e.g. and i.e.) If you have concerns about the level of English in your submission, please ensure that it is proofread before submission by a native English speaker or a scientific editing service.

Cover letter

All submissions for *Proceedings of Anticancer Research* should include a cover letter as a separate file. A cover letter should contain a brief explanation of what was previously known, the conceptual advancement with the findings and its significance to broad readership. The cover letter is confidential and will be read only by the editors. It will not be seen by reviewers.

Title

The title should capture the conceptual significance for a broad audience. The title should not be more than 50 words and should be able to give readers an overall view of the paper's significance. Titles should avoid using uncommon jargons, abbreviations and punctuation.

List of Authors

The names of authors must be spelled out rather than set in initials with their affiliations footnoted. Authors should be listed according to the extent of their contribution, with the major contributor listed first. All corresponding authors (maximum 2) should be identified with an asterisk. Affiliations should contain the following core information: department, institution, city, state, postal code, and country. For contact, email address of only one corresponding author is expected within the manuscript. Please note that all authors must see and approve the final version of the manuscript before submitting.

Abstract

Articles must include an abstract containing a maximum of 200 words. The purpose of abstract is to provide sufficient information for a reader to choose either to proceed to the full text of the article. After the abstract, please give 3-8 key words; please avoid using the same words as those already used in the title.

Section Headings

Please number all section headings, subheadings and sub-subheadings. Use boldface to identify major headings (e.g. **1**, **2**, **3**, etc.) and subheadings (e.g. **1.1**, **1.2**, **2.1**, **2.2** etc.) For the sub-subheadings, please distinguish it further using non-boldface numbers in parenthesis (e.g. (1), (2), (3), etc.)

Introduction

Introduction should provide a background that gives a broad readership an overall outlook of the field and the research performed. It tackles a problem and states its important regarding with the significance of the study. Introduction can conclude with a brief statement of the aim of the work and a comment about whether that aim was achieved.

Materials and Methods

This section provides the general experimental design and methodologies used. The aim is to provide enough detail to for other investigators to fully replicate your results. It is also required to facilitate better understanding of the results obtained. Protocols and procedures for new methods must be included in detail to reproduce the experiments.

Ethics

Ethics information, including IACUC permit numbers and/or IRB name, if applicable. This information should be included in a subheading labelled "Ethics Statement" in the "Methods" section of your manuscript file, in as much detail as possible.

Results

This section can be divided into subheadings. This section focuses on the results of the experiments performed.

Discussion

This section should provide the significance of the results and identify the impact of the research in a broader context. It should not be redundant or similar to the content of the results section.

Conclusion

Please use the conclusion section for interpretation only, and not to summarize information already presented in the text or abstract.

Conflict of Interest

All authors are required to declare all activities that have the potential to be deemed as a source of competing interest in relations to their submitted manuscript. Examples of such activities could include personal or work-related relationships, events, etc. Authors who have nothing to declare are encouraged to add "No conflict of interest was reported by all authors" in this section.

Funding

Authors should declare all financial and non-financial support that have the potential to be deemed as a source of competing interest in relations to their submitted manuscript in this section. Financial supports are generally in the form of grants, royalties, consulting fees and more. Examples of non-financial support could include the following: externally-supplied equipments/biological sources, writing assistance, administrative support, contributions from non-authors etc.

Appendix

This section is optional and is for all materials (e.g. advanced technical details) that has been excluded from the main text but remain essential to readers in understanding the manuscripts. This section is

not for supplementary figures. Authors are advised to refer to the section on 'Supplementary figures' for such submissions.

Text

The text of the manuscript should be in Microsoft Word or Latex. The length of the manuscript cannot be more than 50000 characters (inclusive of spaces) or approximately 7000 words.

Nomenclature for genes and proteins

This journal aims to reach researchers all over the globe. Hence, for both reviewers' and readers' ease in comprehension, authors are highly encouraged to use the appropriate gene and protein nomenclature. Authors may prefer to utilize resources such as http://www.ncbi.nlm.nih.gov/gene

Figures

Authors should include all figures into the manuscript and submit it as 1 file in the OJS system. Reference to the "Instructions for Typesetting manuscript" is strongly encouraged. Figures include photographs, scanned images, graphs, charts and schematic diagrams. Figures submitted should avoid unnecessary decorative effects (e.g. 3D graphs) as well as be minimally processed (e.g. changes in brightness and contrast applied uniformly for the entire figure). It should also be set against a white background. Please remember to label all figures (e.g. axis etc.) and add in captions (below the figure) as required. These captions should be numbered (e.g. **Figure 1**, **Figure 2**, etc.) in boldface. All figures must have a brief title (also known as caption) that describes the entire figure without citing specific panels, followed by a legend defined as description of each panel. Please identify each panel with uppercase letters in parenthesis (e.g. A, B, C, etc.)

The preferred file formats for any separately submitted figure(s) are TIFF or JPEG. All figures should be legible in print form and of optimal resolution. Optimal resolutions preferred are 300 dots per inch for RBG coloured, 600 dots per inch for greyscale and 1200 dots per inch for line art. Although there are no file size limitation imposed, authors are highly encouraged to compress their figures to an ideal size without unduly affecting legibility and resolution of figures. This will also speed up the process of uploading in the submission system if necessary.

The Editor-in-Chief and Publisher reserve the right to request from author(s) the high-resolution files and unprocessed data and metadata files should the need arise at any point after manuscript submission for reasons such as production, evaluation or other purposes. The file name should allow for ease in identifying the associated manuscript submitted.

Tables, lists and equations

Tables, lists and equations must be submitted together with the manuscript. Likewise, lists and equations should be properly aligned and its meaning clear to readers. Tables created using Microsoft Word table function are preferred. Place each table in your manuscript file right after the paragraph in which it is first cited. Do not submit your tables in separate files. The tables should include a concise but sufficiently explanatory title at the top. Vertical lines should not be used to separate columns. Leave some extra space between the columns instead. All tables should be based on three horizontal lines to separate the caption, header and body. A few additional horizontal lines MAY be included as needed (example below). Any explanations essential to the understanding of the table should be given in footnotes at the bottom of the table. SI units should be used.

Supplementary information

This section is optional and contains all materials and figures that have been excluded from the entire manuscript. This information are relevant to the manuscript but remains non-essential to readers' understanding of the manuscript's main content. All supplementary information should be submitted as a separate file in Step 4 during submission. Please ensure the names of such files contain 'suppl. info'.

In-text citations

Reference citations in the text should be numbered consecutively in superscript square brackets. Some examples:

1. Negotiation research spans many disciplines [3, 4].
2. This result was later contradicted by Becker and Seligman [5].
3. This effect has been widely studied [1–3, 7].

Personal communications and unpublished works can only be used in the main text of the submission and are not to be placed in the Reference section. Authors are advised to limit such usage to the minimum. They should also be easily identifiable by stating the authors and year of such unpublished works or personal communications and the word 'Unpublished' in parenthesis.

E.g. (Smith J, 2000, Unpublished)

References

This section is compulsory and should be placed at the end of all manuscripts. Do not use footnotes or endnotes as a substitute for a reference list. The list of references should only include works that are cited in the text and that have been published or accepted for publication. Personal communications and unpublished works should be excluded from this section.

For references in reference list, all authors must be stated. Authors referenced are listed with their surname followed by their initials. All references should be numbered (e.g. 1. 2. 3. etc.) and sequenced according to the order it appears as an in-text citation. References should follow the following pattern: Author(s) followed by year of publication, title of publication, full journal name in italics, volume number, issue number in parenthesis, page range and lastly the DOI (if applicable). If the referred article has more than three authors, list only the first three authors and abbreviate the remaining authors to italicized 'et al.' (meaning: "and others").

Journal

Journal article (print) with one to three authors

[1] Yao Y., Xia B. Application of Phase Frequency Feature Group Delay Algorithm in Database Differential Access. Computer Simulation, 2014, 31(12): 238-241.

Journal article (print) with more than three authors

[2] Gamelin F.X., Baquet G., Berthoin S., et al. Effect of high intensity intermittent training on heart rate variability in prepubescent children. European Journal of Applied Physiology, 2009, 105: 731–738.

Journal article (online) with one to three authors

[3] Jackson D., Firtko A., Edenborough M. Personal resilience as a strategy for surviving and thriving in the face of workplace adversity: a literature review. Journal of Advanced Nursing, 2009, 60(1): 1–9,

Journal article (online) with more than three authors

[4] Hargreave M., Jensen A., Nielsen T.S.S., et al. Maternal use of fertility drugs and risk of cancer in children—A nationwide population-based cohort study in Denmark. International Journal of Cancer, 2015, 136(8): 1931–1939.

Book

Book with one to three authors

[5] Schneider Z., Whitehead D., Elliott D. Nursing and midwifery research: methods and appraisal for evidence-based practice. 3rd edn. 2009, Elsevier Australia, Marrickville, NSW.

Book with more than three authors

[6] Davis M., Charles L., Curry M.J., et al. Challenging spatial norms. 2013, Routledge, London.

Chapter or Article in Book

[7] Knowles M.S. Independent study. In Using learning contracts. 1986, Jossey-Bass, San Francisco, 89–96.

Others

Proceedings of meetings and symposiums, conference papers

[8] Chang S.S., Liaw L. and Ruppenhofer J. (eds). Proceedings of the twenty-fifth annual meeting of the Berkeley Linguistics Society, February 12–15, 1999: general session and parasession on loan word phenomena. 2000, Berkeley Linguistics Society, Berkeley.

Conference proceedings (from electronic database)

[9] Bukowski R.M. Prognostic factors for survival in metastatic renal cell carcinoma: update 2008. Innovations and challenges in renal cancer: proceedings of the third Cambridge conference. Cancer, 2009, 115 (10): 2273, viewed 19 May 2009, Academic OneFile database.

Online Document with author names

[10] Este J., Warren C., Connor L., et al. Life in the clickstream: the future of journalism, Media Entertainment and Arts Alliance, 2008. viewed 27 May 2009, http://www.alliance.org.au/documents/foj_report_final.pdf

Online Document without author name

[11] Developing an argument n.d., viewed March 30 2009, http://web.princeton.edu/sites/writing

/Writing_Center/WCWritingResources.htm

Thesis/Dissertation

[12] Gale L. The relationship between leadership and employee empowerment for successful total quality management. 2000, University of Western Sydney.

Standard

[13] Standards Australia Online. Glass in buildings: selection and installation. AS 1288–2006. 2006, SAI Global database.

Government Report

[14] National Commission of Audit. Report to the Commonwealth Government, Australian Government Publishing Service, 1996, Canberra.

Government report (online)

[15] Department of Health and Ageing. Ageing and aged care in Australia, 2008, viewed 10 November 2008, http://www.health.gov.au/internet/main/publishing.nsf/Content/ageing

No author

[16] Guide to agricultural meteorological practices. 2nd edn, Secretariat of the World Meteorological Organization, 2010, Geneva.

Note: When referencing an entry from a dictionary or an encyclopedia with no author there is no requirement to include the source in the reference list. In these cases, only cite the title and year of the source in-text. For an authored dictionary/encyclopedia, treat the source as an authored book.

Submission Preparation Checklist

As part of the submission process, authors are required to check off their submission's compliance with all of the following items, and submissions may be returned to authors that do not adhere to these guidelines.

1. The submission has not been previously published, nor is it before another journal for consideration (or an explanation has been provided in Comments to the Editor).

2. The submission file is in OpenOffice, Microsoft Word, RTF, or WordPerfect document file format.

3. Where available, URLs for the references have been provided.

4. The text is single-spaced; uses a 12-point font; employs italics, rather than underlining (except with URL addresses); and all illustrations, figures, and tables are placed within the text at the appropriate points, rather than at the end.

5. The text adheres to the stylistic and bibliographic requirements outlined in the Author Guidelines, which is found in About the Journal.

6. If submitting to a peer-reviewed section of the journal, the instructions in Ensuring a Blind Review have been followed.

Integrated Services Platform of International Scientific Cooperation

Innoscience Research (Malaysia), which is global market oriented, was founded in 2016.Innoscience Research focuses on services based on scientific research. By cooperating with universities and scientific institutes all over the world, it performs medical researches to benefit human beings and promotes the interdisciplinary and international exchanges among researchers.

Innoscience Research covers biology, chemistry, physics and many other disciplines. It mainly focuses on the improvement of human health. It aims to promote the cooperation, exploration and exchange among researchers from different countries. By establishing platforms, Innoscience integrates the demands from different fields to realize the combination of clinical research and basic research and to accelerate and deepen the international scientific cooperation.

Cooperation Mode

Clinical Workers

In-service Doctors

Foreign Researchers

Hospital

University

Scientific institutions

BIO-BYWORD
SCIENTIFIC PUBLISHING PTY LTD

OUR JOURNALS

The *Journal of Architectural Research and Development* is an international peer-reviewed and open access journal which is devoted to establish a bridge between theory and practice in the fields of architectural and design research, urban planning and built environment research.

Topics covered but not limited to:

- Architectural design
- Architectural technology, including new technologies and energy saving technologies
- Architectural practice
- Urban planning
- Impacts of architecture on environment

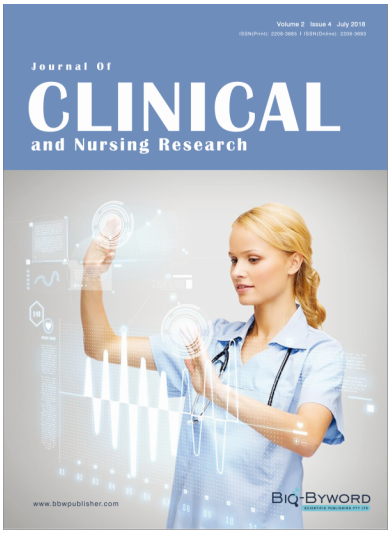

Journal of Clinical and Nursing Research (JCNR) is an international, peer reviewed and open access journal that seeks to promote the development and exchange of knowledge which is directly relevant to all clinical and nursing research and practice. Articles which explore the meaning, prevention, treatment, outcome and impact of a high standard clinical and nursing practice and discipline are encouraged to be submitted as original article, review, case report, short communication and letters.

Topics covered by not limited to:

- Development of clinical and nursing research, evaluation, evidence-based practice and scientific enquiry
- Patients and family experiences of health care
- Clinical and nursing research to enhance patient safety and reduce harm to patients
- Ethics
- Clinical and Nursing history
- Medicine

Journal of Electronic Research and Application is an international, peer-reviewed and open access journal which publishes original articles, reviews, short communications, case studies and letters in the field of electronic research and application.

Topics covered but not limited to:

- Automation
- Circuit Analysis and Application
- Electric and Electronic Measurement Systems
- Electrical Engineering
- Electronic Materials
- Electronics and Communications Engineering
- Power Systems and Power Electronics
- Signal Processing
- Telecommunications Engineering
- Wireless and Mobile Communication